

Stability in isotropic and anisotropic fluids

K. A. McCosh
Department of Mathematics,
University of Strathclyde,
Glasgow, U.K.
September 2009

A thesis submitted in partial fulfilment of the requirements
for the degree of Doctor of Philosophy

I would like to thank my supervisors Dr. André Sonnet and Prof. Iain Stewart for all their help and guidance over the past few years. It has been an education. I would also like to thank both of my examiners, Prof. Paulo Biscari of Politecnico Di Milano and Prof. Nigel Mottram.

I also owe great thank to the three people who inspired and encouraged me to study maths beyond school level - Mr Ian Love and Mr Martin Smith who were teachers at Clyde Valley High School while I was there, and also Count von Count from Sesame Street who taught me to count in the first place.

Finally, I must give great thanks to my mum and dad and the rest of my family and friends and special thanks must go to Chris Logan for understanding the stress and pressure I have been under over the past 4 years.

Abstract

In this thesis, we consider various liquids in different situations to determine whether or not the geometry of the liquid is stable. The types of liquids discussed here are an isotropic liquid, smectic C liquid crystal and nematic liquid crystals.

Smectic C liquid crystals are considered when they are in a concentric circular geometry in the presence of an azimuthal magnetic field. The stability of the solutions for the orientation of the director are considered using variational techniques. Planar layered smectic C liquid crystals are also considered in this context.

A perturbed thin film of nematic liquid crystal is then considered to determine whether the film will dewet. This is first done by considering the Stokes equations and then the Ericksen–Leslie equations. The latter is then subject to a perturbation of the perturbation to analyse the stability of the original perturbation.

Finally, an isotropic fluid is considered when a free surface is acted upon by van der Waal forces caused by an approaching blade. The profile of the free surface rises to meet the blade and whether or not this distortion to the profile changes depends on the distance of the blade, shape of the blade or curvature of the blade, as will be discussed.

Contents

1	Introduction	1
1.1	States of matter	1
1.2	History of liquid crystals	2
1.3	Liquid crystals	3
1.3.1	Nematics	4
1.3.2	Cholesterics	5
1.3.3	Smectics	6
1.3.4	Polymorphism	7
1.4	Outline of thesis	8
2	Liquid Crystal Theory	9
2.1	Notation and terminology	9
2.1.1	Director	10
2.2	Nematic theory	11
2.2.1	Frank–Oseen elastic energy	11
2.2.1.1	One-constant approximation	12
2.2.2	Magnetic and electric fields	13
2.2.3	Bulk energy	14
2.2.4	Ericksen–Leslie dynamic equations	14
2.2.5	Leslie and Miesowicz viscosities	16
2.2.6	Equilibrium equations for nematics	18
2.2.7	Reformulated Ericksen–Leslie equations	18
2.3	Anchoring conditions	21
2.3.1	Strong anchoring	21
2.3.2	Conical anchoring	22
2.3.3	Weak anchoring	22
2.4	Smectic theory	23

2.4.1	Static smectic theory	24
2.4.2	The magnetic and electric energies	27
2.4.3	Equilibrium Equations	27
2.4.4	Dynamic smectic theory	28
3	Calculus of Variations	31
3.1	The minimum of a functional	31
3.2	Rayleigh–Ritz method	32
3.3	Second variation	35
3.3.1	Positive definiteness	36
3.3.2	The Jacobi equation and conjugate points	37
3.3.3	Necessary conditions	38
3.3.4	Sufficient conditions	40
3.4	Positivity criterion	42
4	Smectic C Domain Walls in a Cylinder	45
4.1	Atkin and Stewart’s solutions	45
4.2	Stability	52
4.2.1	Application of the Rayleigh–Ritz method	56
4.2.2	Second variation	57
4.2.2.1	The Euler–Lagrange equation	58
4.2.2.2	The Strengthened Legendre condition	58
4.2.2.3	Strengthened Jacobi condition	59
4.2.3	Positivity criterion	59
4.2.4	The Jacobi equation	66
4.3	Conclusions	68
5	Smectic C Domain Walls in Planar Layers	70
5.1	Solutions	73

5.2	Specific solutions	76
5.3	Stability of the solutions	78
5.4	Conclusions	80
6	Fluctuations of a Thin Nematic Film	81
6.1	Physical setup	82
6.2	Isotropic viscosity	84
6.2.1	Navier–Stokes equation	84
6.2.2	Laplace’s formula	87
6.2.3	Surface conditions	87
6.2.4	Solving the equations	89
6.2.5	Fluctuations	91
6.2.6	Typical values	93
6.3	Thin film with Leslie viscosities	93
6.3.1	Ericksen-Leslie equations	94
6.3.2	Fluctuations	97
6.4	Leslie viscosities with more director freedom	98
6.4.1	Ericksen-Leslie equations	98
6.5	A perturbation to the known solution	100
6.5.1	Different nematic liquid crystals	105
6.5.1.1	5CB	105
6.5.1.2	MBBA	106
6.5.1.3	DDA9	108
6.6	Conclusions	112
7	A Blade Approaching a Free Surface	114
7.1	Blade models	114
7.1.1	Parabolic blade	117
7.1.2	Circular ended blade	120

7.1.3	Comparison of blade shapes	123
7.2	Stability of the profiles	124
7.2.1	Second Variation	125
7.2.2	Rayleigh–Ritz method	127
7.3	Conclusions	128
8	Conclusions and Outlook	129
A	Solutions to the Planar Layer Integral	132

1 Introduction

1.1 States of matter

It is widely accepted that there are three states of matter: solid, liquid and gaseous. There is in fact a fourth state of matter which exists between the solid and liquid state for some substances. These substances have two “melting points” between the solid crystalline state and the liquid state. At the first melting point, the crystal melts into a cloudy liquid then, at a higher temperature, this cloudy liquid clears to form an isotropic liquid (see Fig. 1 below). This

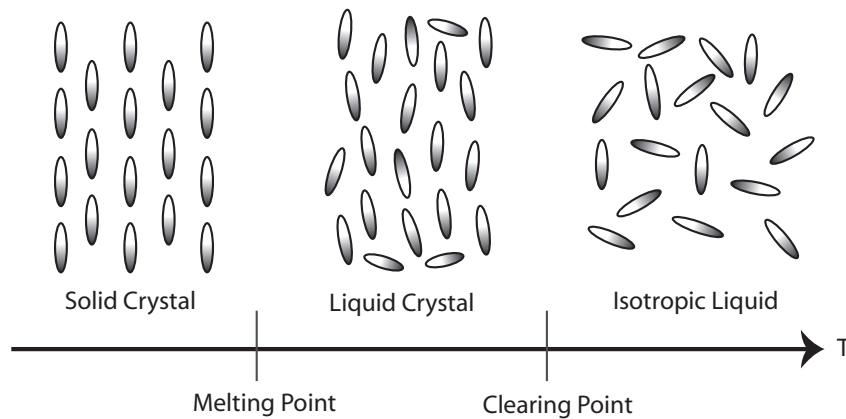


Figure 1: As the temperature is increased a solid crystal sample can “melt” once to form a liquid crystal then “melt” again to form an isotropic liquid.

cloudy liquid is the liquid crystalline state.

Some substances do not form a liquid crystalline phase but those that are more likely to form one tend to have similar physical properties within the chemical structure of their molecules. Molecules of substances which form a liquid crystal phase tend to be elongated “rod-like” molecules which align themselves parallel to one another. They also tend to have flexible ends to their structure with some rigidity in the centre.

Chapters 4, 5 and 6 in this thesis model Liquid Crystals. However, chapter 7 is concerned with isotropic fluids. An introduction will be given to this problem

there.

1.2 History of liquid crystals

A liquid crystal phase was first observed over 150 years ago in the middle of the 19th century by Virchow, Mettenheimer and Valentin [1] although they did not know that that was what they were observing. Many other chemists, biologist and physicists noticed that some materials behaved strangely close to their melting points and that the optical properties of some substances changed unexpectedly with temperature. It was not until 1888 that people began to realise that it was a different phase of matter that they were observing.

In 1888, the Austrian botanist Friedrich Reinitzer was attempting to determine the precise melting point of cholesteryl benzoate. He noticed that it seemed to have two melting points [2]: one at 145.5°C where the solid crystal melted to form a cloudy liquid, then another at 178.5°C where this cloudy liquid cleared to give a transparent liquid. During this transition, unusual optical behaviour was also observed. Reinitzer then turned to Otto Lehmann, an expert in liquid optics, for help. Lehmann had invented a heating microscope which allowed the user to control the temperature of the sample. Lehmann and Reinitzer looked at the sample under the microscope and noticed that the cloudy liquid seemed to have some sort of order to it, while the clear liquid was isotropic. This was when Reinitzer realised that this was another state of matter. It is Otto Lehmann who is credited with coming up with the term “liquid crystal” [3].

In the early 20th century Vorländer discovered that a substance had to have “rod-like” molecules in order to form a liquid crystal phase. This allowed mathematicians to make assumptions and model the substance. Wiener developed the first optical theory for liquid crystals in 1904 and Oseen identified elastic constants which allowed further development in the theory and mathematical modelling of the substances. In the 1920s, a French scientist called George

Friedel conducted experiments on liquid crystal samples which led to them being classified into 3 broad categories: nematic, smectic and cholesteric [4].

From the 1900s to the outbreak of World War II, theorists were very interested in the elastic properties of liquid crystal substances. Oseen derived a static theory for nematic liquid crystals which was then developed further by Frank in the 1950s. Towards the end of that decade liquid crystals were once again being researched as their potential had been realised, and within 10 years the first liquid crystal display had been made.

Until the late 19th century, all liquid crystal substances had been naturally occurring but nowadays it is possible to produce liquid crystals with specific predetermined material properties. Liquid crystals are now used for a whole host of everyday things. They are used in medicine for simple things such as thermometers right through to complex things such as medical lasers. They are also used for screens in mobile phones, televisions and laptops as well as a lot of other things.

1.3 Liquid crystals

Liquid crystals are partially ordered materials between the solid and liquid phase. They are usually thought of as elongated rod like molecules and it is their shape which encourages them to align in a certain direction. The chemical structure of 4-pentyl-4'-cyanobiphenyl, also known as 5CB, is shown below in Fig. 2. This

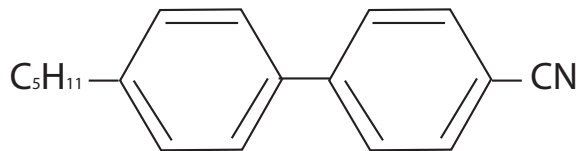


Figure 2: The chemical structure of 4-pentyl-4'-cyanobiphenyl

liquid crystal molecule has a long rod like structure with a “tail” of five carbon

atoms and eleven hydrogen atoms attached to a “centre” consisting of two cyclic groups with a “head” of a carbon and a nitrogen atom.

There are many different liquid crystalline phases, so called mesophases. The three main types are nematic, smectic and cholesteric.

1.3.1 Nematics

The nematic phase is the simplest liquid crystalline phase. Nematic liquid crystals do not have any specific structures within a sample except that there is a general direction to the molecules, which is taken to be the average direction in which all the molecules are pointing as shown in Fig. 3. The direction in which

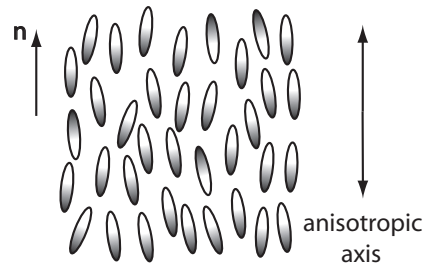


Figure 3: A typical sample of nematic liquid crystal

they are pointing is called the “anisotropic axis”. This direction is described by a unit vector \mathbf{n} , called the nematic director (see Section 2.1.1).

An example of a substance which has a nematic liquid crystalline phase is the aforementioned 4-pentyl-4'-cyanobiphenyl (5CB). Its chemical structure is shown above in Fig. 2. 5CB is nematic between 24°C and 35.4°C [5] and is often used for testing twisted nematic displays since it is stable at room temperature.

It is well known that in a finite sample of liquid crystal there is a competition between the alignment of the director \mathbf{n} at the surface or boundary and the orientation of \mathbf{n} induced within the sample by an externally applied magnetic or electric field [6, p.72]. It is also known that in a thin sample of nematic liquid crystal which has, for example, magnetic anisotropy $\chi_a > 0$, a magnetic field

\mathbf{H} may be in a position to attract the director \mathbf{n} and cause it to begin to align in the bulk to be parallel to \mathbf{H} , and different from its initial sample alignment, when $H = |\mathbf{H}|$ is greater than some critical value H_c , which is often, but not always, greater than zero. In other words, the director alignment throughout the sample will not be influenced by the magnetic field whenever $0 \leq H < H_c$ but will be influenced and begin to adjust its orientation to become more parallel to \mathbf{H} when $H \geq H_c$. This change in director orientation after the magnitude of the field increases through the value H_c is called the Freedericksz transition and H_c is called the critical field strength of Freedericksz threshold.

Although not directly considered in this thesis, the reorientation of \mathbf{n} may occur through electric fields with domain walls which will be considered here in Ch. 4. It is the Freedericksz transition that is important for display technologies and solitons / domain walls are of interest in soliton switching of displays.

1.3.2 Cholesterics

When molecules are chiral, that is, they cannot be superimposed on their own mirror image, and in the nematic phase, they tend to arrange themselves in a twisted geometry: see Fig. 4 below. Cholesterics, also known as chiral nematics, tend to reflect light in bright colours which are dependent on the temperature of the substance. This makes them suitable for use in thermometers and other temperature sensors.

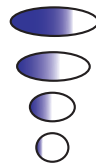


Figure 4: A right handed cholesteric liquid crystal

Cholesterics can have a left or a right handed twist and the director rotates with respect to this twist throughout the sample producing a helix.

1.3.3 Smectics

Smectic liquid crystals still have the same general orientation as nematic liquid crystals but they also align themselves in layers. Within these layers, the liquid crystals move around freely and they tend to align themselves in the same direction within these layers. Smectic A (SmA) molecules line up parallel to the layer normal (on average) in each layer, while smectic C (SmC) line up parallel to one another pointing at an angle θ , usually called the tilt angle, from the layer normal within each layer. The typical structures within SmA and SmC samples are shown below in Fig. 5. The tilt angle of the smectic C phase is temperature

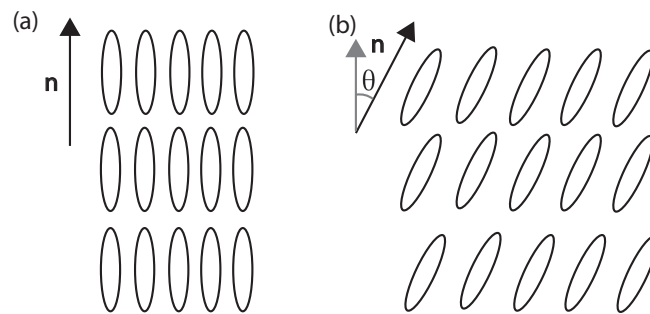


Figure 5: (a) Smectic A liquid crystal. (b) Smectic C liquid crystal

dependent.

One substance which has a smectic phase is terephthalbis-(4n)-butylaniline, also known as TBBA. This substance is in the SmC phase between 144°C and 170°C (at 170°C TBBA becomes SmA). The angle which the director makes with the unit normal of this substance varies from approximately 65° to the SmA phase of 0° over these temperatures [7].

Smectic C liquid crystals have the same tilt angle throughout all of their layers at a certain temperature. If the director is not fixed uniformly in space, but rather rotates around the surface of a fictitious “cone”, as shown below in Fig. 6, then the liquid crystal is chiral smectic C, denoted SmC*. The SmC* phase can occur if the molecules are chiral.

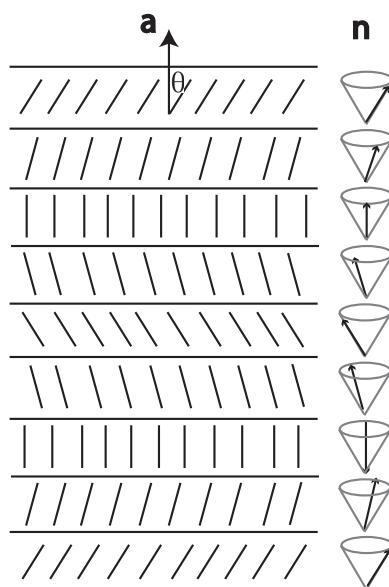


Figure 6: Each layer of SmC* has a slightly different twist angle going from layer to layer so the directors point in a slightly different direction, but are generally uniformly aligned within layers.

1.3.4 Polymorphism

Some liquid crystal materials exhibit more than one mesophase. For example, 4-n-pentylphenyl 4'-n-decyloxythiobenzoate ($\bar{1}O5$) is solid up to 60°C, has a smectic C phase from 60°C to 63°C, a smectic A phase from 63°C to 80°C, then a nematic phase from 80°C to 86°C when it becomes an isotropic liquid.

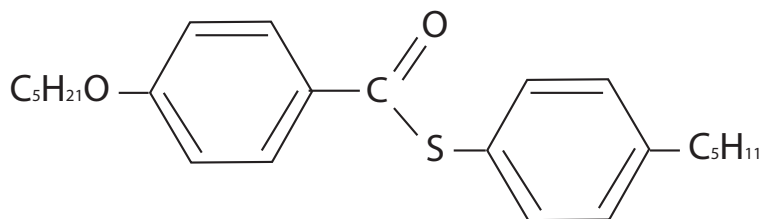


Figure 7: The chemical structure of $\bar{1}O5$

1.4 Outline of thesis

Chapter 2 of this thesis will begin by briefly explaining the basic theory of nematic and smectic liquid crystals which will be used later. It will then go on to explain the basics of the calculus of variations, where a useful inequality is highlighted, before applying these to the equations which arise when considering an azimuthal magnetic field acting upon smectic C liquid crystals in a cylindrical geometry, to consider the stability. This work is then carried on to the next chapter where the same types of equations arise for smectic liquid crystal in a planar layer geometry.

The fluctuation of a thin film of nematic liquid crystal is then discussed as to whether the film wets or dewets. A brief introduction to wetting and dewetting is given at the beginning of Chapter 6. The results of changing some of the simplifications and variables in the problem are looked at as well as the stability of perturbing the Ericksen–Leslie equations for different nematic liquid crystal samples.

The thesis then concludes with some of the methods used in the previous chapters being applied to the problem of a blade approaching a free surface of isotropic liquid. This chapter begins by looking at a parabolic blade approaching the free surface and considering the stability of the deformed surface as the blade approaches from above. The model of the approaching blade is then changed to a circular ended blade. This allows direct comparisons to be drawn between the different models.

2 Liquid Crystal Theory

In this chapter the basic mathematical theories of liquid crystals will be introduced. These theories from [6] cover static and dynamic theory for both nematic and smectic liquid crystals.

The continuum theory for liquid crystals was started by Oseen in 1925 and contributed to by Zöcher, [8] and [9], from 1927 onwards. Oseen derived a static version of the continuum theory for nematics [10] which is the basis for the theories used today. In 1958, significant progress was made by Frank [11] who came up with a more direct approach to the formulation of a static theory for liquid crystals. Ericksen generalised this work in 1961 [12] to incorporate dynamics, culminating in the balance laws for the dynamic behaviour of nematics. Ericksen's work was then developed further by Leslie [13, 14] when the constitutive equations for nematics and anisotropic fluids were derived which led to the celebrated Ericksen-Leslie dynamic theory.

2.1 Notation and terminology

Throughout this thesis the Einstein summation convention is used. That is, wherever there is an index repeated in the same term the term should be summed over all values of the index, e.g.

$$\mathbf{b} \cdot \mathbf{c} = b_i c_i = b_1 c_1 + b_2 c_2 + b_3 c_3,$$

where \mathbf{b} and \mathbf{c} have three components.

The Kronecker delta will also be used within this thesis. The Kronecker delta is

$$\delta_{ij} = \begin{cases} 1 & \text{if } i = j \\ 0 & \text{if } i \neq j. \end{cases} \quad (2.1)$$

Another notation which will be used here is the alternator ϵ_{ijk} . The alterna-

tor is defined to be

$$\epsilon_{ijk} = \begin{cases} 1 & \text{if } i, j \text{ and } k \text{ are unequal and in cyclic order,} \\ -1 & \text{if } i, j \text{ and } k \text{ are unequal and not in cyclic order,} \\ 0 & \text{if any two of } i, j \text{ and } k \text{ are equal.} \end{cases} \quad (2.2)$$

The scalar, vector and scalar triple product will also be used. In cartesian form, the scalar product of two vectors \mathbf{a} and \mathbf{b} is

$$\mathbf{a} \cdot \mathbf{b} = a_i b_i \quad (2.3)$$

and the vector product is defined by

$$\mathbf{a} \times \mathbf{b} = \mathbf{e}_i \epsilon_{ijk} b_j c_k, \quad (2.4)$$

where \mathbf{e}_i is the unit vector in the i direction. The scalar triple product of three vectors \mathbf{a} , \mathbf{b} and \mathbf{c} is defined by

$$\mathbf{a} \cdot (\mathbf{b} \times \mathbf{c}) = a_i \epsilon_{ijk} b_j c_k. \quad (2.5)$$

2.1.1 Director

The director of a liquid crystal is described by a unit vector which indicates the general direction in which the molecules are aligned. This is found by taking the average directions of all the molecules within the sample. The unit vector for nematics can be parametrised as

$$\mathbf{n} = (\cos \theta \cos \phi, \cos \theta \sin \phi, \sin \theta) \quad (2.6)$$

where θ and ϕ are as shown below in Fig. 8.

There are two choices for the direction of the director in every sample, up or down, left or right etc., but these directions are equivalent. Also, the director can point in any direction at all of its own accord, but it can be made to point in a specific direction using anchoring (see Section 2.3). The director in a liquid crystal sample is influenced by electric fields, magnetic fields and the presence of a solid boundary. This will be discussed later.

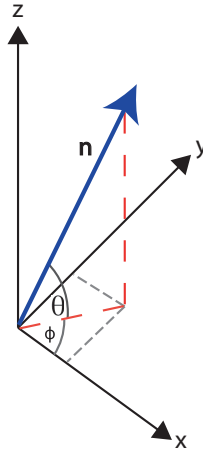


Figure 8: Parametrisation of the director in terms of the two angles θ and ϕ .

2.2 Nematic theory

2.2.1 Frank–Oseen elastic energy

The structure of liquid crystals is elastic. A sample can be distorted by external forces but once those forces have been removed the sample returns to its original undistorted state. For example, flow within a sample will cause elastic distortions, as can squeezing a sample. These distortions cause the director of the liquid crystal to change throughout the whole sample. These distortions can be described in terms of the Frank elastic constants [15, 11]. It is assumed that the liquid crystal sample is incompressible so the mass density of the sample remains constant.

The Frank elastic constants are K_1 , K_2 , K_3 and K_4 . The K_1 constant is a measure of how splayed the director structure if a sample of liquid crystal is, K_2 is a measure of how twisted it is and K_3 tells how bent it is while $K_2 + K_4$ is the saddle-splay constant. Fig. 9 shows graphical representations of the deformations pertaining to K_i with $i = 1, 2, 3$.

The Frank-Oseen elastic energy, also known as the free energy density, for

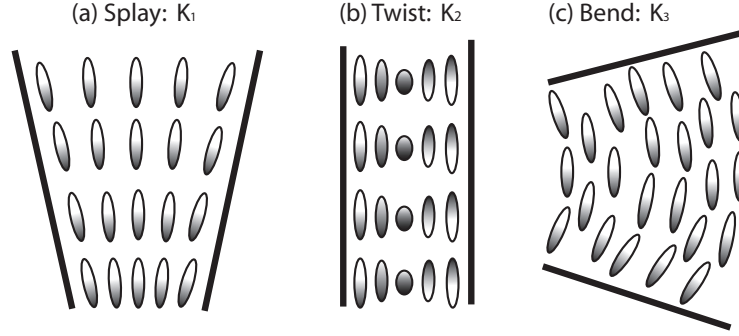


Figure 9: The elastic constants

non-cholesteric nematics is given by

$$\begin{aligned}
 w_{elast} &= \frac{1}{2} (K_1 (\nabla \cdot \mathbf{n})^2 + K_2 (\mathbf{n} \cdot \nabla \times \mathbf{n})^2 + \\
 &\quad K_3 (\mathbf{n} \times \nabla \times \mathbf{n})^2 + (K_2 + K_4) \nabla \cdot [(\mathbf{n} \cdot \nabla) \mathbf{n} - (\nabla \cdot \mathbf{n}) \mathbf{n}]) \quad (2.7) \\
 &= \frac{1}{2} ((K_1 - K_2 - K_4) (n_{i,i})^2 + K_2 n_{i,j} n_{i,j} \\
 &\quad + K_4 n_{i,j} n_{j,i} + (K_3 - K_2) n_j n_{i,j} n_k n_{i,k}) , \quad (2.8)
 \end{aligned}$$

from [6]. The saddle-splay term, $K_2 + K_4$, is often ignored as it does not contribute to the bulk energy equations when there is strong anchoring. A full derivation of this can be found in [6].

From (2.8), the Frank elastic constants must satisfy the following Ericksen inequalities [11]:

$$\begin{aligned}
 K_1 &\geq 0, & K_2 &\geq 0, & K_3 &\geq 0 \\
 K_2 &\geq |K_4| & 2K_1 &\geq K_2 + K_4 & \geq 0, & \quad (2.9)
 \end{aligned}$$

since the elastic energy must be non-negative.

2.2.1.1 One-constant approximation

Sometimes, for example when the relative values of the K_i are unknown or when the resulting equilibrium equations are complicated, the one-constant approxi-

mation is made. This means that the Frank constants are set to be

$$K_1 = K_2 = K_3 \equiv K \quad \text{and} \quad K_4 = 0. \quad (2.10)$$

This allows the free energy to be simplified to become

$$w_F = \frac{1}{2}K \|\nabla \mathbf{n}\|^2 \quad (2.11)$$

$$= \frac{1}{2}K n_{i,j} n_{i,j}. \quad (2.12)$$

2.2.2 Magnetic and electric fields

It has been common practice from early research in liquid crystals to apply a magnetic field to align samples of nematic or cholesteric liquid crystals. The alignment so produced encourages the director to be parallel to the field for the majority of nematics and perpendicular to the field in many cholesterics. Similar effects can be produced by an electric field. These electric and magnetic fields have corresponding energies in liquid crystals.

The magnetic energy density that will be used in Ch. 4 will be [6, p. 30]

$$w_{mag} = -\frac{1}{2} \frac{\Delta\chi}{\mu_0} (\mathbf{n} \cdot \mathbf{B})^2, \quad (2.13)$$

where $\Delta\chi$ is the magnetic anisotropy, μ_0 is the permeability of free space, \mathbf{n} is the director and \mathbf{B} is the magnetic induction.

The electric potential is very similar in form to the magnetic potential. The electric energy density which is normally used is [15, p. 134]

$$w_{elec} = -\frac{1}{2} \varepsilon_0 \varepsilon_a (\mathbf{n} \cdot \mathbf{E})^2, \quad (2.14)$$

where ε_0 is the permittivity of free space, ε_a is the dielectric anisotropy, \mathbf{n} is the director as before and \mathbf{E} is the electric field. The sign of ε_a signals whether the director wants to orient parallel or perpendicular to the electric field, see Fig. 10. When $\varepsilon_a > 0$ the director wants to align itself parallel to the electric field \mathbf{E} and when $\varepsilon_a < 0$ it aligns perpendicular to the field.

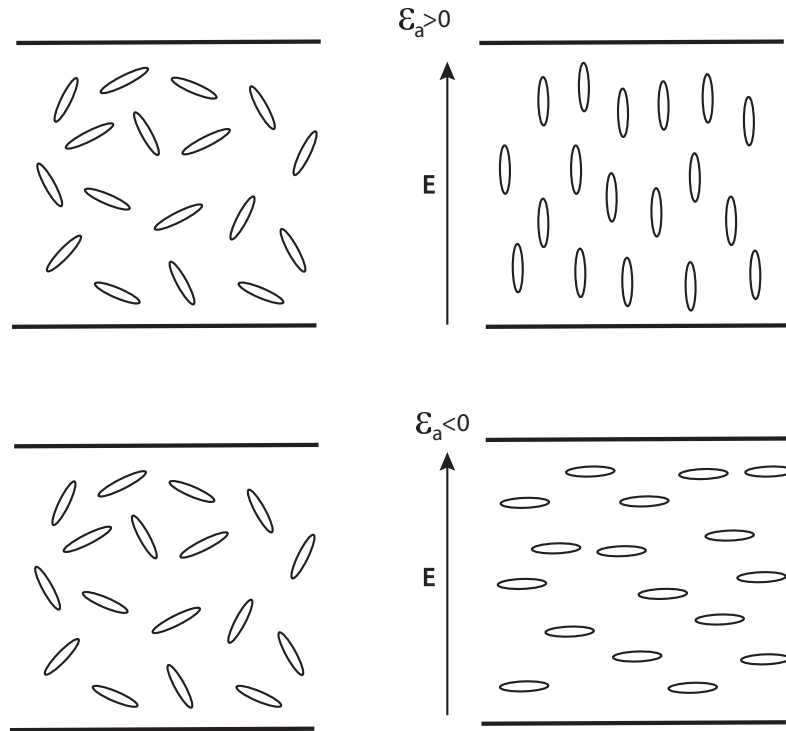


Figure 10: The sign of ε_a determines how the director aligns.

2.2.3 Bulk energy

The bulk energy density is defined as the sum of the elastic energy and the magnetic (or electric) density such that

$$w_F = w_{elast} + w_{mag}. \quad (2.15)$$

It is clear from this that in the absence of an electric or magnetic field the bulk energy reduces to the elastic energy given by (2.12).

2.2.4 Ericksen–Leslie dynamic equations

The Ericksen–Leslie dynamic equations for nematic liquid crystals are derived from the balances of linear and angular momentum and mass conservation [6]. There are two equations, one for linear momentum and one for angular momen-

tum. The linear momentum equation is

$$\rho \dot{v}_i = \rho F_i - (p + w_F)_{,i} + \tilde{g}_j n_{j,i} + G_j n_{j,i} + \tilde{t}_{ij,j}, \quad (2.16)$$

where ρ is the density of the liquid crystal, \dot{v}_i is the material time derivative of the component of the velocity in the i direction, F_i is the external body force per unit mass, p is the pressure, w_F is the bulk energy density for nematic liquid crystals given by (2.8), G_j is the generalised body force, n_j is the component of the director in the j direction and the vector \tilde{g}_j and \tilde{t}_{ij} , the dynamic stress terms, are given by

$$\begin{aligned} \tilde{t}_{ij} = & \alpha_1 n_k A_{kp} n_p n_i n_j + \alpha_2 N_i n_j + \alpha_3 n_i N_j \\ & + \alpha_4 A_{ij} + \alpha_5 n_j A_{ik} n_k + \alpha_6 n_i A_{jk} n_k \end{aligned} \quad (2.17)$$

$$\tilde{g}_i = -\gamma_1 N_i - \gamma_2 A_{ip} n_p \quad (2.18)$$

with

$$\gamma_1 = \alpha_3 - \alpha_2 \geq 0 \quad (2.19)$$

$$\gamma_2 = \alpha_3 + \alpha_2 \quad (2.20)$$

$$A_{ij} = \frac{1}{2} (v_{i,j} + v_{j,i}) \quad (2.21)$$

$$N_i = \dot{n}_i - W_{ij} n_j \quad (2.22)$$

$$W_{ij} = \frac{1}{2} (v_{i,j} - v_{j,i}), \quad (2.23)$$

where α_i are the Leslie viscosities, v_i is the component of the velocity in the i direction and \dot{n}_i is the material time derivative of the director.

The angular momentum equation is

$$\left(\frac{\partial w_F}{\partial n_{i,j}} \right)_{,j} - \frac{\partial w_F}{\partial n_i} + \tilde{g}_i + G_i = \lambda n_i \quad (2.24)$$

where λ is a Lagrange multiplier coming from the $\mathbf{n} \cdot \mathbf{n} = 1$ condition which can be determined by multiplying (2.24) with n_i and summing over i .

The Parodi relation is [16], based upon Onsager relations,

$$\alpha_3 + \alpha_2 = \alpha_6 - \alpha_5. \quad (2.25)$$

When this relation holds, then the viscous dissipation function is given by [6, p. 147]

$$\begin{aligned} \mathcal{D} = & \alpha_1 (n_i A_{ij} n_j)^2 + 2\gamma_2 N_i A_{ij} n_j + \alpha_4 A_{ij} A_{ij} \\ & + (\alpha_5 + \alpha_6) n_i A_{ij} A_{jk} n_k + \gamma_1 N_i N_i \geq 0, \end{aligned} \quad (2.26)$$

by standard thermodynamic assumptions.

2.2.5 Leslie and Miesowicz viscosities

It is well known that the six Leslie viscosities must satisfy the following inequalities for (2.26) to hold [6, p. 146]:

$$\gamma_1 = \alpha_3 - \alpha_2 \geq 0, \quad (2.27)$$

$$\alpha_4 \geq 0, \quad (2.28)$$

$$2\alpha_4 + \alpha_5 + \alpha_6 \geq 0, \quad (2.29)$$

$$2\alpha_1 + 3\alpha_4 + 2\alpha_5 + 2\alpha_6 \geq 0, \quad (2.30)$$

$$4\gamma_1(2\alpha_4 + \alpha_5 + \alpha_6) \geq (\alpha_2 + \alpha_3 + \gamma_2)^2. \quad (2.31)$$

It is not trivial to measure the Leslie viscosities individually but they are measurable in combinations, known as the Miesowicz viscosities η_i . The viscosities η_1 , η_2 and η_3 are shear viscosities, γ_1 is the director rotational viscosity and η_{12} is important when the director is not aligned with an axis.

The viscosity η_1 can be measured by having a shear flow, with the flow velocity \mathbf{v} parallel to the director, \mathbf{n} , η_2 can be measured by considering a flow where \mathbf{n} is parallel to $\nabla\mathbf{v}$, the gradient of the velocity, and η_3 can be found by considering a flow where \mathbf{n} is orthogonal to both \mathbf{v} and $\nabla\mathbf{v}$ [17].

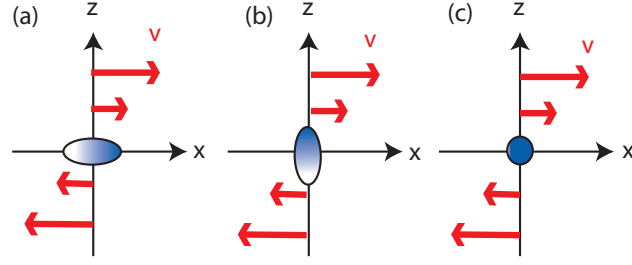


Figure 11: These are the Miesowicz viscosities where a) is η_1 where the director is parallel to the velocity, b) is η_2 where the director is parallel to the gradient of the velocity and c) is η_3 where the director is orthogonal to the velocity and the gradient of the velocity.

In terms of the Leslie viscosities, the Miesowicz viscosities are

$$\eta_1 = \frac{1}{2}(\alpha_3 + \alpha_4 + \alpha_6) = \frac{1}{2}(\alpha_2 + 2\alpha_3 + \alpha_4 + \alpha_5), \quad (2.32)$$

$$\eta_2 = \frac{1}{2}(-\alpha_2 + \alpha_4 + \alpha_5), \quad (2.33)$$

$$\eta_3 = \frac{1}{2}\alpha_4, \quad (2.34)$$

$$\eta_{12} = \alpha_1, \quad (2.35)$$

$$\gamma_1 = \alpha_3 - \alpha_2, \quad (2.36)$$

$$\gamma_2 = \alpha_6 - \alpha_5 = \alpha_3 + \alpha_2. \quad (2.37)$$

The Miesowicz viscosities can be measured by experiments and the values of the α_i can be found via the relationships given by

$$\alpha_1 = \eta_{12}, \quad (2.38)$$

$$\alpha_2 = \frac{1}{2}(\eta_1 - \eta_2 - \gamma_1), \quad (2.39)$$

$$\alpha_3 = \frac{1}{2}(\eta_1 - \eta_2 + \gamma_1), \quad (2.40)$$

$$\alpha_4 = 2\eta_3, \quad (2.41)$$

$$\alpha_5 = \frac{1}{2}(\eta_1 + 3\eta_2 - 4\eta_3 - \gamma_1), \quad (2.42)$$

$$\alpha_6 = \frac{1}{2}(3\eta_1 + \eta_2 - 4\eta_3 - \gamma_1), \quad (2.43)$$

which can be written in terms of the splay, twist and bend viscosities:

$$\eta_{splay} = \gamma_1 - \frac{(\eta_1 - \eta_2 + \gamma_1)^2}{4\eta_1} = \gamma_1 - \frac{\alpha_3^2}{\eta_1}, \quad (2.44)$$

$$\eta_{twist} = \gamma_1 = \alpha_3 - \alpha_2, \quad (2.45)$$

$$\eta_{bend} = \gamma_1 - \frac{(\eta_1 - \eta_2 - \gamma_1)^2}{4\eta_2} = \gamma_1 - \frac{\alpha_2^2}{\eta_2}. \quad (2.46)$$

The twist viscosity determines the relaxation rate of the director, and γ_2 characterises the contribution of torque due to a shear velocity gradient.

2.2.6 Equilibrium equations for nematics

The equilibrium equations which describe the linear and angular momentum balance of a liquid crystal are

$$\left(\frac{\partial w_F}{\partial n_{i,j}} \right)_{,j} - \frac{\partial w_F}{\partial n_i} + G_i = -\lambda n_i, \quad (2.47)$$

$$t_{ij,j} + \rho F_i = 0, \quad (2.48)$$

where w_F is the total energy, n_i is the component of the director \mathbf{n} in the i direction, G is the generalised body force, λ is a Lagrange multiplier, ρ is the density, F is the body force per unit volume and the stress tensor t_{ij} is given by

$$t_{ij} = -\frac{\partial w_F}{\partial n_{k,j}} n_{k,i} - p \delta_{ij} \quad (2.49)$$

where p is an arbitrary pressure coming from the assumed incompressibility of nematic liquid crystals.

A full derivation of these equations and relations can be found in [6].

2.2.7 Reformulated Ericksen–Leslie equations

If the director is represented in the form

$$\mathbf{n} = \mathbf{f}(\theta_1, \theta_2) \quad \text{where} \quad \mathbf{f} \cdot \mathbf{f} = 1 \quad (2.50)$$

and

$$w_F = \hat{w}_F(\theta_\alpha, \theta_{\alpha,i}) \quad \alpha, i = 1, 2 \quad (2.51)$$

then the Ericksen–Leslie equations can be formulated in a more convenient way. Here, θ_1 and θ_2 can be functions of space and time and an example of a possible director which satisfies this is

$$\mathbf{n} = (\cos \theta_1(x, z, t) \cos \theta_2(x, z, t), \cos \theta_1(x, z, t) \sin \theta_2(x, z, t), \sin \theta_1(x, z, t)) . \quad (2.52)$$

When the Parodi relation applies then the dissipation function is linked to the \tilde{g}_i and \tilde{t}_{ij} by the properties

$$\tilde{g}_i = -\frac{1}{2} \frac{\partial \mathcal{D}}{\partial \dot{n}_i} \quad (2.53)$$

and

$$\tilde{t}_{ij} = \frac{1}{2} \frac{\partial \mathcal{D}}{\partial v_{i,j}} . \quad (2.54)$$

If the potential, Ψ given by

$$\rho F_i = \frac{\partial \Psi}{\partial x_i}, \quad G_i = \frac{\partial \Psi}{\partial n_i} \quad (2.55)$$

can be reformulated such that

$$\Psi(n_i, x_i) = \hat{\Psi}(\theta_\alpha, x_i), \quad i = 1, 2, 3, \quad \alpha = 1, 2 \quad (2.56)$$

and the dissipation can be reformulated such that

$$\mathcal{D}(A_{ij}, N_i, n_i) = 2\hat{\mathcal{D}}(v_{i,j}, \dot{\theta}_\alpha, \theta_\alpha), \quad i = 1, 2, 3, \quad \alpha = 1, 2 \quad (2.57)$$

and the chain rule

$$\dot{n}_k = \frac{\partial f_k}{\partial \theta_\alpha} \dot{\theta}_\alpha \quad (2.58)$$

is used, eqs. (2.53) and (2.54) can be combined to give the result

$$\begin{aligned} \frac{\partial \hat{\mathcal{D}}}{\partial \dot{\theta}_\alpha} &= \frac{1}{2} \frac{\partial \mathcal{D}}{\partial \dot{n}_k} \frac{\partial \dot{n}_k}{\partial \dot{\theta}_\alpha} \\ &= -\tilde{g}_k \frac{\partial f_k}{\partial \theta_\alpha} . \end{aligned} \quad (2.59)$$

Using this result, along with

$$n_{i,j} = \frac{\partial f_i}{\partial \theta_\alpha} \theta_{\alpha,j}, \quad (2.60)$$

the equation

$$\tilde{g}_j n_{j,i} = \tilde{g}_j \frac{\partial f_j}{\partial \theta_\alpha} \theta_{\alpha,i}$$

becomes

$$\tilde{g}_j n_{j,i} = - \frac{\partial \hat{\mathcal{D}}}{\partial \theta_\alpha} \theta_{\alpha,i}. \quad (2.61)$$

The G_i term can be expressed as

$$G_i = \frac{\partial \Psi}{\partial n_i}. \quad (2.62)$$

If this is used along with (2.56) then

$$\begin{aligned} \frac{\partial \hat{\Psi}}{\partial \theta_\alpha} &= \frac{\partial \Psi}{\partial n_i} \frac{\partial f_i}{\partial \theta_\alpha} \\ &= G_i \frac{\partial f_i}{\partial \theta_\alpha}. \end{aligned} \quad (2.63)$$

Using eqs. (2.61) and (2.63) along with

$$\left(\frac{\partial \hat{w}}{\partial \theta_{\alpha_i}} \right)_{,i} - \frac{\partial \hat{w}}{\partial \theta_\alpha} = \left[\left(\frac{\partial w}{\partial n_{k,i}} \right)_{,i} - \frac{\partial w}{\partial n_k} \right] \frac{\partial f_k}{\partial \theta_\alpha}, \quad (2.64)$$

which arises from the bulk equilibrium equations, the following equation is obtained,

$$\left(\frac{\partial \hat{w}_F}{\partial \theta_{\alpha_i}} \right)_{,i} - \frac{\partial \hat{w}_F}{\partial \theta_\alpha} - \frac{\partial \hat{\mathcal{D}}}{\partial \theta_\alpha} + \frac{\partial \hat{\Psi}}{\partial \theta_\alpha} = \left[\left(\frac{\partial w_F}{\partial n_{k,i}} \right)_{,i} - \frac{\partial w_F}{\partial n_k} + \tilde{g}_k + G_k \right] \frac{\partial f_k}{\partial \theta_\alpha}, \quad (2.65)$$

and so by

$$n_i \frac{\partial f_i}{\partial \theta_\alpha} = 0 \quad (2.66)$$

and by eq. (2.24), the reformulated angular momentum equation is given by

$$\left(\frac{\partial \hat{w}_F}{\partial \theta_{\alpha_i}} \right)_{,i} - \frac{\partial \hat{w}_F}{\partial \theta_\alpha} - \frac{\partial \hat{\mathcal{D}}}{\partial \theta_\alpha} + \frac{\partial \hat{\Psi}}{\partial \theta_\alpha} = 0 \quad \alpha = 1, 2. \quad (2.67)$$

The linear momentum equation is given by

$$\rho \dot{v}_i = \left(\frac{\partial \hat{\mathcal{D}}}{\partial v_{i,j}} \right)_{,j} - \frac{\partial \hat{\mathcal{D}}}{\partial \theta_\alpha} \theta_{\alpha,i} - \tilde{p}_{,i} \quad i = 1, 2, 3 \quad (2.68)$$

where

$$\tilde{p} = p + \hat{w}_F - \hat{\Psi} \quad (2.69)$$

which is found by combining eqs. (2.54), (2.57) and (2.61).

2.3 Anchoring conditions

The energy equations can be modified to account for a surface energy which depends on the alignment of the director at boundaries or interfaces. This can be done by including a surface energy term in the free energy. The description of the alignment of the director there is called anchoring.

There are three different types of anchoring which can be applied to a sample of liquid crystal so that the director points in a certain direction. These are strong, conical and weak anchoring.

2.3.1 Strong anchoring

At the boundary with a solid substrate a liquid crystal can be fixed such that the director points in a certain direction and only that direction. This is called strong anchoring. This can be achieved by rubbing the boundary in one direction so that the liquid crystal wants to lie in that direction. Strong anchoring does not require any additional terms in the free energy.

If the sample is between two solid boundaries and is aligned so that the director lies along the boundaries then the director is said to have homogeneous alignment and if the director is perpendicular to the boundaries then the alignment is said to be homeotropic.

2.3.2 Conical anchoring

Conical anchoring is where the director \mathbf{n} makes an angle ψ with the tangent plane of the boundary. This means that the director has a cone of preferred directions as shown in Fig. 12. The director at the surface satisfies the constraint

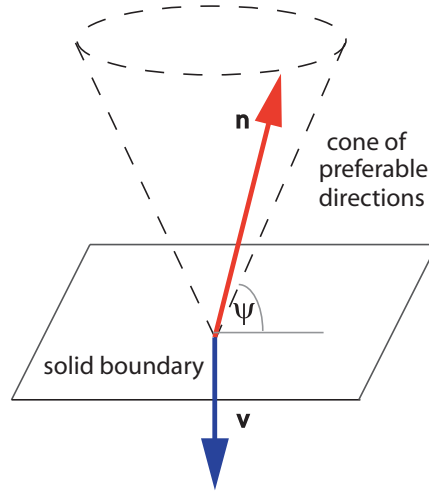


Figure 12: The liquid crystal has a cone of preferable directions where the director makes an angle ψ with the tangent plane of the boundary.

$$(\mathbf{n} \cdot \boldsymbol{\nu})^2 = \sin^2 \psi \quad (2.70)$$

where $\boldsymbol{\nu}$ is the outward unit normal of the boundary. It is usually assumed that $0 < \psi < \frac{\pi}{2}$. If $\psi = \frac{\pi}{2}$ then the conical anchoring becomes strong homeotropic anchoring. Conical anchoring does not require any additional terms in the free energy as the restriction can be applied as a boundary condition.

2.3.3 Weak anchoring

Weak anchoring occurs if the director has some freedom with the angle it makes at the boundary. This means that the angle between the director and the boundary or surface interface can vary under the influence of forces such as electric or magnetic fields. An additional surface energy is needed. The Rapini and

Papoular [18] surface energy density is the simplest such energy. This is

$$w_s = \frac{1}{2}\tau_0 (1 + \omega(\mathbf{n} \cdot \boldsymbol{\nu})^2) , \quad (2.71)$$

where $\tau_0 > 0$, $\omega > -1$ and $\boldsymbol{\nu}$ is the outward unit normal to the boundary or interface as it was for conical anchoring. When $-1 < \omega < 0$, the director will prefer to align itself parallel to $\boldsymbol{\nu}$ so the favoured orientation of \mathbf{n} is homeotropic since this will minimise the energy w_s . If $\omega > 0$, the energy will be minimised when \mathbf{n} is orthogonal to $\boldsymbol{\nu}$ so the preferred orientation will be homogeneous.

The total energy for a sample Ω with surface S and with weak anchoring is now given by

$$W = \int_{\Omega} w_F d\Omega + \int_S w_s dS , \quad (2.72)$$

where w_F is the bulk energy. In general, this leads to two coupled equilibrium equations and boundary conditions, one in the bulk and one on the surface.

2.4 Smectic theory

The smectic theory for liquid crystals was developed in the early 1990s by Leslie, Stewart and Nakagawa [19] and many of the results are analogous to those for nematics, but with some clear smectic properties. Throughout this section it is assumed that the smectic C liquid crystal is not chiral.

For smectic liquid crystals, the director is described by

$$\mathbf{n} = \mathbf{a} \cos \theta + \mathbf{c} \sin \theta \quad (2.73)$$

where \mathbf{a} is a unit vector defining the layer normal, and \mathbf{c} is the unit orthogonal projection of \mathbf{n} onto the smectic plane and θ . The layer normal \mathbf{n} is shown below in Fig. 13. The vectors \mathbf{a} and \mathbf{c} are subject to the constraints

$$\mathbf{a} \cdot \mathbf{a} = \mathbf{1} , \quad \mathbf{c} \cdot \mathbf{c} = \mathbf{1} , \quad \mathbf{a} \cdot \mathbf{c} = \mathbf{0} , \quad \nabla \times \mathbf{a} = \mathbf{0} , \quad (2.74)$$

this latter constraint being due to Oseen [20].

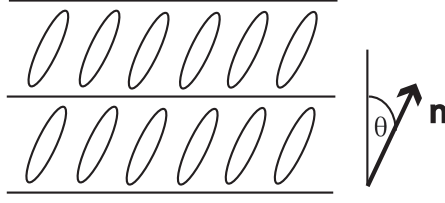


Figure 13: The angle θ is the angle which the director makes with the layer normal.

2.4.1 Static smectic theory

This smectic energy is conveniently expressed in vector form in terms of \mathbf{b} and \mathbf{c} [21] where

$$\mathbf{b} = \mathbf{a} \times \mathbf{c}. \quad (2.75)$$

The energy can then be expressed as

$$\begin{aligned} w = & \frac{1}{2}A_{12}(\mathbf{b} \cdot \nabla \times \mathbf{c})^2 + \frac{1}{2}A_{21}(\mathbf{c} \cdot \nabla \times \mathbf{b})^2 + A_{11}(\mathbf{b} \cdot \nabla \times \mathbf{c})(\mathbf{c} \cdot \nabla \times \mathbf{b}) \\ & + \frac{1}{2}B_1(\nabla \cdot \mathbf{b})^2 + \frac{1}{2}B_2(\nabla \cdot \mathbf{c})^2 + \frac{1}{2}B_3 \left[\frac{1}{2}(\mathbf{b} \cdot \nabla \times \mathbf{b} + \mathbf{c} \cdot \nabla \times \mathbf{c}) \right]^2 \\ & + B_{13}(\nabla \cdot \mathbf{b}) \left[\frac{1}{2}(\mathbf{b} \cdot \nabla \times \mathbf{b} + \mathbf{c} \cdot \nabla \times \mathbf{c}) \right] \\ & + C_1(\nabla \cdot \mathbf{c})(\mathbf{b} \cdot \nabla \times \mathbf{c}) + C_2(\nabla \cdot \mathbf{c})(\mathbf{c} \cdot \nabla \times \mathbf{b}). \end{aligned} \quad (2.76)$$

The smectic elastic constants above are related to the distortions of the smectic layers. The constants A_{11} , A_{12} and A_{21} are related to the bending of the smectic layers and B_1 , B_2 , B_3 and B_{13} are related to the reorientation of the c -director within or across layers. The two remaining constants, C_1 and C_2 , are related to couplings of these deformations.

Fig. 14 shows the five basic distortions for a sample of smectic C liquid crystal. The bold lines in parallel to the layers represent the c -director. Fig. 14 a) shows the layer with no distortions, b) shows the plane bent such that the layer normal changes along the direction of the c -director. If the layer is bent so that the layer normal changes perpendicular to the c -director then Fig. 14 c) would result. The cases where the smectic layer is not bent but the c -director

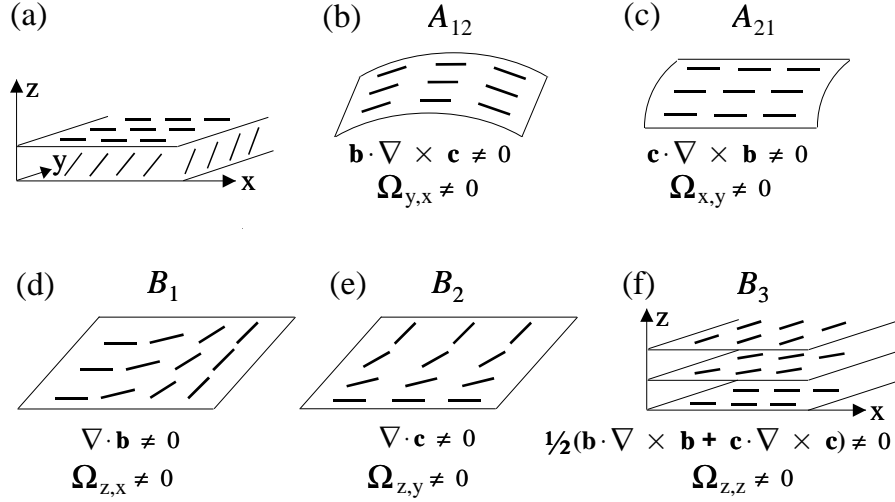


Figure 14: This diagram shows the five basic distortions where Ω is an arbitrary small rotation of the smectic layers. Each distortion is related to an elastic constant.

rotates parallel or perpendicular to the original alignment of the c -director is shown in Fig. 14 d) and e) respectively. The final distortion shown in Fig. 14 f) relates to the c -director remaining constant within each layer but rotating along the layer normal.

From [21], the smectic elastic constants must satisfy the following inequalities.

$$A_{12}, A_{21}, B_1, B_2, B_3 \geq 0, \quad (2.77)$$

$$A_{12}A_{21} - A_{11}^2 \geq 0, \quad (2.78)$$

$$B_1B_3 - B_{13}^2 \geq 0, \quad (2.79)$$

$$B_2A_{12} - C_1^2 \geq 0, \quad (2.80)$$

$$B_2A_{21} - C_2^2 \geq 0. \quad (2.81)$$

Inequality (2.78) implies that if A_{12} or A_{21} equals 0 then A_{11} must also be 0. Similarly, if B_1 or B_3 is 0 then $B_{13} = 0$; if B_2 or A_{12} equals 0 then $C_1 = 0$; if $B_2 = 0$ or $A_{21} = 0$ then $C_2 = 0$. More inequalities can be derived from the ones above. For more details see [6].

The energy density for SmC was given an alternative form by Leslie, Stewart, Carlsson and Nakagawa [22] to be, ignoring surface contributions,

$$\begin{aligned}
w &= \frac{1}{2}K_1(\nabla \cdot \mathbf{a})^2 + \frac{1}{2}K_2(\nabla \cdot \mathbf{c})^2 + \frac{1}{2}K_3(\mathbf{a} \cdot \nabla \times \mathbf{c})^2 + \frac{1}{2}K_4(\mathbf{c} \cdot \nabla \times \mathbf{c})^2 \\
&\quad + \frac{1}{2}K_5(\mathbf{b} \cdot \nabla \times \mathbf{c})^2 + K_6(\nabla \cdot \mathbf{a})(\mathbf{b} \cdot \nabla \times \mathbf{c}) + K_7(\mathbf{a} \cdot \nabla \times \mathbf{c})(\mathbf{c} \cdot \nabla \times \mathbf{c}) \\
&\quad + K_8(\nabla \cdot \mathbf{c})(\mathbf{b} \cdot \nabla \times \mathbf{c}) + K_9(\nabla \cdot \mathbf{a})(\nabla \cdot \mathbf{c})
\end{aligned} \tag{2.82}$$

$$\begin{aligned}
&= \frac{1}{2}K_1(a_{i,i})^2 + \frac{1}{2}(K_2 - K_4)(c_{i,i})^2 + \frac{1}{2}(K_3 - K_4)c_{i,j}c_jc_{i,k}c_k \\
&\quad + \frac{1}{2}K_4c_{i,j}c_{i,j} + \frac{1}{2}(K_5 - K_3)(c_{i,j}c_j)^2 + K_6a_{i,i}(c_ja_{j,k}c_k) \\
&\quad - K_7c_{i,j}c_jc_{i,k}a_k + (K_8 - K_7)c_{i,i}(c_ja_{j,k}c_k) + K_9a_{i,i}c_{j,j}
\end{aligned} \tag{2.83}$$

where \mathbf{b} represents the vector given by

$$\mathbf{b} = \mathbf{a} \times \mathbf{c} \tag{2.84}$$

and K_i are smectic elastic constants. The smectic elastic constants are given by

$$K_1 = A_{21} \tag{2.85}$$

$$K_2 = B_2 \tag{2.86}$$

$$K_3 = B_1 \tag{2.87}$$

$$K_4 = B_3 \tag{2.88}$$

$$K_5 = 2A_{11} + A_{12} + A_{21} + B_3 \tag{2.89}$$

$$K_6 = -\left(A_{11} + A_{21} + \frac{1}{2}B_3\right) \tag{2.90}$$

$$K_7 = -B_{13} \tag{2.91}$$

$$K_8 = C_1 + C_2 - B_{13} \tag{2.92}$$

$$K_9 = -C_2. \tag{2.93}$$

where these A_{ij} , B_i and C_i are constants. We note for completeness that the Orsay group had the same notation except for A_{11} and C_1 which are [23]

$$A_{11} = -\frac{1}{2}A_{11}^{Orsay} \quad \text{and} \quad C_1 = -C_1^{Orsay}. \tag{2.94}$$

2.4.2 The magnetic and electric energies

Often it is assumed that the magnetic and electric energy densities for smectic C liquid crystals are the same as the nematic ones given by (2.13) and (2.14) respectively.

2.4.3 Equilibrium Equations

There are three sets of equilibrium equations for smectic C liquid crystals.

The balance of forces is given by

$$t_{ij,j} + F_i = 0 \quad (2.95)$$

where t_{ij} is the stress tensor given by

$$t_{ij} = -p\delta_{ij} + \beta_p \epsilon_{pjk} a_{k,i} - \frac{\partial w}{\partial a_{k,j}} a_{k,i} - \frac{\partial w}{\partial c_{k,j}} c_{k,i} \quad (2.96)$$

and F_i is the external body force, p is the pressure and β_p is a Lagrange multiplier that arises from the $\nabla \times \mathbf{a} = \mathbf{0}$ constraint from (2.74).

The two equations

$$\Pi_i^a + G_i^a + \gamma a_i + \mu c_i + \epsilon_{ijk} \beta_{k,j} = 0 \quad (2.97)$$

$$\Pi_i^c + G_i^c + \tau c_i + \mu a_i = 0, \quad (2.98)$$

where

$$\Pi_i^a = \left(\frac{\partial w}{\partial a_{i,j}} \right)_{,j} - \frac{\partial w}{\partial a_i} \quad (2.99)$$

$$\Pi_i^c = \left(\frac{\partial w}{\partial c_{i,j}} \right)_{,j} - \frac{\partial w}{\partial c_i}, \quad (2.100)$$

are equivalent to a balance of moments. Here, γ , μ and τ are the Lagrange multipliers which arise from the first three constraints in (2.74).

It is useful to note the vector form of $\mathbf{\Pi}^c$ from [6] as this will be used later:

$$\begin{aligned}
\mathbf{\Pi}^c = & K_2 \nabla(\nabla \cdot \mathbf{c}) - K_3 \nabla \times \{(\mathbf{a} \cdot \nabla \times \mathbf{c})\mathbf{a}\} \\
& - K_4 [\nabla \times \{(\mathbf{c} \cdot \nabla \times \mathbf{c})\mathbf{c}\} + (\mathbf{c} \cdot \nabla \times \mathbf{c})(\nabla \times \mathbf{c})] \\
& + K_5 [(\mathbf{b} \cdot \nabla \times \mathbf{c})(\mathbf{a} \times \nabla \times \mathbf{c}) - \nabla \times \{(\mathbf{b} \cdot \nabla \times \mathbf{c})\mathbf{b}\}] \\
& + K_6 [(\nabla \cdot \mathbf{a})(\mathbf{a} \times \nabla \times \mathbf{c}) - \nabla \times \{(\nabla \cdot \mathbf{a})\mathbf{b}\}] \\
& - K_7 [\nabla \times \{(\mathbf{a} \cdot \nabla \times \mathbf{c})\mathbf{c} + (\mathbf{c} \cdot \nabla \times \mathbf{c})\mathbf{a}\} + (\mathbf{a} \cdot \nabla \times \mathbf{c})(\nabla \times \mathbf{c})] \\
& + K_8 [\nabla(\mathbf{b} \cdot \nabla \times \mathbf{c}) - \nabla \times \{(\nabla \cdot \mathbf{c})\mathbf{b}\} + (\nabla \cdot \mathbf{c})(\mathbf{a} \times \nabla \times \mathbf{c})] \\
& + K_9 \nabla(\nabla \cdot \mathbf{a}) + \frac{\Delta\chi}{\mu_0} \sin \theta \{(\mathbf{a} \cdot \mathbf{B}) \cos \theta + (\mathbf{c} \cdot \mathbf{B}) \sin \theta\} \mathbf{B}, \quad (2.101)
\end{aligned}$$

where \mathbf{B} is the magnetic field. There is a similar formulation for the $\mathbf{\Pi}^a$ term but it is not used within this thesis. For details, see [6].

2.4.4 Dynamic smectic theory

The governing dynamic equations for smectic C liquid crystals are

$$\rho \dot{v}_i = \rho F_i - \tilde{p}_{,i} + G_k^a a_{k,i} + G_k^c c_{k,i} + \tilde{g}_k^a a_{k,i} + \tilde{g}_k^c c_{k,i} + \tilde{t}_{ij,j} \quad (2.102)$$

where

$$\tilde{p} = p + w \quad (2.103)$$

and

$$\Pi_i^a + G_i^a + \tilde{g}_i^a + \gamma a_i + \mu c_i + \epsilon_{ijk} \beta_{k,j} = 0 \quad (2.104)$$

$$\Pi_i^c + G_i^c + \tilde{g}_i^c + \tau c_i + \mu a_i = 0, \quad (2.105)$$

with γ , μ , τ and β as Lagrange multipliers. F_i is the external body force per unit mass, \tilde{t}_{ij} is the dynamic stress, G_i^a and G_i^c are the generalised body forces per unit volume related to \mathbf{a} and \mathbf{c} respectively, p is the pressure and w within

Π_i^a and Π_i^c is the elastic energy for smectic C liquid crystals and

$$\begin{aligned} \tilde{g}_i^a &= -2 \left(\lambda_1 D_i^a + \lambda_3 c_i c_p D_p^a + \lambda_4 A_i + \lambda_6 c_i c_p A_p \right. \\ &\quad \left. + \tau_2 D_i^c + \tau_3 c_i a_p D_p^a + \tau_4 c_i c_p D_p^c + \tau_5 C_i \right) \end{aligned} \quad (2.106)$$

$$\tilde{g}_i^c = -2 \left(\lambda_2 D_i^c + \lambda_5 C_i + \tau_1 D_i^a + \tau_5 A_i \right) \quad (2.107)$$

with

$$D_i^a = D_{ij} a_j \quad \text{and} \quad D_i^c = D_{ij} c_j \quad (2.108)$$

where

$$D_{ij} = \frac{1}{2} (v_{i,j} + v_{j,i}) \quad (2.109)$$

and where τ_i , $i = 1..5$ and λ_j , $j = 1..6$ are viscosities associated with the dynamic stress. The dynamic stress term \tilde{t}_{ij} is given by

$$\tilde{t}_{ij} = \tilde{t}_{ij}^s + \tilde{t}_{ij}^{ss} \quad (2.110)$$

where \tilde{t}_{ij}^s and \tilde{t}_{ij}^{ss} are the symmetric and skew-symmetric parts of the viscous stress given by [6, p. 294]

$$\begin{aligned} \tilde{t}_{ij}^s &= \mu_0 D_{ij} + \mu_1 a_p D_p^a a_i a_j + \mu_2 (D_i^a a_j + D_j^a a_i) + \mu_3 c_p D_p^c c_i c_j \\ &\quad + \mu_4 (D_i^c c_j + D_j^c c_i) + \mu_5 c_p D_p^a (a_i c_j + a_j c_i) \\ &\quad + \lambda_1 (A_i a_j + A_j a_i) + \lambda_2 (C_i c_j + C_j c_i) + \lambda_3 c_p A_p (a_i c_j + a_j c_i) \\ &\quad + \kappa_1 (D_i^a c_j + D_j^a c_i + D_i^c a_j + D_j^c a_i) \\ &\quad + \kappa_2 [a + p D_p^a (a_i c_j + a_j c_i) + 2 a_p D_p^c a_i a_j] \\ &\quad + \kappa_3 [c_p D_p^c (a_i c_j + a_j c_i) + 2 a_p D_p^c c_i c_j] \\ &\quad + \tau_1 (C_i a_j + C_j a_i) + \tau_2 (A_i c_j + A_j c_i) \\ &\quad + 2 \tau_3 c_p A_p a_i a_j + 2 \tau_4 c_p A_p c_i c_j, \end{aligned} \quad (2.111)$$

where μ_i and λ_i are the viscosity coefficients associated with contributions to the dynamic stress which are even in the vector \mathbf{c} while κ_i and τ_i are linked to

term which are odd in the vector \mathbf{c} , and

$$\begin{aligned}
\tilde{t}_{ij}^{ss} = & \lambda_1 (D_j^a a_i - D_i^a a_j) + \lambda_2 (D_j^c c_i - D_i^c c_j) + \lambda_3 c_p D_p^a (a_i c_j - a_j c_i) \\
& \lambda_4 (A_j a_i - A_i a_j) + \lambda_5 (C_j c_i - C_i c_j) + \lambda_6 c_p A_p (a_i c_j - a_j c_i) \\
& \tau_1 (D_j^a c_i - D_i^a c_j) + \tau_2 (D_j^c a_i - D_i^c s_j) + \tau_3 a_p D_p^a (a_i c_j - a_j c_i) \\
& \tau_4 c_p D_p^c (a_i c_j - a_j c_i) + \tau_5 (A_j c_i - A_i c_j + C_j a_i - C_i a_j) . \quad (2.112)
\end{aligned}$$

There are twenty viscosity co-efficients in (2.111) and (2.112). These viscosities have been classified in [6, p. 296].

Equation (2.102) is the balance of linear momentum and (2.104) and (2.105) are coupled equations for the angular momentum, commonly referred to as the “ a -equations” and “ c -equations”, respectively.

3 Calculus of Variations

In this chapter some of the theory and methods of calculus of variations will be discussed. These methods will then be used in the following work. The chapter closes with section 3.4 where an inequality for integrals, which was first derived by Gartland [24], is introduced which will allow the application of the theory and methods.

Throughout this thesis, there are problems whose solution y minimises functionals $J[y]$ of the form

$$J[y] = \int_a^b F(x, y, y') dx . \quad (3.1)$$

There are different methods that can be used to minimise such functionals. Here, the second variation will be considered as well as the Rayleigh–Ritz method of minimising functionals. The Rayleigh–Ritz method is a direct method in the calculus of variations, since it does not use a differential equation to look at the problem (3.1), but instead looks at the functional directly. This method allows the eigenvalues and corresponding eigenvectors for the problem to be found, and from these, we can consider the stability of the problem. The second variation of the problem considers the derivatives of the integrand of the functional and has necessary and sufficient conditions for both weak and strong minima.

3.1 The minimum of a functional

From Sagan [25, p.46], a function $y_0(x) \in \Sigma$ is said to be a weak relative minimum for $J[y]$, where Σ is the space of competing functions, which for our purposes is taken to be $C^1[a, b]$ which is the space of all real valued functions with a continuous derivative on the interval $[a, b]$, if

$$J[y] - J[y_0] \geq 0 \quad (3.2)$$

for all $y \in \Sigma$ for which $y \in N^\delta(y_0)$, for some $\delta > 0$, where from Sagan [25, p. 45] the strong δ neighbourhood, $N^\delta(y_0)$, is the set

$$\{(x, y, y') | x \in [a, b], |y - y_0(x)| < \delta, |y' - y'_0(x)| < \delta\} . \quad (3.3)$$

If $y_0(x)$ is a strong relative minimum, then (3.2) must be true for all $y \in \Sigma$ for which $y \in N_\omega^\delta(y_0)$, for some δ , where $N_\omega^\delta(y_0)$ from [25, p. 45], is a weak δ neighbourhood, the set

$$\{(x, y) | x \in [a, b], |y - y_0(x)| < \delta\} . \quad (3.4)$$

The subscript ω denotes the weak minimum, no subscript denotes strong.

3.2 Rayleigh–Ritz method

The Rayleigh–Ritz method allows the eigenvalues and corresponding eigenvectors for the functional (3.1) to be found, and from these, the stability of the solution y can be considered. These can be found by considering a perturbation over an interval to a solution. This interval can be $-\infty$ to ∞ but often it is chosen to be a finite interval from $-L$ to L or if y is even or odd then the interval of 0 to L can be considered via symmetry. A symmetrical graph with the interval of 0 to L perturbed is illustrated in Fig. 15 below.

This technique looks at functionals of the form

$$J[y] = \int_a^b \left[p(x) \{y'(x)\}^2 - q(x) \{y(x)\}^2 \right] dx \quad (3.5)$$

defined on some space \mathcal{M} of admissible functions, usually taken to be a normed linear space for simplicity. It is assumed that there are functions in \mathcal{M} such that $J[y] < \infty$ and that the infimum of the functional is a number greater than $-\infty$.

This method works by looking for the minimum of the functional of the problem by choosing known functions, which make it easier to evaluate the

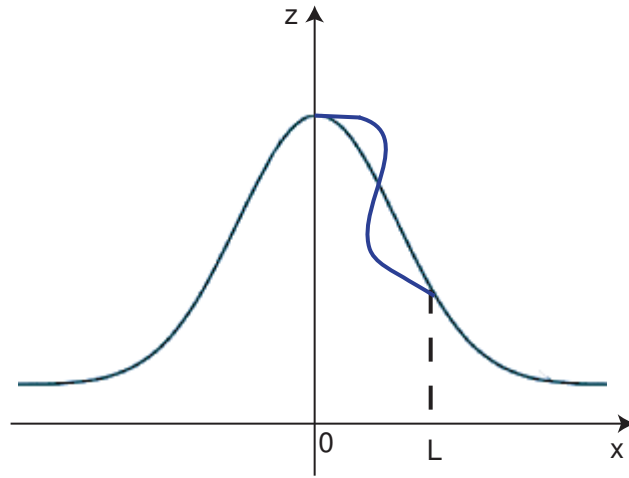


Figure 15: This shows a perturbation from 0 to L to a solution. The interval has been chosen to be 0 to L because of the presumed symmetry of the solution, $y(x) = y(-x)$.

integral, to be y . This is done by considering

$$\phi_1, \phi_2, \phi_3, \dots \tag{3.6}$$

an infinite sequence of functions in \mathcal{M} which satisfy the boundary conditions of the problem, and \mathcal{M}_n , the set of all linear combinations of the form

$$y_n := \alpha_1\phi_1 + \alpha_2\phi_2 + \alpha_3\phi_3 + \dots + \alpha_n\phi_n, \tag{3.7}$$

where the α_n are real constants. If we let y be this linear combination then we have

$$J[y_n] = J[\alpha_1\phi_1 + \dots + \alpha_n\phi_n], \tag{3.8}$$

which can be considered as a function of the n variables, α_n . This is then evaluated and the α_n are chosen such that (3.8) is minimised. This minimised value of (3.8) is the lowest eigenvalue for the problem for that value of n , denoted μ_n ,

$$\mu_n := \min_{\{\alpha_1, \dots, \alpha_n\}} J[\alpha_1\phi_1 + \alpha_2\phi_2 + \dots + \alpha_n\phi_n]. \tag{3.9}$$

It is clear that the value of this eigenvalue cannot increase with n since any linear combination of ψ_1, \dots, ψ_n is also a linear combination of $\psi_1, \dots, \psi_n, \psi_{n+1}$, [26], so

$$\mu_1 \geq \mu_2 \geq \mu_3 \geq \dots \quad (3.10)$$

The following definition and theorem from [26] show that the sequence of the μ_n converges to the infimum of $J[y]$ on \mathcal{M} .

Definition 1 *The sequence (3.6) is complete if, given any $y \in \mathcal{M}$ and any $\epsilon > 0$, there is a linear combination y_n of the form (3.7) such that $\|y_n - y\| < \epsilon$ (where n depends on ϵ).*

This definition is needed for:

Theorem 1 *If the functional $J[y]$ is continuous, and if the sequence (3.6) is complete, then*

$$\lim_{n \rightarrow \infty} \mu_n = \mu, \quad (3.11)$$

where

$$\mu = \inf_y J[y]. \quad (3.12)$$

For proof of this theorem, see [26] p 196.

If this method is applied to a problem and any μ_n is found to be negative, then the solution is unstable. If μ_n is positive then the series μ_1, μ_2, \dots has to be looked at to see whether or not μ , the limit of this series, is positive or null. If the series is tending towards a positive value then the solution is stable, but if $\mu = 0$ then the problem needs to be looked at further. If the series becomes negative at any point, then the solution y is unstable.

The eigensolution for the problem is given by (3.7) with the minimised α_n . For further details see [26].

3.3 Second variation

The second variation is used to determine whether or not a function y_0 is an extremal function of a functional. If the functional does not attain a minimum value then the function is not a minimum of the problem.

The first variation (Gâteaux variation) of

$$J[y] = \int_a^b F(x, y, y') dx \quad (3.13)$$

at $y = y_0$ is defined as

$$\delta J[h] = \left. \frac{d}{dt} J(y_0 + th) \right|_{t=0} \quad (3.14)$$

provided the right-hand side exists for all h , where $h = h(x)$ is an admissible function which satisfies $h(a) = h(b) = 0$ and $h(x) \not\equiv 0$. For $J[y]$ to have a minimum for a function y_0 it is necessary that the first variation is zero and the second variation must be greater than or equal to zero.

If the functional

$$J[y] = \int_a^b F(x, y, y') dx, \quad (3.15)$$

where $F(x, y, y')$ is a function with continuous partial derivatives up to third order, is defined on an open subset Y of a normed linear space \mathcal{S} and has a second Gâteaux variation so that, for all $y_0 \in Y$,

$$J[y_0 + h] - J[y_0] = \delta J[h] + \frac{1}{2} \delta^2 J[h] + \alpha[h], \quad (3.16)$$

for all $h \in \mathcal{S}$ for which $\|h\| < \delta$ for some $\delta > 0$ and

$$\lim_{t \rightarrow 0} \left(\frac{\alpha[th]}{t^2} \right) = 0, \quad (3.17)$$

then $\delta^2 J[h]$ is the second variation of the functional. The second variation is given by

$$\delta^2 J[h] = \int_a^b \left(P \{h'\}^2 + Q h^2 \right) dx, \quad (3.18)$$

where

$$P \equiv P(x) = \frac{1}{2} F_{y'y'} \quad \text{and} \quad Q \equiv Q(x) = \frac{1}{2} \left(F_{yy} - \frac{d}{dx} F_{yy'} \right). \quad (3.19)$$

3.3.1 Positive definiteness

A necessary condition for a functional $J[y]$ to have a minimum is

$$\delta^2 J[h] > 0, \quad (3.20)$$

for all admissible $h \in \mathcal{S}$. This means that if the integral is positive definite then the solution, y , is stable. If the integrand is positive definite, this forces the integral to be positive definite. It is worth noting at this point that a positive definite integrand guarantees a positive definite integral, however, it is not true to say that a positive definite integral requires a positive definite integrand. An example of this is

$$J = \int_0^1 \{(h')^2 - h^2\} dx. \quad (3.21)$$

The integrand $(h')^2 - h^2$ is, in matrix form,

$$\begin{bmatrix} h' & h \end{bmatrix} \begin{bmatrix} 1 & 0 \\ 0 & -1 \end{bmatrix} \begin{bmatrix} h' \\ h \end{bmatrix}. \quad (3.22)$$

The eigenvalues for this problem are clearly $\lambda = \pm 1$. Since we have a negative eigenvalue, it is not known for sure whether or not the integrand is positive definite. However, using the Poincaré inequality [27]

$$\int_0^1 \{h'\}^2 dx \geq \int_0^1 \pi h^2 dx, \quad (3.23)$$

with the conditions that $h(x)$ vanishes at the ends points but is not identically zero, we have

$$\begin{aligned} J &= \int_0^1 \{h'^2 - h^2\} dx, \\ &\geq \int_0^1 \{\pi h^2 - h^2\} dx = (\pi - 1) \int_0^1 h^2 dx, \\ &\geq 0. \end{aligned} \quad (3.24)$$

This means that the integral is positive definite. This illustrates that an integral can be positive definite without having a positive definite integrand.

3.3.2 The Jacobi equation and conjugate points

A functional of the form of (3.1) has the second variation given by

$$\delta^2 J[h] = \int_a^b (Ph'^2 + Qh^2) dx, \quad (3.25)$$

where $h(x)$ satisfies $h(a) = h(b) = 0$ and $h(x) \not\equiv 0$. The Jacobi equation is defined to be the Euler–Lagrange equation of the second variation, i.e.

$$\frac{d}{dx} (P(x)h'(x)) - Q(x)h(x) = 0. \quad (3.26)$$

Since it is necessary that $h(x) \not\equiv 0$, we can choose $h'(a) = \alpha$ where $\alpha \neq 0$. For more details see [26].

The point c ($a < c < b$) is said to be conjugate to a if the Jacobi equation (3.26) has a solution which has a zero at $x = a$ and $x = c$ but is not identically zero. These conjugate points affect the positive definiteness of the integral through the following theorem from [26]:

Theorem 2 *If*

$$P(x) > 0 \quad (a \leq x \leq b) \quad (3.27)$$

for all $x \in [a, b]$ and the interval (a, b) contains no points conjugate to a , then the quadratic functional

$$\int_a^b (P \{h'\}^2 + Q \{h\}^2) dx \quad (3.28)$$

is positive definite for all $h(x)$ such that $h(a) = h(b) = 0$.

From [25, p. 404], this leads to the following theorem.

Theorem 3 *If $P(x) > 0$ for all $x \in [a, b]$, the second variation is positive definite if and only if (a, b) contains no point conjugate to a .*

So, for a solution to be stable, there must be a solution to the Jacobi equation (3.26) which never touches the x -axis. If a solution is found and it does cross the axis then it must be unstable since the solution to the Jacobi equation is unique by the existence and uniqueness theorem in [28].

3.3.3 Necessary conditions

From [26] and [25], there are five necessary conditions for $y = y_0(x)$ to be a minimum for $J[y]$.

To guarantee that the extremal $y_0(x)$ is a weak relative minimum, both the Euler–Lagrange equation, (3.29), and the Legendre condition (3.30) must be satisfied. For a strong relative minimum, these must be satisfied as well as the Jacobi condition, (3.40).

If $y = y_0(x)$ is a regular extremal (an extremal that consists of regular lineal elements, i.e., elements (x_0, y_0, y'_0) such that $f_{y'y'} \neq 0$), then for a strong relative minimum it must satisfy the Euler–Lagrange equation, (3.29), the Legendre condition, (3.30), Weierstraß' necessary condition, (3.32), and the Jacobi condition, (3.40). For a weak relative minimum it must satisfy the Euler–Lagrange equation, (3.29), the strengthened Legendre condition, (3.31), and the Jacobi condition, (3.40).

Euler–Lagrange equation

The functional $J[y]$ to have $y_0(x)$ as a minimum must satisfy the Euler–Lagrange equation. That is,

$$F_y(x, y_0, y'_0) - \frac{d}{dx} F_{y'}(x, y_0, y'_0) = 0. \quad (3.29)$$

Legendre condition

Legendre's Condition for $y_0(x)$ to be a relative minimum for a function $J[y]$ is

$$F_{y'y'}(x, y_0, y'_0) \geq 0 \quad (3.30)$$

for a minimum $\forall x \in [a, b]$.

Strengthened Legendre condition

The strengthened Legendre Condition is

$$F_{y'y'}(x, y_0, y'_0) > 0 \quad (3.31)$$

for a minimum $\forall x \in [a, b]$.

Weierstraß' necessary condition

If extremal $y = y_0(x)$ gives a strong relative minimum for $J[y]$, it must satisfy

$$\varepsilon(x, y_0(x), y'_0(x), \omega(x)) \geq 0 \quad (3.32)$$

for a minimum $\forall x \in [a, b]$ and $-\infty < \omega(x) < \infty$ where $\varepsilon(x, y_0, y'_0, \omega)$ is the Weierstraß excess function, which is defined by

$$\varepsilon(x, y, y', \omega) = F(x, y, \omega) - F(x, y, y') + (y' - \omega)F_{y'}(x, y, y') \quad (3.33)$$

for a functional given by

$$J[y] = \int_a^b F(x, y, y')dx. \quad (3.34)$$

Here $\omega(x)$ is the derivative with respect to x of an arbitrary function satisfying the boundary conditions of the problem.

An example of applying the Weierstraß Necessary Condition, taken from [29, p. 89], is the function

$$J[y] = \int_0^1 F(x, y, y')dx \quad (3.35)$$

where

$$F(x, y, y') = F(y') = (y')^2 + (y')^3. \quad (3.36)$$

For this function, the Weierstraß excess function is

$$\begin{aligned} \varepsilon(x, y, y', \omega) &= F(\omega) - F(y') - (\omega - y')F'(y') \\ &= (\omega^2 + \omega^3) - ((y')^2 + (y')^3) - (\omega - y')(2y' + 3(y')^2) \\ &= (\omega - y')^2(1 + \omega + 2y'). \end{aligned} \quad (3.37)$$

For the endpoints $(0, 0)$ and $(1, 0)$, the extremal joining them is a straight line, $y' = 0$. So the Weierstraß excess function becomes

$$\varepsilon(x, y, 0, \omega) = \omega^2(1 + \omega). \quad (3.38)$$

If $\omega < -1$ then the excess function (3.38) is negative so it is not a strong minimum. Legendre's condition gives

$$F''(y') = 2 + 6y' = 2 \geq 0, \quad (3.39)$$

so Legendre's condition is satisfied. This is not a contradiction since Weierstraß's condition and Legendre's condition are both only necessary.

Jacobi condition

For $y_0(x)$ to yield a weak relative minimum for $J[y]$

$$(a, b) \text{ contains no point that is conjugate to } a. \quad (3.40)$$

Proof that these five conditions are necessary for minima of the functional can be found in [25] and [29].

3.3.4 Sufficient conditions

There are three sufficient conditions for an extremal $y_0(x)$ to yield a minimum to the functional $J[y]$.

The extremal $y_0(x)$ is a strong relative minimum for $J[y]$ if it satisfies the Euler–Lagrange equation, (3.29) and the Weierstraß condition (3.42) and is either embeddable in a field, (3.41), or satisfies the strengthened Jacobi condition given by (3.43).

The extremal is a weak minimum if it satisfies the Euler–Lagrange equation, (3.29), the strengthened Legendre condition, (3.31), and the strengthened Jacobi condition, (3.43).

Embeddable in a field

For the extremal $y_0(x)$ to be a minimum of $J[y]$,

$$y_0 \text{ must be embeddable in a field.} \tag{3.41}$$

From Sagan [25, p. 133], a field is defined as

Definition 2 (A field) *Let \mathcal{A} denote a bounded and simply connected domain in the x, y plane. The vector function $(1, \phi(x, y))$ is said to define a field $\mathcal{F} = \{(1, \phi(x, y)) \mid (x, y) \in \mathcal{A}\}$ in \mathcal{A} for $J[y]$ if $\phi_x, \phi_y \in C(\mathcal{A})$ and if every solution of $y' = \phi(x, y)$ in \mathcal{A} is an extremal of $J[y]$.*

Definition 3 (Embeddable in a field) *An extremal $y_0(x)$ of $J[y]$ is said to be embeddable in a field, \mathcal{F} , if:*

- \mathcal{F} is defined on a simply connected domain \mathcal{A} that contains a weak delta neighbourhood $N_\omega^\delta(y_0)$, and
- $y = y_0(x)$ is a solution on \mathcal{A} of $y' = \phi(x, y)$, where $\phi(x, y)$ defines the field.

Weierstraß condition

The Weierstraß condition states that if $y_0(x)$ is embeddable in a field and if

$$\varepsilon(x, y, y', \omega) \geq 0 \tag{3.42}$$

$$\forall (x, y) \in N_\omega^\delta(y_0) \text{ and all } -\infty < y' < \infty \text{ and } -\infty < \omega < \infty$$

where $\varepsilon(x, y, y', \omega)$ is given by (3.32), then $y_0(x)$ gives a strong minimum.

Strengthened Jacobi Condition

The strengthened Jacobi condition is

$$(a, b] \text{ does not contain a conjugate point to } a. \tag{3.43}$$

The difference between this and the Jacobi condition (3.40) is that b must not be conjugate to a in the strengthened condition, but it can be in (3.40).

Proof that these conditions are sufficient for a minimum can be found in [25] and [29].

3.4 Positivity criterion

Inequalities can be used to determine whether or not an integral is positive definite. One such inequality is a positivity criterion due to Gartland, [24], which will be reviewed in this section. First consider the functional

$$\int_0^1 \left\{ (\phi'(x))^2 + q(x)\phi^2(x) \right\} dx, \quad (3.44)$$

$$= \int_0^1 (\phi'(x))^2 dx + \int_0^1 q(x)\phi^2(x) dx, \quad (3.45)$$

where $q(x)$ crosses the axis so that it has negative and positive parts and $\phi \in C^1$. It is assumed that $\phi(0) = \phi(1) = 0$. The first integral is always ≥ 0 so only the second one, which involves $q(x)$, needs to be considered. Let the negative parts of $q(x)$ be $q_-(x)$ and the positive parts be $q_+(x)$ so

$$q_-(x) = \begin{cases} q(x) & \text{for } q(x) < 0, \\ 0 & \text{for } q(x) \geq 0, \end{cases} \quad (3.46)$$

and

$$q_+(x) = \begin{cases} 0 & \text{for } q(x) < 0, \\ q(x) & \text{for } q(x) \geq 0. \end{cases} \quad (3.47)$$

Since $q_-(x) < 0$,

$$\begin{aligned} 0 \leq \int_0^1 -q_-(x)\phi^2(x) dx &= \int_0^1 |q_-(x)|\phi^2(x) dx, \\ &\leq \|\phi\|_{L^\infty(0,1)}^2 \int_0^1 |q_-(x)| dx \end{aligned} \quad (3.48)$$

by Hölder's inequality, where $\|\cdot\|_{L^\infty}$ is the supremum norm.

Also, $\|\phi\|_{L^\infty} = |\phi(x_1)|$ for some $x_1 \in (0, 1)$ since $\phi \in C^1$, and so with $\phi(0) = 0$:

$$\|\phi\|_{L^\infty} = \left| \int_0^{x_1} \phi'(x) dx \right| \quad \text{since } \phi(0) = 0, \quad (3.49)$$

$$\leq \int_0^{x_1} |\phi'(x)| dx, \quad (3.50)$$

$$\leq \left(\int_0^{x_1} 1^2 dx \right)^{\frac{1}{2}} \left(\int_0^{x_1} |\phi'(x)|^2 dx \right)^{\frac{1}{2}}, \quad (3.51)$$

using the Cauchy-Schwartz inequality. This is

$$\|\phi\|_{L^\infty} \leq \sqrt{x_1} \left(\int_0^{x_1} |\phi'(x)|^2 dx \right)^{\frac{1}{2}}, \quad (3.52)$$

$$\leq \sqrt{x_1} \left(\int_0^1 |\phi'(x)|^2 dx \right)^{\frac{1}{2}}, \quad (3.53)$$

$$= \sqrt{x_1} \|\phi'(x)\|_{L^2}. \quad (3.54)$$

Similarly

$$\|\phi\|_{L^\infty} \leq \sqrt{1-x_1} \|\phi'(x)\|_{L^2} \quad (3.55)$$

since $\phi = 0$ on both boundaries. Hence

$$\|\phi\|_{L^\infty}^2 \leq \min\{x_1, 1-x_1\} \cdot \left(\int_0^1 \phi'(x)^2 dx \right), \quad (3.56)$$

$$\leq \frac{1}{2} \int_0^1 \phi'(x)^2 dx. \quad (3.57)$$

Hence, from (3.48),

$$-\int_0^1 q_-(x) \phi^2(x) dx \leq \frac{1}{2} \int_0^1 |q_-(x)| dx \int_0^1 \phi'(x)^2 dx. \quad (3.58)$$

The integral (3.45) is now considered again, giving

$$\int_0^1 (\phi'(x))^2 dx + \int_0^1 q(x)\phi^2(x)dx \tag{3.59}$$

$$= \int_0^1 (\phi'(x))^2 dx + \int_0^1 q_+(x)\phi^2(x)dx + \int_0^1 q_-(x)\phi^2(x)dx, \tag{3.60}$$

$$\geq \int_0^1 (\phi'(x))^2 dx + \int_0^1 q_+(x)\phi^2(x)dx - \frac{1}{2} \int_0^1 |q_-(x)|dx \cdot \int_0^1 (\phi')^2 dx \tag{3.61}$$

$$= \int_0^1 q_+(x)\phi^2(x)dx + \int_0^1 (\phi'(x))^2 dx \left[1 - \frac{1}{2} \int_0^1 |q_-(x)|dx \right], \tag{3.62}$$

$$\geq 0 \quad \text{provided} \quad \int_0^1 |q_-(x)|dx \leq 2. \tag{3.63}$$

This condition,

$$\int_0^1 |q_-(x)|dx \leq 2, \tag{3.64}$$

will be referred to as the positivity criterion throughout this thesis. It is worth noting that this criterion could still be valid even if the function was entirely negative between the finite end points.

The above argument can easily be changed to an arbitrary domain. If the domain of x is extended to $x \in [0, a]$, then the positivity criterion (3.64) is given by

$$\int_0^a |q_-(x)|dx \leq \frac{2}{a}, \tag{3.65}$$

since

$$\min\{x_1, a - x_1\} \leq \frac{a}{2} \quad \text{for } 0 < x_1 < a. \tag{3.66}$$

This is a generalised positivity criterion. This criterion is a sufficient but not a necessary condition since, if the function $q(x)$ does not satisfy it, then the solution could still be stable. Another technique would need to be used to determine its stability.

4 Smectic C Domain Walls in a Cylinder

Atkin and Stewart considered the problem of the stability of solutions for the orientation of smectic C liquid crystals molecules in a concentric circular geometry in the presence of an azimuthal magnetic field. They found five different solutions [30, 31] when they looked at an infinite sample of concentric circular cylinders of smectic C liquid crystal with a fixed inner radius r_0 . Within this chapter we will consider the stability of these solutions. Previously, only the stability of one of these solutions had been looked at and only resolved with constraints. Here we will resolve all five stability cases.

Because of the symmetry of the problem, cylindrical polar co-ordinates are used with basis vectors $\hat{\mathbf{r}}$, $\hat{\boldsymbol{\alpha}}$ and $\hat{\mathbf{z}}$ for convenience, where r measures the radial distance (so $\hat{\mathbf{r}} = \mathbf{a}$), z is the axis of the cylinder and α is the polar angle. This is shown below in Fig. 16. Here, ϕ is the orientation angle of \mathbf{c} within the smectic layers.

4.1 Atkin and Stewart's solutions

The solutions which Atkin and Stewart found in [30, 31] were for $\phi = \phi(r)$. From Fig. 16

$$\mathbf{a} = \hat{\mathbf{r}}, \quad (4.1)$$

$$\mathbf{c} = \hat{\boldsymbol{\alpha}} \sin \phi + \hat{\mathbf{z}} \cos \phi, \quad (4.2)$$

$$\mathbf{n} = \mathbf{a} \cos \theta + \mathbf{c} \sin \theta, \quad (4.3)$$

$$= \hat{\mathbf{r}} \cos \theta + \hat{\boldsymbol{\alpha}} \sin \theta \sin \phi + \hat{\mathbf{z}} \sin \theta \cos \phi, \quad (4.4)$$

and a new vector \mathbf{b} can be introduced such that

$$\mathbf{b} = \mathbf{a} \times \mathbf{c}, \quad (4.5)$$

$$= -\hat{\boldsymbol{\alpha}} \cos \phi + \hat{\mathbf{z}} \sin \phi. \quad (4.6)$$

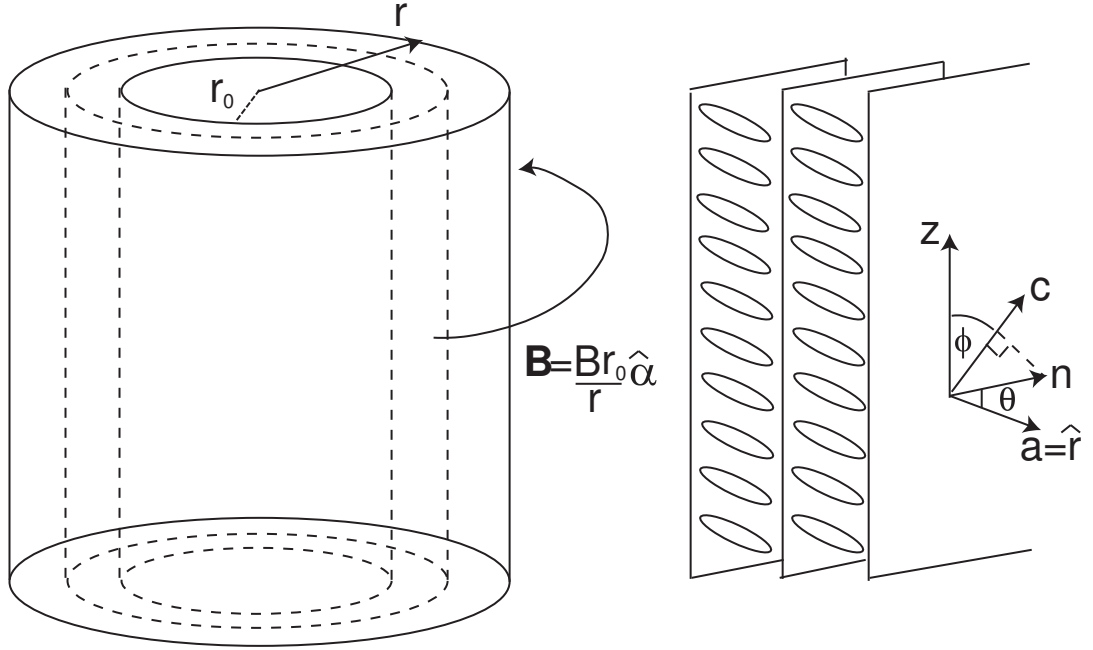


Figure 16: A physical representation of the geometry of the problem and of the unit vectors. Fig (a) shows the cylinder with inner radius r_0 with equidistant cylindrical layers of smectic C liquid crystals, and Fig (b) shows the director in relation to the layer normal.

In [30, 32] the solutions to this problem were found by considering the total energy of the system. From [6], the bulk energy density, w_b , is given in terms of \mathbf{b} and \mathbf{c} in (2.76) with B_1 , B_2 , C_1 and C_2 equal to zero. From (2.77-2.78), the remaining elastic constants must satisfy

$$A_{12}, A_{21}, B_3 > 0 \quad \text{and} \quad A_{12} + A_{21} \pm 2A_{11} > 0, \quad (4.7)$$

since

$$(A_{12} \pm A_{11})^2 = A_{12}^2 + A_{11}^2 \pm 2A_{12}A_{11} \geq 0 \quad (4.8)$$

and then adding (2.78) gives

$$A_{12} (A_{12} + A_{21} \pm 2A_{11}) \geq 0 \quad (4.9)$$

and since $A_{12} > 0$ then the second inequality in (4.7) arises.

Since cylindrical polar co-ordinates are being used then the divergence and curl of the vectors are not as straight forward as they would be if Cartesian co-ordinates were being used. In cylindrical polars, from [6] and [33] the divergence of a vector \mathbf{n} given by

$$\mathbf{n} = n_1 \hat{\mathbf{r}} + n_2 \hat{\boldsymbol{\alpha}} + n_3 \hat{\mathbf{z}} \quad (4.10)$$

EPT FOR THE SPELLING M is

$$\nabla \cdot \mathbf{n} = \frac{1}{r} \frac{\partial}{\partial r} (rn_1) + \frac{1}{r} \frac{\partial n_2}{\partial \alpha} + \frac{\partial n_3}{\partial z}. \quad (4.11)$$

The curl of \mathbf{n} in polars is

$$\nabla \times \mathbf{n} = \frac{1}{r} \begin{vmatrix} \hat{\mathbf{r}} & r\hat{\boldsymbol{\alpha}} & \hat{\mathbf{z}} \\ \frac{\partial}{\partial r} & \frac{\partial}{\partial \alpha} & \frac{\partial}{\partial z} \\ n_1 & rn_2 & n_3 \end{vmatrix}. \quad (4.12)$$

Using the above formulae, the bulk energy density becomes

$$\begin{aligned} w_b &= \frac{1}{2} A_{12} \frac{1}{r^2} \sin^4 \phi + \frac{1}{2} A_{21} \frac{1}{r^2} \cos^4 \phi \\ &\quad - A_{11} \frac{1}{r^2} \cos^2 \phi \sin^2 \phi + \frac{1}{2} B_3 \left(\frac{d\phi}{dr} \right)^2, \end{aligned} \quad (4.13)$$

$$\begin{aligned} &= \frac{1}{2} r^{-2} [(A_{12} + A_{11}) \sin^4 \phi + (A_{21} + A_{11}) \cos^4 \phi - \sin^2 \phi \cos^2 \phi A_{11}] \\ &\quad + \frac{1}{2} B_3 [\phi'(r)]^2. \end{aligned} \quad (4.14)$$

If there is a magnetic field \mathbf{B} such that

$$\mathbf{B} = B \frac{r_0}{r} \hat{\boldsymbol{\alpha}}, \quad (4.15)$$

where B is the field strength at $r = r_0$, then the magnetic energy density is given by

$$w_{mag} = -\frac{1}{2} \frac{\Delta\chi}{\mu_0} (\mathbf{n} \cdot \mathbf{B})^2, \quad (4.16)$$

where $\Delta\chi$ is the magnetic anisotropy of the smectic C liquid crystal and μ_0 is the permeability of free space. This gives

$$w_{mag} = -\frac{1}{2} \frac{\Delta\chi}{\mu_0} \frac{B^2 r_0^2}{r^2} \sin^2 \theta \sin^2 \phi. \quad (4.17)$$

Now, the total energy is given by

$$W = \int_{\Omega} (w_b + w_m) r dr d\alpha dz \quad (4.18)$$

$$= \int_{\Omega} \bar{w} r dr d\alpha dz \quad (4.19)$$

where Ω is the sample region and

$$\bar{w} = r (w_b + w_m) . \quad (4.20)$$

The governing equation is found by considering the Euler–Lagrange equation of the total energy, i.e.

$$\frac{\partial}{\partial r} \left(\frac{\partial \bar{w}}{\partial \phi_r} \right) + \frac{\partial}{\partial \theta} \left(\frac{\partial \bar{w}}{\partial \phi_\theta} \right) - \frac{\partial \bar{w}}{\partial \phi} = 0. \quad (4.21)$$

which gives

$$\begin{aligned} B_3 \left[r^2 \frac{d^2 \phi}{dr^2} + r \frac{d\phi}{dr} \right] - 2 (A_{12} + A_{21} + 2A_{11}) \sin^3 \phi \cos \phi \\ + \left[2 (A_{21} + A_{11}) + \frac{\Delta \chi}{\mu_0} B^2 r_0^2 \sin^2 \theta \right] \sin \phi \cos \phi = 0 . \end{aligned} \quad (4.22)$$

If the following new variables and constants, for ease, given by

$$s = \ln \left(\frac{r}{r_0} \right), \quad (4.23)$$

$$\psi = 2\phi, \quad (4.24)$$

$$a = \frac{1}{B_3} \left(A_{12} - A_{21} - \frac{\Delta \chi}{\mu_0} B^2 r_0^2 \sin^2 \theta \right), \quad (4.25)$$

$$b = \frac{1}{2B_3} (A_{12} + A_{21} + 2A_{11}), \quad (b > 0 \text{ by (4.7)}), \quad (4.26)$$

are introduced, (4.22) can be rewritten as

$$\frac{d^2 \psi}{ds^2} = a \sin \psi - b \sin 2\psi. \quad (4.27)$$

If this is now multiplied by $\frac{d\psi}{ds}$ and integrated, (4.27) becomes

$$\frac{d\psi}{ds} = \pm \sqrt{b \cos(2\psi) - 2a \cos \psi + c} \quad (4.28)$$

where c is a constant of integration. This is a first order ordinary differential equation (ODE) which depends upon a , b and the solution ψ . This ODE also depends upon the parameter c and has a further constant of integration.

Atkin and Stewart [30, 31] looked at the phase portraits for this problem with $b > 0$. From these, shown in Fig. 17, they found five possible explicit solutions depending upon the constants a and b . These are:

$$\psi_1 = -2n\pi - 2 \arctan \left\{ \tanh \left(\frac{\eta}{2} \right) \tan \left(\sqrt{\frac{b}{2}} \sinh(\eta) s \right) \right\}, \quad (4.29)$$

$$\frac{\pi(2n-1)}{\sqrt{2b} \sinh \eta} < s < \frac{\pi(2n+1)}{\sqrt{2b} \sinh \eta}, \quad n = 0, 1, 2, \dots, \quad a > 2b,$$

$$\psi_2 = 0, \quad a = 2b, \quad (4.30)$$

$$\psi_3 = 2 \arctan \left\{ \tan \left(\frac{\psi_0}{2} \right) \tanh \left(\sqrt{\frac{b}{2}} \sin(\psi_0) s \right) \right\}, \quad |a| < 2b, \quad (4.31)$$

$$\psi_4 = 2 \arctan \left(\sqrt{2b} s \right), \quad a = -2b, \quad (4.32)$$

$$\psi_5 = 2 \arctan \left\{ \sqrt{\frac{a}{a+2b}} \sinh \left(\sqrt{-(a+2b)} s \right) \right\}, \quad a < -2b, \quad (4.33)$$

where

$$\eta = \operatorname{arccosh} \left(\frac{a}{2b} \right), \quad \text{for } a > 2b \quad (4.34)$$

and

$$\psi_0 = \arccos \left(\frac{a}{2b} \right). \quad (4.35)$$

These solutions can be found by considering the differential equation (4.28). This equation is solved using boundary conditions chosen from the phase portraits with the value of c chosen in terms of a and b in such a way that it completes the square on the right hand side allowing the equation to be solved analytically. Other values of c could be chosen but analysis would not be as straight forward. The solutions could have $2n\pi$ added to them and they would also be solution to the differential equation but they would not satisfy the boundary conditions chosen from our phase portrait.

Introducing the parameter

$$k = -\frac{a}{2b}, \quad (4.36)$$

(4.34) and (4.35) become

$$\begin{aligned} \eta &= \operatorname{arccosh}(-k), \quad \text{for } |k| < 1 \\ \psi_0 &= \arccos(k). \end{aligned} \quad (4.37)$$

Substituting this into (4.29-4.33) and reverting back to ϕ ($\psi = 2\phi$) yields

$$\phi_1(k, s) = -n\pi - \arctan \left\{ \sqrt{\frac{k+1}{k-1}} \tan \left(\sqrt{\frac{b}{2}} \sqrt{k^2-1} s \right) \right\}, \quad (4.38)$$

with

$$\frac{\pi(2n-1)}{\sqrt{2b(k^2-1)}} < s < \frac{\pi(2n+1)}{\sqrt{2b(k^2-1)}}, \quad n = 0, 1, 2, \dots, \quad k < -1,$$

$$\phi_2(k, s) = 0, \quad k = -1, \quad (4.39)$$

$$\phi_3(k, s) = \arctan \left\{ \sqrt{\frac{1+k}{1-k}} \tanh \left(\sqrt{\frac{b}{2}} \sqrt{1-k^2} s \right) \right\}, \quad |k| < 1, \quad (4.40)$$

$$\phi_4(k, s) = \arctan \left(\sqrt{2b} s \right), \quad k = 1, \quad (4.41)$$

$$\phi_5(k, s) = \arctan \left\{ \sqrt{\frac{k}{k-1}} \sinh \left(\sqrt{2b} \sqrt{k-1} s \right) \right\}, \quad k > 1. \quad (4.42)$$

It is interesting to note here that the extrapolation length of $\psi_3(s)$ is proportional to $\sqrt{1-k^2}$ but as k increases such that $k > 1$, the extrapolation length changes to be proportional to $\sqrt{k-1}$. If the phase diagrams for these solutions are considered, then it can be seen that these five solutions connect together continuously as k changes, that is why these five were selected by Atkin and Stewart.

The graphs of $\psi_1(s)$, $\psi_3(s)$, $\psi_4(s)$ and $\psi_5(s)$ are shown below in Fig. 18. This shows that as s tends to infinity, $\psi_3(s)$ tends to $\arctan \frac{\sqrt{1+k}}{1-k}$ and $\phi_4(s)$ and $\phi_5(s)$ both tend to π . The ϕ_2 solution is omitted since it is simply the trivial zero solution.

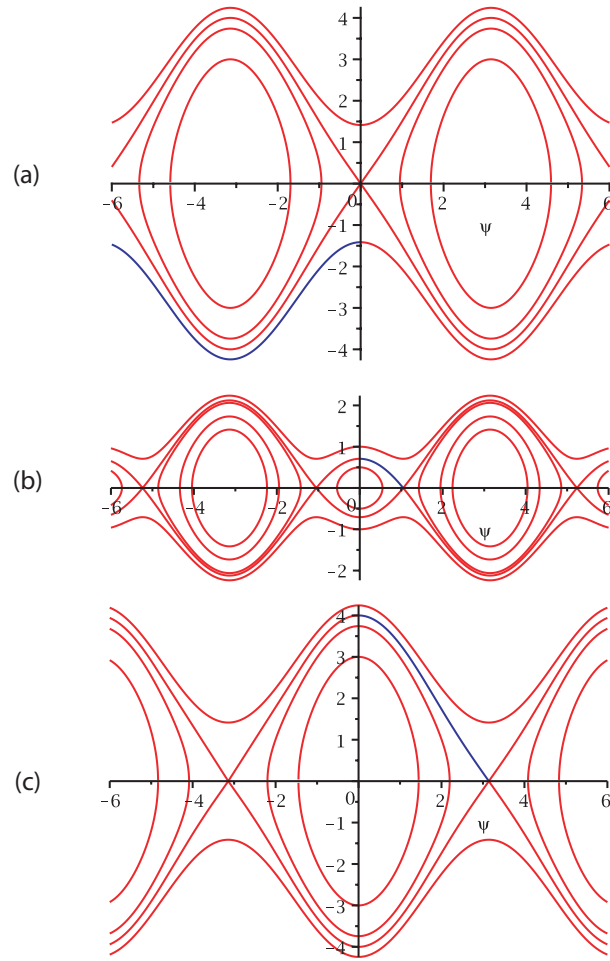


Figure 17: These are the phase portraits for (a) $k < -1$, (b) $|k| < 1$ and (c) $k > 1$.

The stability of these five solutions will be considered here. The energy of the solutions may be compared for different cases, but this is beyond the scope of the Thesis at present. Atkin and Stewart looked at the stability of (4.40) in [34]. In that paper, they looked at the stability analytically and they found that the solution was indeed stable with the restrictions that

$$b \geq \frac{1}{40} \quad \text{and} \quad |a| \leq \sqrt{2b(2b-1)}. \quad (4.43)$$

Here results will be achieved without any restrictions on the values of a or b for four of the five solutions, and a result with some restrictions on the value of k

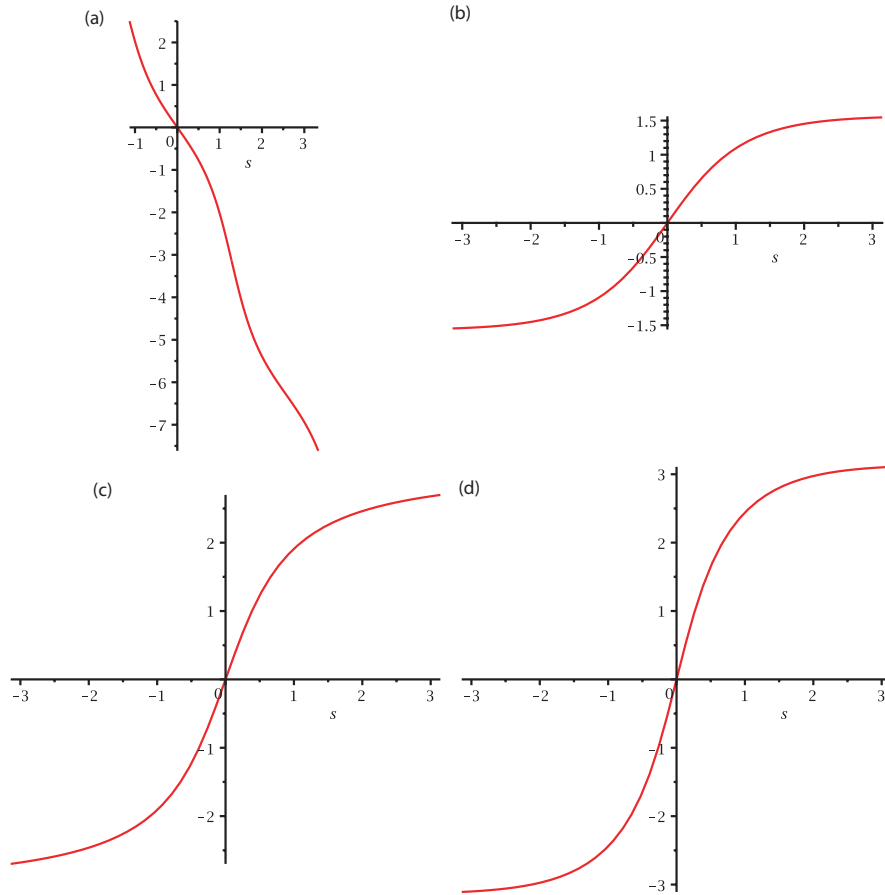


Figure 18: These are the graphs of (a) ψ_1 , (b) ψ_3 (c) ψ_4 and (d) ψ_5 .

will be obtained for the ϕ_1 solution.

4.2 Stability

The analysis of the stability of these solutions begins by looking at the Rayleigh–Ritz method for computing eigenvalues. To apply this method to our problem, we must cast it in the form of (3.5). To get the problem into the required form for the method, the same method is used as Atkin and Stewart used in [34]; a time dependence will be assumed. This is a commonly used technique in considering the stability of static solutions and leads to the introduction of a dynamic term.

From the dynamic theory of smectic C liquid crystals, the governing dynamic

equations are given by (2.102), (2.104) and (2.105). There is no flow involved in this problem so equation (2.102) is gone and since there is no flow and \mathbf{a} is constant, the equation for the a -director (2.104) is also gone. For more details, see [6, p. 303-304] and for an explicit example in cylindrical geometry, see [35].

The remaining equation is (2.105), which reduces to

$$\Pi_i^c + \tilde{g}_i^c + \tau c_i + \mu a_i = 0 \quad (4.44)$$

since we have no external body force. The dynamic contribution, \tilde{g}_i^c is reduced to

$$\tilde{g}_i^c = -2\lambda_5 C_i, \quad (4.45)$$

since there is no velocity, where

$$C_i = \dot{c}_i - W_{ik} c_k = \dot{c}_i. \quad (4.46)$$

For $i = 1$ the second angular momentum equation is given by

$$\mu a_1 = 0 \quad \Rightarrow \quad \mu = 0 \quad (4.47)$$

since $a_1 = 1$ and $c_1 = 0$ from (4.1) and (4.2).

When $i = 2$ and $i = 3$, the remaining angular momentum equations are

$$\Pi_2^c - 2\lambda_5 \dot{c}_2 + \tau c_2 = 0 \quad \text{for } i = 2, \quad (4.48)$$

$$\Pi_3^c - 2\lambda_5 \dot{c}_3 + \tau c_3 = 0 \quad \text{for } i = 3. \quad (4.49)$$

These are

$$\Pi_2^c - 2\lambda_5 \cos \phi \dot{\phi} + \tau \sin \phi = 0 \quad (4.50)$$

and

$$\Pi_3^c + 2\lambda_5 \sin \phi \dot{\phi} + \tau \cos \phi = 0 \quad (4.51)$$

when the expressions for c_i are inserted from (4.2). Eliminating the Lagrange multiplier τ leaves the single equation

$$\Pi_2^c \cos \phi - \Pi_3^c \sin \phi - 2\lambda_5 \dot{\phi} = 0. \quad (4.52)$$

From [6], the $\mathbf{\Pi}_i^c$ term is given in general vector form in (2.101). The K_i elastic constants from (2.83) that enter the model equations are

$$K_1 = A_{21}, \quad K_4 = B_3, \quad K_5 = 2A_{11} + A_{12} + A_{21} + B_3 \quad (4.53)$$

$$K_6 = - \left(A_{11} + A_{21} + \frac{1}{2}B_3 \right). \quad (4.54)$$

The other K_i are absent because of the geometry of the problem. The divergence and curl of the terms in (4.52) are given by equations (4.11) and (4.12) respectively and the gradient of a scalar function, p , is given by

$$\nabla p = \frac{\partial p}{\partial r} \hat{\mathbf{r}} + \frac{1}{r} \frac{\partial p}{\partial \alpha} \hat{\boldsymbol{\alpha}} + \frac{\partial p}{\partial z} \hat{\mathbf{z}}. \quad (4.55)$$

After the non-trivial calculation of $\mathbf{\Pi}^c$ and reverting back to the Orsay elastic constants and rescaling time by setting

$$\bar{t} = \frac{B_3}{2\lambda_5} t, \quad (4.56)$$

we get

$$r^2 \frac{\partial^2 \psi}{\partial r^2} + r \frac{\partial \psi}{\partial r} - r^2 \frac{\partial \psi}{\partial t} = a \sin \psi - b \sin 2\psi \quad (4.57)$$

where the bar on t has been dropped for convenience and where

$$\psi = 2\phi, \quad (4.58)$$

and

$$a = \frac{1}{B_3} \left(A_{12} - A_{21} - \frac{\Delta\chi}{\mu_0} B^2 r_0^2 \sin^2 \theta \right) \quad (4.59)$$

$$b = \frac{1}{2B_3} (A_{12} + A_{21} + 2A_{11}) \quad (4.60)$$

as before.

It is now convenient to rescale the problem. If the problem is first rescaled via (4.23), as before, then a new variable \hat{s} is introduced such that

$$\hat{s} = \sqrt{\frac{b}{2}} s \quad \Rightarrow \quad \frac{d\hat{s}}{ds} = \sqrt{\frac{b}{2}} \quad \Rightarrow \quad \frac{d^2}{ds^2} = \frac{b}{2} \frac{d^2}{d\hat{s}^2}. \quad (4.61)$$

Eq. (4.27) becomes

$$\frac{d^2\psi}{d\hat{s}^2} = 2\frac{a}{b}\sin\psi - 2\sin 2\psi, \quad (4.62)$$

$$= -4k\sin\psi - 2\sin 2\psi. \quad (4.63)$$

The five solutions must also be rescaled using \hat{s} from (4.61). When we do this, our solutions become

$$\psi_1 = -2n\pi - 2\arctan\left\{\sqrt{\frac{k+1}{k-1}}\tan\left(\sqrt{k^2-1}\hat{s}\right)\right\}, \quad (4.64)$$

$$\frac{\pi(2n-1)}{2\sqrt{(k^2-1)}} < \hat{s} < \frac{\pi(2n+1)}{2\sqrt{(k^2-1)}}, \quad n = 0, 1, 2, \dots, \quad k < -1,$$

$$\psi_2 = 0, \quad k = -1, \quad (4.65)$$

$$\psi_3 = 2\arctan\left\{\sqrt{\frac{1+k}{1-k}}\tanh\left(\sqrt{1-k^2}\hat{s}\right)\right\}, \quad |k| < 1 \quad (4.66)$$

$$\psi_4 = 2\arctan(2\hat{s}), \quad k = 1, \quad (4.67)$$

$$\psi_5 = 2\arctan\left\{\sqrt{\frac{k}{k-1}}\sinh\left(2\sqrt{k-1}\hat{s}\right)\right\}, \quad k > 1. \quad (4.68)$$

From now on, s will represent the rescaled \hat{s} .

It is known from (4.62) that

$$\psi''(s) = -4k\sin\psi - 2\sin 2\psi. \quad (4.69)$$

A dependence on time is now assumed so that $\psi = \psi(s, t)$ giving

$$\frac{\partial^2\psi}{\partial s^2} - \frac{\partial\psi}{\partial t} = -4k\sin\psi - 2\sin 2\psi. \quad (4.70)$$

The time independent solutions still satisfy this since their partial derivative with respect to time is 0. A time-dependent perturbation $\varepsilon(s, t)$ is then considered, where

$$\psi(s, t) = \bar{\psi}(s) + \varepsilon(s, t), \quad |\varepsilon| \ll 1, \quad (4.71)$$

where $\varepsilon(0, t) = \varepsilon(\infty, t) = 0$. Substituting (4.71) into (4.70) gives the linearised perturbation equation

$$\frac{\partial^2\varepsilon}{\partial s^2} - \frac{\partial\varepsilon}{\partial t} = (-4k\cos(\bar{\psi}(s)) - 4\cos(2\bar{\psi}(s)))\varepsilon. \quad (4.72)$$

Setting

$$2\varepsilon(s, t) = \bar{\varepsilon}e^{-\lambda t}, \quad (4.73)$$

and substituting this into (4.72) gives the eigenvalue problem

$$\frac{\partial^2 \bar{\varepsilon}}{\partial s^2} + 4 \{k \cos(\psi(s)) + \cos(2\psi(s))\} \bar{\varepsilon} = -\lambda \bar{\varepsilon}. \quad (4.74)$$

Solutions to this problem will be stable whenever $\lambda \geq 0$ (or $\text{Re}(\lambda) \geq 0$). Equation (4.74) can be written as

$$\lambda v(s) = -v''(s) + q(s)v, \quad (4.75)$$

where, for easier notation,

$$q(s) = -4 [k \cos \psi + \cos(2\psi)] \quad \text{and} \quad v(s) = \varepsilon(s). \quad (4.76)$$

Multiplying (4.75) by $v(s)$ and using integration by parts, gives

$$\lambda \int_0^\infty v^2 ds = \int_0^\infty (v')^2 ds + \int_0^\infty q(s)v^2 ds. \quad (4.77)$$

It is clear from this that $\lambda \geq 0$ if the right hand side of this equation is positive.

Therefore we consider the functional

$$J[v] := \int_0^\infty \left\{ (v')^2 + q(s)v^2 \right\} ds, \quad (4.78)$$

with

$$q(s) = -4 [k \cos \psi + \cos(2\psi)]. \quad (4.79)$$

The functional (4.78) is of the form (3.5) so the method outlined in section 3.2 can be applied.

4.2.1 Application of the Rayleigh–Ritz method

To apply the Rayleigh–Ritz method to the problem, a numerical program was written, using Simpson’s numerical method to evaluate the integral (4.78). The ψ_3 solution (4.31) was considered first since a stability result from the Atkin and

Stewart paper [34] was already known. If the program produced the same results as the paper, this would indicate whether or not the program was working correctly. The Rayleigh–Ritz program produced positive eigenvalues for given values of a and b which confirmed the result already known. Since there was confidence in the routine, the ψ_2 , ψ_4 and ψ_5 solutions (4.65), (4.67) and (4.68) were now looked at, all of which were found to have positive eigenvalues and therefore to be stable. [The stability for these solutions were only found numerically and only for certain k values, so this is not a complete picture for these solutions.]

When the ψ_1 solution, (4.38), was considered, the Rayleigh–Ritz program could only find second, third and fourth eigenvalues, but not the first. This means that some other method is needed to look at the stability of this solution.

4.2.2 Second variation

Since the Rayleigh–Ritz method failed for the ψ_1 solution and does not give a complete picture for the other solutions, the second variation of the problem was considered. To consider the second variation of this problem, it has to be in the form of (3.15), where $F(s, \phi, \phi')$ is given by the bulk energy (4.14) added to the magnetic energy (4.16) in this case. This can be non-dimensionalised, as was done previously, by introducing

$$s = \ln \left(\frac{r}{r_0} \right), \quad (4.80)$$

then $F(s, \phi, \phi')$ becomes

$$F(s, \phi, \phi') = \frac{1}{2} \left\{ (A_{12} + A_{11}) \sin^4 \phi + (A_{21} + A_{11}) \cos^4 \phi \right. \quad (4.81)$$

$$\left. - A_{11} + B_3 (\phi')^2 - \frac{\Delta\chi}{\mu_0} B^2 r_0^2 \sin^2 \theta \sin^2 \phi \right\}. \quad (4.82)$$

This means that, for this problem,

$$\delta^2 J[h] = \frac{1}{B_3} \int_0^{\psi(s)} \left[p(s) \left(\frac{dh}{ds} \right)^2 + B_3 q(s) h(s)^2 \right] ds \quad (4.83)$$

where

$$p(s) = 1 \quad \text{and} \quad q(s) = \frac{a}{2} \cos \psi - b \cos 2\psi(s) + \frac{2}{B_3} (A_{21} + A_{11}) . \quad (4.84)$$

From [31], the final term of this equation is

$$\frac{2}{B_3} (A_{21} + A_{11}) > 0 \quad (4.85)$$

so if this term is neglected and the second variation given by (4.83) with

$$q(s) = \frac{a}{2} \cos \psi - b \cos 2\psi(s) \quad (4.86)$$

is found to be positive definite then it will still be positive definite once this term has been reinstated.

For the solutions to be stable, the functional by (3.15) must have a minimum. From Section 3.3, a necessary condition for the functional to have a minimum is

$$\delta^2 J[h] > 0 , \quad (4.87)$$

for all admissible h . This does not mean that if the integral is positive definite then the solutions are stable since it is only a necessary condition. From section 3.3.4, the sufficient conditions for a weak minimum are the Euler–Lagrange equation, (3.29), the strengthened Legendre condition, (3.31), and the strengthened Jacobi condition, (3.43).

4.2.2.1 The Euler–Lagrange equation

The Euler–Lagrange equation is the governing equation used to find these solutions, given by (4.22). The solutions automatically satisfy this condition.

4.2.2.2 The Strengthened Legendre condition

The strengthened Legendre condition from (3.31) is

$$F_{\phi'\phi'}(x, \phi_0, \phi_0') \geq 0. \quad (4.88)$$

In particular, here

$$F_{\phi'\phi'} = B_3 \tag{4.89}$$

and $B_3 > 0$ from (4.7), so the strengthened Legendre condition is satisfied by all of our solutions.

4.2.2.3 Strengthened Jacobi condition

The theorem from Section 3.3.2, says that the solutions found by Atkin and Stewart will have no conjugate points and, therefore, satisfy the strengthened Jacobi Condition if the integrand is positive definite. For the integrand to be positive definite, we need

$$p(s)h'(s)^2 + q(\psi_i(s))h(s)^2 > 0. \tag{4.90}$$

For our solutions, $p(s) = 1$ so we have

$$h'(s)^2 + q(\psi_i(s))h(s)^2 > 0, \tag{4.91}$$

but since q depends on ψ_i , we have to look at $q(\psi_i)$ for each of the solutions in turn. If $q \geq 0$ for a solution, then the integrand for that particular solution is positive definite. For ψ_2 we have $q \equiv 0$ and so this solution is stable with no restrictions on the values of the constants a and b . The function q for ψ_i , where $i = 1, 3, 4, 5$, changes sign so the integrand is not positive definite. This does not rule out stability altogether since the integral might still be positive definite as is the case with (3.21), so the integrand needs to be considered in more detail.

4.2.3 Positivity criterion

Before the positivity criterion, (3.65) from Section 3.4, is used to look at the solutions, the point where $q(\psi_i)$ crosses the horizontal s -axis needs to be found. For the ψ_3 to ψ_5 solutions, the $q(\psi_i)$ function only crosses the s -axis at one

point, $s = x_{c_i}$ say, but for ψ_1 the function $q(\psi_1)$ oscillates. The ψ_1 solution will be considered separately later, and for now ψ_3 to ψ_5 will be concentrated on.

The q function for an arbitrary solution ψ_i is given by

$$q(s) = -bk \cos \psi_i - 2b \cos^2 \psi_i + b \quad (4.92)$$

so the point where this cuts the s -axis can be found by considering $q(\psi_i(x_{c_i})) = 0$

$$-bk \cos \psi_i(x_{c_i}) - 2b \cos^2 \psi_i(x_{c_i}) + b = 0, \quad (4.93)$$

$$2 \cos^2 \psi_i(x_{c_i}) + k \cos \psi_i(x_{c_i}) - 1 = 0, \quad (4.94)$$

$$2 \left[\cos \psi_i(x_{c_i}) + \frac{k}{4} \right]^2 - \frac{k^2}{8} = 1, \quad (4.95)$$

$$\cos \psi_i(x_{c_i}) + \frac{k}{4} = \sqrt{\frac{8+k^2}{16}}. \quad (4.96)$$

Looking at each of the ψ_i in turn, the following x_c values are found

$$\psi_3 : \quad x_{c_3} = \sqrt{\frac{2}{b(1-k^2)}} \operatorname{arctanh} \left(\sqrt{\frac{(1-k)(4+k-\sqrt{8+k^2})}{(1+k)(4-k+\sqrt{8+k^2})}} \right), \quad (4.97)$$

$$\psi_4 : \quad x_{c_4} = \sqrt{\frac{1}{6b}}, \quad (4.98)$$

$$\psi_5 : \quad x_{c_5} = \frac{1}{\sqrt{2b(k-1)}} \operatorname{arcsinh} \left(\sqrt{\frac{(k-1)(4+k-\sqrt{8+k^2})}{k(4-k+\sqrt{8+k^2})}} \right). \quad (4.99)$$

These x_{c_i} values will be the upper limit for the integral that will be considered with the generalised positivity criterion. For $s > x_{c_i}$, $q(\psi_i(s)) > 0$, so only the integral from 0 to x_{c_i} needs to be considered. This will make the integrand negative over the whole domain. If the positivity criterion gives stability in this range of s , then we have stability over the whole of $s > 0$. Since only the region up to x_c is being considered, the generalised positivity criterion (3.65) becomes

$$\int_0^{x_{c_i}} |q_-(s)| ds \leq \frac{2}{x_c}. \quad (4.100)$$

The next thing to be considered is the integral of $q(s)$. To simplify, the

integration variable can be changed. This gives

$$\begin{aligned}
 \int_0^{x_{c_i}} |q(s)| ds &= - \int_0^{x_{c_i}} q(s) ds, \\
 &= - \int_0^{\psi(x_{c_i})} q(\psi) \frac{ds}{d\psi} d\psi, \\
 &= - \int_0^{\psi(x_{c_i})} q(\psi) \frac{1}{\psi'(s)} d\psi.
 \end{aligned} \tag{4.101}$$

From (4.28), it is known that

$$\begin{aligned}
 \frac{d\psi}{ds} &= \pm \sqrt{b \cos(2\psi) - 2a \cos \psi + c}, \quad c = \text{const. of int.}, \\
 &= \pm \sqrt{b \cos(2\psi) + 4bk \cos \psi + c} \quad k = -\frac{a}{2b},
 \end{aligned} \tag{4.102}$$

but the value of the integration constant c has to be specified for each solution. For each of the solutions, the constant of integration was chosen so that it completes the square in (4.102) to simplify the problem. For this to happen,

$$c = b - \frac{a^2}{2b}. \tag{4.103}$$

Substituting (4.103) into (4.102)

$$\begin{aligned}
 & - \int_0^{\psi_i(x_c)} \frac{(-bk \cos \psi - 2b \cos^2 \psi + b)}{\sqrt{2b}(\cos \psi + k)} d\psi \\
 &= - \left[\sqrt{2bk} \frac{\psi_i(x_c)}{2} - 2\sqrt{2b} \frac{\tan \frac{\psi_i(x_c)}{2}}{\tan^2 \frac{\psi_i(x_c)}{2} + 1} \right. \\
 & \quad \left. + \frac{\sqrt{2b}}{\sqrt{(1-k)(1+k)}} (1-k^2) \arctan \left\{ \frac{(k-1) \tan \frac{\psi_i(x_c)}{2}}{\sqrt{(1-k)(1+k)}} \right\} \right].
 \end{aligned} \tag{4.104}$$

This evaluated integral will be called $I(b, k)$ from now on.

Looking at the $\frac{\psi_i(x_{c_i})}{2}$ term for the ψ_i solutions, the following results are obtained after simplification

$$\frac{\psi_3(x_{c_3})}{2} = \arctan \left\{ \frac{(4+k - \sqrt{8+k^2})}{(4-k + \sqrt{8+k^2})} \right\}, \tag{4.105}$$

$$\frac{\psi_4(x_{c_4})}{2} = \arctan \left\{ \frac{1}{\sqrt{3}} \right\} = \frac{\pi}{6}, \tag{4.106}$$

$$\frac{\psi_5(x_{c_5})}{2} = \arctan \left\{ \frac{(4+k - \sqrt{8+k^2})}{(4-k + \sqrt{8+k^2})} \right\}. \tag{4.107}$$

Notice that (4.105) is the same as (4.107) even though their x_c values are different. These values of $\psi_i(x_{c_i})/2$ were then substituted back into (4.104) for each ψ_i .

To allow the behaviour of the integral (4.104), in relation to the positivity criterion, to be considered easily, we can consider the function, given by

$$f_i(b, k) = \frac{2}{x_{c_i}} - I(b, k). \quad (4.108)$$

If $f_i(b, k) > 0 \forall b > 0$ and $\forall k$ in the range for the specific solution, then our positivity criterion is satisfied and our solution is stable.

Straight away this can be used to look at the ψ_4 solution, (4.32), which is

$$\psi_4 = 2 \arctan\left(\sqrt{2b} s\right), \quad a = -2b \quad \text{i.e., } k = 1. \quad (4.109)$$

The value of our integral for this solution is

$$\begin{aligned} I(b) &= - \left[\frac{\sqrt{2b}}{\sqrt{3}} - \frac{2\sqrt{2b}}{\sqrt{3}(\frac{1}{3} + 1)} \right], \\ &= - \left[\frac{\sqrt{2b}}{\sqrt{3}} - \frac{\sqrt{3b}}{\sqrt{2}} \right], \end{aligned} \quad (4.110)$$

$$= \frac{\sqrt{b}}{\sqrt{6}} > 0 \quad \forall b > 0. \quad (4.111)$$

It is known that the x_{c_4} value for this solution, given by (4.98), is

$$x_{c_4} = \sqrt{\frac{1}{6b}}, \quad (4.112)$$

so

$$f_4(b, k) = f_4(b) = 2\sqrt{6b} - \frac{\sqrt{b}}{\sqrt{6}}, \quad (4.113)$$

$$= \frac{11\sqrt{b}}{\sqrt{6}}, \quad (4.114)$$

$$> 0 \quad \forall b > 0. \quad (4.115)$$

This means that the ψ_4 solution satisfies the generalised positivity criterion (3.65) and since this is satisfied, it means that the integral is positive definite and the solution is stable $\forall b > 0$.

For the ψ_3 and ψ_5 solutions, the analysis is not so straightforward. These solutions are valid for different ranges of k so using polar co-ordinates simplifies the problem. For this, it has to be remembered that, from (4.36),

$$k = \frac{-a}{2b}, \quad (4.116)$$

so k depends on a and b . If we set

$$a = r \cos \alpha \quad (4.117)$$

and

$$b = r \sin \alpha, \quad (4.118)$$

and substitute these into (4.105), (4.107) and (4.104) we can look at the bounding curve for each of the solutions given by (4.108) with r ranging from 0 to ∞ and the α range depending on the solution.

For the ψ_3 solution, $f_3(b, k)$ is given by

$$f_3(b, k) = \frac{2}{x_{c3}} - I(b, k(a, b)). \quad (4.119)$$

Substituting (4.117) and (4.118) into this gives

$$f_3(r, \alpha) = \sqrt{\frac{r \tan(\alpha/2)}{1 + \tan^2(\alpha/2)}} \left[\frac{\sqrt{4 - \frac{1}{\tan^2(\alpha)}}}{\operatorname{arctanh}\left(\frac{1 + 2 \tan(\alpha)}{2 \tan(\alpha)} g(\alpha)\right)} + \frac{\operatorname{arctan}\left(\sqrt{g(\alpha)}\right)}{\tan \alpha} \right. \\ \left. + \frac{4\sqrt{g(\alpha)}}{g(\alpha) + 1} + \frac{\operatorname{arctan}\left(\sqrt{-1 - 2 \tan(\alpha)} \sqrt{g(\alpha)}\right)}{\sqrt{\left(1 - \frac{1}{2 \tan \alpha}\right) \left(\frac{-1}{2 \tan \alpha} - 1\right)}} \left(-2 + \frac{1}{2 \tan^2 \alpha}\right) \right], \quad (4.120)$$

$$f_3(r, \alpha) := \sqrt{r} h_3(\alpha), \quad (4.121)$$

where

$$g(\alpha) = \frac{4 - \frac{1}{2 \tan \alpha} - \sqrt{8 + \frac{1}{4 \tan^2 \alpha}}}{4 + \frac{1}{2 \tan \alpha} + \sqrt{8 + \frac{1}{4 \tan^2 \alpha}}}. \quad (4.122)$$

For this solution, the α variable has the range $\arctan\left(\frac{1}{2}\right) < \alpha < \pi - \arctan\left(\frac{1}{2}\right)$ since $|a| < 2b$ for the solution to be valid. Only the function $h_3(\alpha)$ needs to be considered to determine whether or not this solution is stable since r is always positive. If this function is plotted for an arbitrary r then the following graph in Fig. 19 is obtained. This graph shows that $h_3(\alpha)$ is never less than 0 within

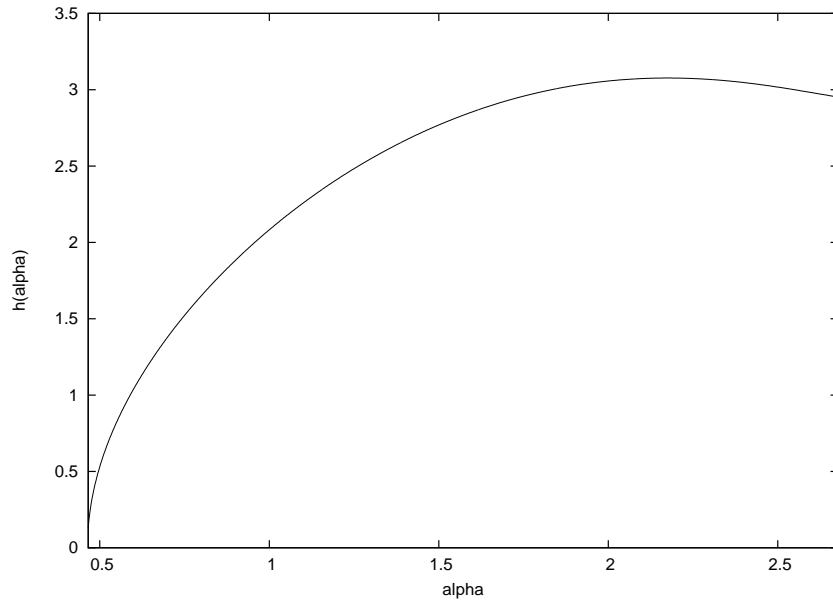


Figure 19: The graph never touches 0 so $h_3(\alpha) > 0$ for all $\arctan\left(\frac{1}{2}\right) < \alpha < \pi - \arctan\left(\frac{1}{2}\right)$ since $|a| < 2b$

the specified range of α . The limit of $h_3(\alpha)$ as α approaches $\arctan\left(\frac{1}{2}\right)$ is

$$\lim_{\alpha \rightarrow \arctan\left(\frac{1}{2}\right)} h_3(\alpha) = 0, \quad (4.123)$$

and as $\alpha \rightarrow \pi - \arctan\left(\frac{1}{2}\right)$ the limit of $h_3(\alpha)$ is

$$\lim_{\alpha \rightarrow \pi - \arctan\left(\frac{1}{2}\right)} h_3(\alpha) \approx 2.952297924. \quad (4.124)$$

This means that the function $f_3(b, k)$, given by (4.108), never crosses the s -axis within the α range for this solution, so the positivity criterion holds for this solution $\forall b > 0$ and $\forall k$ such that $|k| < 1$ and so the ψ_3 solution is stable.

For the ψ_5 solution, the range of α for which the solution is valid is $\pi - \arctan\left(\frac{1}{2}\right) < \alpha < \pi$. This covers all k values greater than 1. (The $k = 1$ case is the ψ_4 solution). The analysis of this solution carries through in exactly the same way and $f(b, k)$ is of the form

$$f_5(r, \alpha) = \sqrt{r} h_5(\alpha), \quad (4.125)$$

as before. The graph of $h_5(\alpha)$ in the interval $[\pi - \arctan\left(\frac{1}{2}\right), \pi]$ is shown below in Fig. 20. As was the case with the ψ_3 solution, the ψ_5 solution is stable since

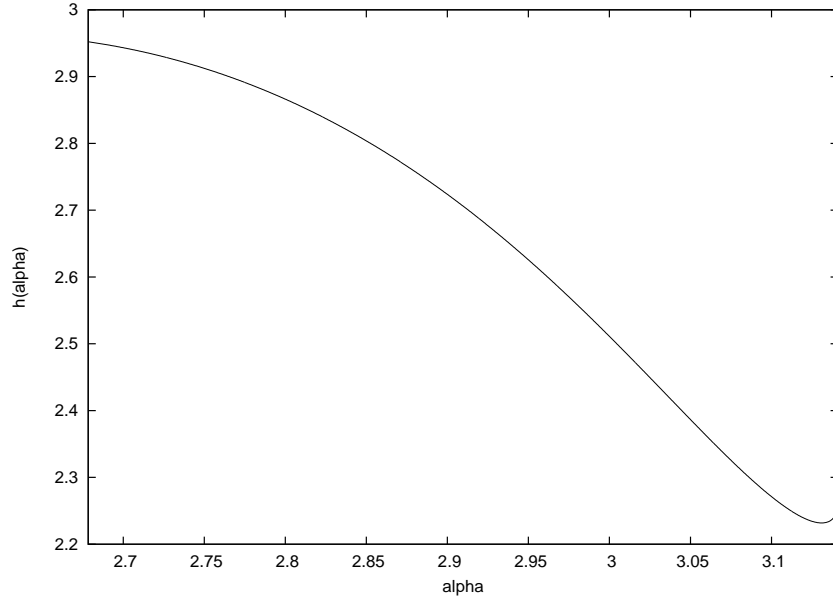


Figure 20: The graph never touches 0 so $h_5(\alpha) > 0$ for all $\pi - \arctan\left(\frac{1}{2}\right) < \alpha < \pi$

it satisfies the generalised positivity criterion given by (3.65). For this solution,

the limits of $h_5(\alpha)$ as α tends towards the limits of its range are

$$\lim_{\alpha \rightarrow \pi - \arctan(\frac{1}{2})} h_5(\alpha) \approx 2.952297924, \quad (4.126)$$

which agrees with the limit for the ψ_3 solution, and

$$\lim_{\alpha \rightarrow \pi} h_5(\alpha) \approx 2.269185314. \quad (4.127)$$

This only leaves the ψ_1 with its stability unknown. To look at this we are going to have to use a different method as our positivity criterion is not satisfied for this solution because of its oscillatory periodic behaviour. We will try to use the Jacobi equation of the functional (3.15) for this.

4.2.4 The Jacobi equation

From section 3.3.2, the Jacobi equation can be used to determine whether or not the second variation of a functional is positive. If the Jacobi equation has a solution which crosses the x -axis within the x range of the problem, then the solution is not stable.

Before beginning to look for a solution to the Jacobi equation (3.26), we need to establish whether or not a solution exists to this equation for the ψ_1 solution. For this solution, the Jacobi equation is

$$u'' - q(x)u = 0, \quad (4.128)$$

where $q(x)$ is given by (4.79). If we let $v = u'$, we have

$$\begin{aligned} u' &= v, \\ v' &= qu. \end{aligned}$$

This gives the system

$$\begin{bmatrix} u \\ v \end{bmatrix}' = \begin{bmatrix} 0 & 1 \\ q(s) & 0 \end{bmatrix} \begin{bmatrix} u \\ v \end{bmatrix} + \begin{bmatrix} 0 \\ 0 \end{bmatrix}, \quad (4.129)$$

which is of the form

$$\underline{\mathbf{y}}' = M\underline{\mathbf{y}} + \underline{\mathbf{f}}, \quad (4.130)$$

where M is a square matrix and $\underline{\mathbf{f}}$ is a continuous vector. The existence of a unique solution is guaranteed [28] since the system is of the correct form and the initial values are

$$\begin{bmatrix} u(0) \\ v(0) \end{bmatrix} = \begin{bmatrix} u(0) \\ u'(0) \end{bmatrix} = \begin{bmatrix} 0 \\ \alpha \end{bmatrix}, \quad (4.131)$$

where α is any number, see [26]. If this solution is found, then for the problem to be stable, it must never touch the x -axis for $x > 0$ or it will have conjugate points.

In the general case, this system is very difficult to solve. The behaviour of the solution with k large and negative was looked at. Since $k = \frac{-a}{2b}$ this is the same as taking a positive and very large compared to b . When k is very large and negative

$$\sqrt{\frac{k+1}{k-1}} \simeq 1$$

and

$$\sqrt{k^2 - 1} \simeq -k, \quad (4.132)$$

so the ψ_1 solution becomes

$$\psi(s) = -2n\pi + 2\sqrt{\frac{b}{2}} ks, \quad (4.133)$$

$$= -2n\pi + \sqrt{2b} ks. \quad (4.134)$$

If this is substituted into the $q(s)$ given by (4.79) we get

$$q(s) = -bk \cos(\sqrt{2b} ks) - 2b \cos^2(\sqrt{2b} ks) + b. \quad (4.135)$$

For $k \gg b$, this behaves like

$$q(s) = -bk \cos(\sqrt{2b} ks). \quad (4.136)$$

Now substituting (4.136) into the Jacobi equation (4.128) and setting $u(0) = 0$ and $u'(0) = 1$ and solving gives the solution

$$u(s) = \frac{2}{\sqrt{b}k} \text{MathieuS} \left(0, \frac{1}{-k}, \frac{\sqrt{b}}{2} ks \right), \quad (4.137)$$

where

$$\text{MathieuS} \left(0, \frac{-1}{k}, \frac{\sqrt{b}}{2} ks \right) \quad (4.138)$$

is the odd solution to the Mathieu equation

$$y''(x) + (a - q \cos(2x))y = 0 \quad (4.139)$$

with $a = 0$ and $q = -\frac{1}{k}$. This solution $u(s)$ oscillates and crosses the s -axis many times so, for k sufficiently large in relation to b , the Jacobi equation has conjugate points so the ψ_1 solution is unstable.

4.3 Conclusions

In this chapter, the stability of the five solutions to the equations arising from considering smectic C domain walls in a cylindrical geometry, found by Atkin and Stewart (4.29)-(4.33), has been analysed. This analysis began by looking at the Rayleigh–Ritz method for finding eigenvalues. This found that, for specific values of k and b , the ψ_2 , ψ_3 , ψ_4 and ψ_5 solutions were stable but it was unable to determine whether or not the ψ_1 case was stable.

The second variation of the problem was then considered. The solutions automatically satisfied the Euler–Lagrange equations and the strengthened Legendre condition was satisfied so only the Jacobi condition was left to be satisfied to guarantee stability. The functional (3.15) with $P(s)$ and $Q(s)$ given by (4.84) had a positive definite integrand for ψ_2 meaning that there were no conjugate points and so the strengthened Jacobi condition was satisfied and the solution was stable. The positivity criterion from section 3.4 was used to prove that the

ψ_3 , ψ_4 and ψ_5 solutions were also stable with no restrictions on the values of a and b .

The ψ_1 case proved to be more complicated. The Jacobi equation (4.128) was used to prove that, for k sufficiently large and negative, the ψ_1 solution is unstable. Unfortunately, the case for k approaching -1 from below could not be tackled in the same way. This means that there is still more work to be done on this solution to determine whether or not it is unstable for all $b > 0$ and all $k < -1$.

The same governing equation (4.28) would arise if an electric field was applied to an infinite sample of planar layers of smectic C liquid crystals. Instead of a magnetic energy, there would be an electric energy, and the bulk energy would differ, but equation (4.27) still comes out as the governing equilibrium equation. This means the same analysis of the phase diagrams could be done and we would have the same solutions, with different a and b values. These bulk and electric energies are given by Atkin and Stewart in [36]. This will be considered in the following chapter.

5 Smectic C Domain Walls in Planar Layers

As mentioned in the previous chapter, the equation (4.27) occurs if an electric field was applied to an infinite sample of planar layers of smectic C liquid crystals. In this chapter new solutions will be found to this equation and the stability of these will be briefly considered for the case which may occur within this set up where the term b is negative. Here, no influence of the director on the field was taken into account, as is normal practice in the first approaches to specific liquid crystal problems.

Suppose that an electric field is applied to a sample at an angle α where α is the angle between the electric field and the plane of the layers, and the x -axis is chosen such that the electric field is in the (x, z) -plane, and

$$0 < \alpha < \frac{\pi}{2}. \quad (5.1)$$

If the layers are parallel to the xy plane and the layer normal is parallel to the z axis then the vectors \mathbf{a} and \mathbf{c} are given by

$$\mathbf{a} = (0, 0, 1) \quad (5.2)$$

and

$$\mathbf{c} = (\cos \phi(z), \sin \phi(z), 0), \quad (5.3)$$

and the electric field is given by

$$\mathbf{E} = E_0 (\cos \alpha, 0, \sin \alpha), \quad (5.4)$$

where E_0 is the strength of the electric field. The set up is shown below in Fig. 21.

From [36], the bulk and electric energies for this problem are given by

$$w_b = \frac{1}{2} B_3 [\phi'(z)]^2 \quad (5.5)$$

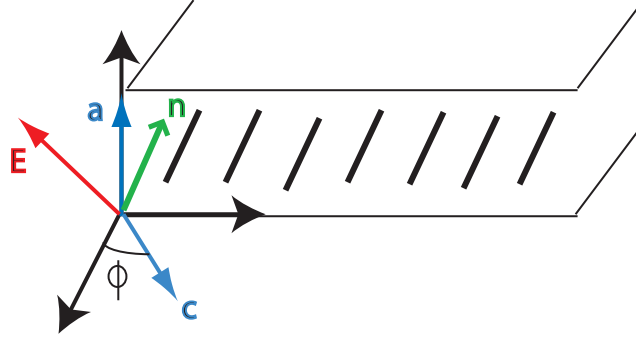


Figure 21: A physical representation of the geometry of the problem.

and

$$w_e = -\frac{1}{2}\epsilon_0\epsilon_a E_0^2 (\mathbf{n} \cdot \mathbf{E})^2 \quad (5.6)$$

$$= -\frac{1}{2}\epsilon_0\epsilon_a E_0^2 (\sin \alpha \cos \theta + \cos \alpha \sin \theta \cos \phi)^2 \quad (5.7)$$

respectively, where ϵ_0 is the permittivity of free space (and $\epsilon_0 > 0$) and ϵ_a is the dielectric anisotropy of the liquid crystal and \mathbf{n} is given by

$$\mathbf{n} = (\cos \phi \sin \theta, \sin \phi \sin \theta, \cos \theta). \quad (5.8)$$

As before, the governing equilibrium equation reduces to (4.27), namely

$$\frac{d^2\psi}{ds^2} = a \sin \psi - b \sin 2\psi, \quad (5.9)$$

but, from [36], the values of a and b are now given by

$$a = \frac{1}{B_3} (\epsilon_0\epsilon_a E_0^2 \sin \alpha \cos \alpha \sin \theta \cos \theta) \quad (5.10)$$

and

$$b = -\frac{1}{2B_3} (\epsilon_0\epsilon_a E_0^2 \cos^2 \alpha \sin^2 \theta). \quad (5.11)$$

This means that if $\epsilon_a > 0$ then $a > 0$ but $b < 0$ (and so $k > 0$), whereas with the cylindrical case $b > 0$.

The phase portraits for the $b < 0$ case can be seen below in Fig. 22 where k is defined as before in (4.36). Comparing these with Fig. 17, the phase portraits

for the $b > 0$ case, it can be seen that the phase portrait for $b = 1$ with $k = -2$ is the same as $b = -1$ with $k = 2$ and similarly $b = 1$ with $k = 2$ is the same as $b = -1$ with $k = -2$. However, the phase portraits for $b = 1$ with $k = \frac{1}{2}$ and is different from those for $b = -1$ with $k = -\frac{1}{2}$ and $k = \frac{1}{2}$. The phase portrait for $k = -\frac{1}{2}$ will be looked at in more detail.

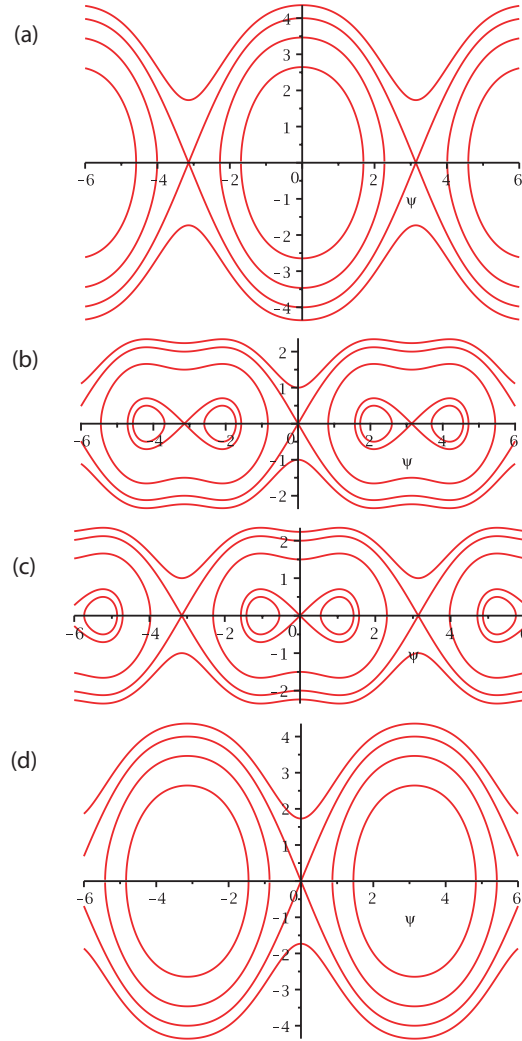


Figure 22: These are the phase portraits for (a) $k < -1$, (b) $-1 < k < 0$, (c) $0 < k < 1$ and (d) $k > 1$.

From the types of solutions shown on the phase portrait, it is physically reasonable for us to expect the homoclinic and heteroclinic orbits to be related

to travelling waves. We expect the periodic phase portraits to be energetically unfavourable.

5.1 Solutions

From above, it is known that

$$\frac{d\psi}{ds} = \pm \sqrt{b \cos 2\psi - 2a \cos \psi + c} \quad (5.12)$$

and taking the positive square root for convenience, gives

$$\frac{d\psi}{ds} = \sqrt{2b \cos^2 \psi + 4bk \cos \psi + c - b}, \quad (5.13)$$

where c is an arbitrary constant. This leads to the equation

$$\int \frac{d\psi}{\sqrt{2b \cos^2 \psi + 4bk \cos \psi + c - b}} = \int ds. \quad (5.14)$$

The following substitutions can be made to the left hand side of the equation

$$\cos \psi = \frac{1 - t^2}{1 + t^2} \quad (5.15)$$

and

$$\frac{d\psi}{dt} = \frac{2}{1 + t^2} \quad (5.16)$$

where

$$t = \tan\left(\frac{\psi}{2}\right). \quad (5.17)$$

After this substitution the equation becomes

$$\int \frac{2 dt}{\sqrt{t^4(b + c - 4bk) + t^2(-6b + 2c) + (b + c + 4bk)}} = \int ds \quad (5.18)$$

$$\int \frac{2 dt}{\sqrt{t^4 a_1 + t^2 b_1 + c_1}} = \int ds \quad (5.19)$$

where

$$a_1 = b + c - 4bk \quad (5.20)$$

$$b_1 = -6b + 2c \quad (5.21)$$

$$\text{and } c_1 = b + c + 4bk. \quad (5.22)$$

This is the full solution for the problem. The value of c can be chosen to find specific solutions as it is this value which dictates where the solution starts in the phase portrait.

From (5.19), a_1 can be taken outside the left hand side integral to give

$$\int \frac{2 dt}{\sqrt{t^4 a_1 + t^2 b_1 + c_1}} = \frac{1}{\sqrt{a_1}} \int \frac{2 dt}{\sqrt{t^4 + t^2 \frac{b_1}{a_1} + \frac{c_1}{a_1}}} \quad (5.23)$$

If the substitution

$$x = t^2 \quad \text{with} \quad dt = \frac{dx}{2\sqrt{x}} \quad (5.24)$$

is made then (5.19) becomes

$$\frac{1}{\sqrt{a_1}} \int \frac{dx}{\sqrt{x^3 + x^2 \frac{b_1}{a_1} + x \frac{c_1}{a_1}}} = \int ds \quad (5.25)$$

$$\frac{1}{\sqrt{a_1}} \int \frac{dx}{\sqrt{x(x-A)(x-B)}} = \int ds \quad (5.26)$$

where

$$\begin{aligned} A &= \frac{-b_1}{2a_1} + \frac{1}{2} \sqrt{\frac{b_1^2}{a_1^2} - 4 \frac{c_1}{a_1}} \\ &= \frac{3b - c}{b + c - 4bk} + \frac{1}{2(b + c - 4bk)} \sqrt{(-6b + 2c)^2 - 4(b + c + 4bk)(b + c - 4bk)} \\ &= \frac{3b - c}{b + c - 4bk} + \frac{2\sqrt{2}}{(b + c - 4bk)} \sqrt{b^2 - bc + 2b^2k^2}, \end{aligned} \quad (5.27)$$

and similarly

$$B = \frac{3b - c}{b + c - 4bk} - \frac{2\sqrt{2}}{(b + c - 4bk)} \sqrt{b^2 - bc + 2b^2k^2}. \quad (5.28)$$

The denominator in 5.26 has three roots, namely 0, A and B . From Gradstein and Ryshik [37], the integral

$$\int \frac{dx}{\sqrt{x(x-A)(x-B)}} \quad (5.29)$$

depends on the relative sizes of the roots, r_1 , r_2 and r_3 . If the roots are ordered in size such that $r_1 > r_2 > r_3$ (where r_1 , r_2 and r_3 are either 0, A or B) then

there are 8 different possible solutions depending on where the variable u (the solution, in this case) lies. Here only one of these solutions is explained in detail. For the remaining seven solutions, please see the Appendix A.

Case 1: $r_1 > r_2 > r_3 \geq u$

If it is the case that all three roots are greater than u or the final root is equal to u then the integral gives a solution of the form of

$$\int_{-\infty}^u \frac{dx}{\sqrt{(r_1-x)(r_2-x)(r_3-x)}} = \frac{2}{\sqrt{r_1-r_3}} F(\alpha, p) \quad (5.30)$$

where

$$\alpha = \arcsin \left(\sqrt{\frac{r_1-r_3}{r_1-u}} \right) \quad (5.31)$$

and

$$p = \sqrt{\frac{r_1-r_2}{r_1-r_3}}. \quad (5.32)$$

The function F is the elliptic integral of the first kind (from [37]) which is

$$\begin{aligned} F(\varphi, k) &= \int_0^\varphi \frac{d\alpha}{\sqrt{1-k^2 \sin^2 \alpha}} \\ &= \int_0^{\sin \varphi} \frac{dx}{\sqrt{(1-x^2)(1-k^2 x^2)}}. \end{aligned} \quad (5.33)$$

For this scenario, the full equation becomes

$$\begin{aligned} \frac{2}{\sqrt{r_1-r_3}} F \left(\arcsin \left(\sqrt{\frac{r_1-r_3}{r_1-u}} \right), \sqrt{\frac{r_1-r_2}{r_1-r_3}} \right) &= \sqrt{a_1} s \\ \Rightarrow F \left(\arcsin \left(\sqrt{\frac{r_1-r_3}{r_1-u}} \right), \sqrt{\frac{r_1-r_2}{r_1-r_3}} \right) &= \frac{\sqrt{r_1-r_3}}{2} \sqrt{a_1} s. \end{aligned} \quad (5.34)$$

This solution has to be rearranged in terms of u . To do this, the inverse of the elliptic function has to be taken. From Gradstein and Ryshik [37], the inverse of the elliptic function $F(\varphi, k)$ is the amplitude function, so that

$$\text{am}(F(\varphi, k), k) = \varphi. \quad (5.35)$$

The amplitude function can be is represented by a power series as

$$\begin{aligned} \operatorname{amu} = & u - \frac{k^2}{3!}u^3 + \frac{k^2(4+k^2)}{5!}u^5 - \frac{k^2(16+44k^2+k^4)}{7!}u^7 \\ & + \frac{k^2(64+912k^2+408k^4+k^6)}{9!}u^9 - \dots \end{aligned} \quad (5.36)$$

for

$$|u| < |\mathbf{K}'| \quad (5.37)$$

where u has a period of $4\mathbf{K}'i$ where K is the elliptic integral with $\mathbf{K}(\sqrt{1-k^2}) = \mathbf{K}' = \mathbf{K}(k')$.

Applying the amplitude function to both sides, (5.34) becomes

$$\arcsin\left(\sqrt{\frac{r_1-r_3}{r_1-u}}\right) = \operatorname{am}\left(\frac{\sqrt{r_1-r_3}}{2}\sqrt{a_1}s, \sqrt{\frac{r_1-r_2}{r_1-r_3}}\right) \quad (5.38)$$

Rearranging this for u gives

$$u = r_1 - (r_1 - r_3) \operatorname{csc}^2\left(\operatorname{am}\left(\frac{\sqrt{r_1-r_3}}{2}\sqrt{a_1}s, \sqrt{\frac{r_1-r_2}{r_1-r_3}}\right)\right) \quad (5.39)$$

The variable u here is a dummy for t^2 so

$$t^2 = r_1 - (r_1 - r_3) \operatorname{csc}^2\left(\operatorname{am}\left(\frac{\sqrt{r_1-r_3}}{2}s, \sqrt{\frac{r_1-r_2}{r_1-r_3}}\right)\right) \quad (5.40)$$

$$\tan^2\frac{\psi}{2} = r_1 - (r_1 - r_3) \operatorname{csc}^2\left(\operatorname{am}\left(\frac{\sqrt{r_1-r_3}}{2}\sqrt{a_1}s, \sqrt{\frac{r_1-r_2}{r_1-r_3}}\right)\right) \quad (5.41)$$

so rearranging this for ψ gives

$$\psi = 2 \arctan\left(\sqrt{r_1 - (r_1 - r_3) \operatorname{csc}^2\left(\operatorname{am}\left(\frac{\sqrt{r_1-r_3}}{2}\sqrt{a_1}s, \sqrt{\frac{r_1-r_2}{r_1-r_3}}\right)\right)}\right) \quad (5.42)$$

This is the solution for the differential equation when $\tan^2\frac{\psi}{2}$ is less than or equal to the lowest of the roots 0, A and B .

5.2 Specific solutions

If k is chosen to be $\frac{1}{2}$ and b to be -1 , all the solutions within the phase plane can be found. There are five qualitatively different solutions. These are shown below

in Fig. 23 where one of each type of solution has been coloured differently to allow easy distinction between them. Starting from the top most solution and working towards zero, the first two solutions are 2π periodic with the second one being a separatrix. The third solution is a heteroclinic orbit, the fourth is a homoclinic orbit and the fifth is periodic.

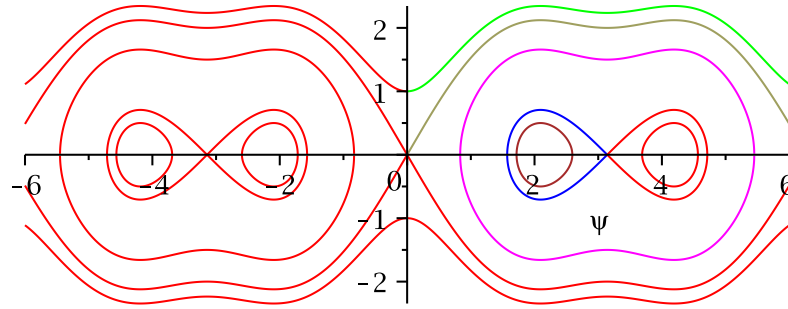


Figure 23: These are the phase portraits for $k = \frac{1}{2}$ with $b = -1$.

Starting from the outside of the phase portrait and working towards the ψ axis, the first solution (which has been plotted in green) is given by

$$\psi_1(s) = 2 \arctan \left(\sqrt{\frac{17(J_1(s)^2 - 1)}{(4\sqrt{2} - 7)J_1(s)^2 + 7 + 4\sqrt{2}}} \right) \quad (5.43)$$

where

$$J_1(s) = \text{am} \left(\frac{1}{4}i\sqrt{7 + 4\sqrt{2}}s, \frac{\sqrt{17}}{7 + 4\sqrt{2}} \right). \quad (5.44)$$

The khaki coloured solution is given by

$$\psi_2(s) = 2 \arctan (\cosh(s)) . \quad (5.45)$$

This solution, in general terms is given by

$$\psi_2(s) = 2 \arctan \left(\cosh(\sqrt{-b} s) \right) \quad (5.46)$$

and only occurs when $k = \frac{1}{2}$.

The next solution to be considered is the pink one. This is given by

$$\psi_3(s) = 2 \arctan \left(\sqrt{\frac{8\sqrt{2} - (5 + 4\sqrt{2})J_3(s)^2}{J_3(s)^2}} \right) \quad (5.47)$$

where

$$J_3(s) = \operatorname{am} \left(2^{\frac{1}{4}} s, \frac{2^{\frac{1}{4}}}{4} \sqrt{5 + 4\sqrt{2}} \right) . \quad (5.48)$$

The fourth type of solution within the phase plane is the homoclinic orbit shown in blue. This solution is given by

$$\psi_4(s) = 2 \arctan \left(\sqrt{3} \sqrt{\frac{1}{\cosh^2(\sqrt{3} s) - 1}} \right) \quad (5.49)$$

The final type of solution within this phase plane is the orbit shown in brown. This is given by

$$\psi_5(s) = 2 \arctan \left(\sqrt{7 + 2\sqrt{11}} s \sqrt{\frac{1 - J_5(s)^2}{J_5(s)^2}} \right) \quad (5.50)$$

with

$$J_5(s) = \operatorname{sn} \left(\frac{1}{2} \sqrt{7 + 2\sqrt{11}} s, \sqrt{2} i \right) . \quad (5.51)$$

5.3 Stability of the solutions

The stability of each of the five solutions above will be considered in turn. The analysis of the second variation is the same for the planar case as it is for the

cylindrical case so the q function is the same as previously, given by (4.92), namely

$$q(x) = -bk \cos \psi_i - 2b \cos^2 \psi_i + b. \quad (5.52)$$

All five of the solutions were first of all considered using the Rayleigh–Ritz stability method over the range of $s = 0$ to $s = 1$. For this range of s the solutions were all found to be stable. However, this changed as the interval was increased and the stability results from this for $\psi_1(s)$, $\psi_3(s)$ and $\psi_5(s)$ changed over a short range $s = 0$ to $s = \pi$.

To consider the stability further, the second variation along with the positivity criterion from Section 3.4 was considered as in the previous chapter. This requires that

$$\int_0^{x_{c_b}} |q_-(x)| dx \leq \frac{2}{x_c}, \quad (5.53)$$

where x_c is the point where $q(x)$ cuts the x axis. For $\psi_1(s)$, $\psi_3(s)$ and $\psi_5(s)$ the $q(\psi(s))$ function crossed the axis multiple times, so the positivity criterion failed. However, for the other two solutions the graph had the same qualitative behaviour as the stable solutions from the preceding chapter. In the case of $\psi_4(s)$ the positivity criterion held, and so we have stability for this solution. However, the positivity criterion failed for the $\psi_2(s)$ case. In this case the negative area was only slightly greater than required for stability. It is probable that the solution is stable but further analysis is required.

The next step which should be followed is to look at the Jacobi equation for the remaining four solutions to determine if there are any conjugate points within the second variation. As noted before, if a conjugate point arises then we have instability. This would be the next step but unfortunately time constraints have not allowed us to complete the story with these solutions.

5.4 Conclusions

Within this chapter we have found five new solutions to the differential equation (4.27). The stability of these five solutions was considered using the Rayleigh–Ritz method, and the positivity criterion due to Gartland [24] was used to try to determine whether or not the integrand of the second variation was positive definite. The only case which was conclusively found to be stable was the case for $\psi_4(s)$, further analysis on the other cases is needed.

The work in this and the preceding chapter may have implications for experimentalists. From [36], the motivation for this work is that it is hoped that the solutions may lead to experiments which can determine the unknown elastic constants A_{ij} as there is very little experimental data on these constants.

6 Fluctuations of a Thin Nematic Film

Dewetting is the term used to describe when a thin fluid ruptures on a substrate to create droplets. The opposite of this, when the thin film spreads out, is called wetting. Wetting is important for many applications including coating and lubrication and dewetting is unwanted as it ruins the thin film applied. The dewetting may occur because of dust on the substrate or defects within it or it may be caused by fluctuations of the free surface. Dewetting caused by these fluctuations is called spinodal dewetting.

The problem of nematic liquid crystal dewetting was looked at in [38] by Vandembrouck et al. with a linear director profile with a fixed director angle at the surface to find out more information about when dewetting occurs. The work in that paper is covered within the following work but is done in a more rigorous mathematical fashion. Some of the approximations and simplifications are then removed which allows comparisons between the methods, and finally the director angle is given more freedom to see what can be achieved.

In this chapter, the problem being considered is a thin film of nematic liquid crystal of a depth h_0 which has its surface perturbed. Using the resultant equations, the velocities in the x and z directions can be obtained, and from these the stability of the film can be assessed as to whether or not the film will dewet (stability or instability).

This chapter begins with a review of the work carried out by Vandembrouck et al. [38] and then the problem is developed further by introducing non-isotropic viscosities. The chapter concludes by considering the model with different liquid crystal materials to see which materials it is valid for, and which ones it is not.

6.1 Physical setup

The original undisturbed level of the surface is h_0 and this is perturbed to give a free surface described by

$$h(x, t) = h_0 + \xi_0(t) \sin(qx), \quad (6.1)$$

where q is the wave vector of the fluctuation caused by the perturbation and it is assumed that $\xi_0 \ll h_0$. This is illustrated below in Fig. 24.

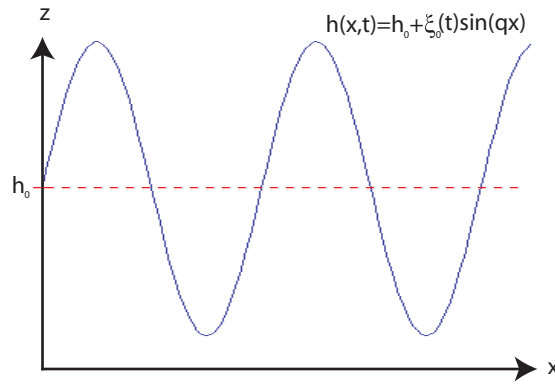


Figure 24: The set up of the problem.

It is assumed that the director has a linear profile in z where the director angle is 0 at $z = 0$ and θ , a fixed constant, at $z = h(x, t)$, the surface of the thin film given by (6.1), as shown in Fig. 25. This means that the angle of the director is given by

$$f(x, z, t) = \frac{\theta}{h(x, t)} z, \quad (6.2)$$

where $h(x, t)$ is given by (6.1).

The director for the sample of liquid crystal is

$$\mathbf{n} = (\cos(f(x, z, t)), 0, \sin(f(x, z, t))) \quad (6.3)$$

where $f(x, z, t)$ is assumed to be small. This means that the director for this problem is given by

$$\mathbf{n} \approx (1, 0, f(x, z, t)) . \quad (6.4)$$

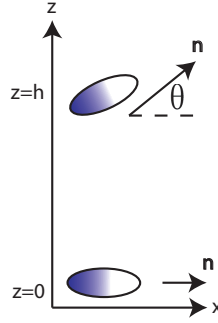


Figure 25: The director has a linear profile in z from $\theta_0 = 0$ at $z = 0$ to $\theta_1 = \theta$ at $z = h$.

The free-energy functional fit to describe the equilibrium properties of the fluid can now be constructed from the nematic energy (2.12) and the dispersion potential for a wetting liquid [39]. From (2.12)

$$w_F = \frac{1}{2}K \left(\left(\frac{\partial f}{\partial x} \right)^2 + \left(\frac{\partial f}{\partial z} \right)^2 \right) + \frac{A}{6\pi h^3}. \quad (6.5)$$

The lubrication approximation that the length scale in the x direction is much greater than in the z direction will be assumed so the x derivative can be ignored and so

$$w_F = \frac{1}{2}K \left(\frac{\partial f}{\partial z} \right)^2 + \frac{A}{6\pi h^3} \quad (6.6)$$

$$= \frac{1}{2} \frac{K\theta^2}{h^2} + \frac{A}{6\pi h^3}. \quad (6.7)$$

The free surface energy density of the problem is given by

$$F(h) = \int w_F dh \quad (6.8)$$

$$= \frac{1}{2} \frac{K\theta^2}{h} - \frac{A}{12\pi h^2} + C \quad (6.9)$$

where the constant term would contain the surface tensions between the solid boundary and the liquid crystal film and the surface tension between the air and the film. This means that the free energy per unit surface can be written as

$$F(h) = \gamma_{sl} + \gamma_{lv} + \frac{1}{2} \frac{K\theta^2}{h} - \frac{A}{12\pi h^2} \quad (6.10)$$

where γ_{sl} is the surface tension between the solid and the liquid and γ_{lv} is the surface tension between the liquid and air.

This problem is only considered in 2D so there are only velocities in the x and z direction, so

$$\mathbf{v} = (u(x, z, t), 0, v(x, z, t)) . \quad (6.11)$$

These will be found from the equations for the problem.

The fluid is assumed to be incompressible and it is also a requirement that mass is conserved, so it is required that

$$\nabla \cdot \mathbf{v} = 0 \quad \text{i.e.,} \quad u_x + v_z = 0 . \quad (6.12)$$

6.2 Isotropic viscosity

If the assumption is made that the viscosity of the liquid crystal is isotropic then the equations to be solved become a lot simpler. For an isotropic viscosity it is assumed that the dynamic viscosity is given by

$$\eta = \eta_3 = \frac{1}{2}\alpha_4 \quad (6.13)$$

while

$$\alpha_i = 0 \quad \text{for } i \neq 4 . \quad (6.14)$$

Using this assumption, the \tilde{t}_{ij} term in the Ericksen–Leslie equations simply becomes

$$\tilde{t}_{ij} = \eta (v_{i,ii} + v_{i,jj}) \quad (6.15)$$

which means that they are reduced to the Navier–Stokes equations.

6.2.1 Navier–Stokes equation

The Navier–Stokes equations, from [40], are

$$\frac{\partial \mathbf{v}}{\partial t} + (\mathbf{v} \cdot \nabla) \mathbf{v} = -\frac{1}{\rho} \nabla p + \nu \nabla^2 \mathbf{v} + \mathbf{g} \quad (6.16)$$

$$\nabla \cdot \mathbf{v} = 0 \quad (6.17)$$

where ν is the viscosity and ∇^2 is the Laplace operator.

For this problem, the left hand side of (6.16) is assumed to be 0 and the gravity term \mathbf{g} is neglected so these become Stokes equations. The p term in (6.16) is replaced by \tilde{p} which is

$$\tilde{p} = p + w_F, \quad (6.18)$$

where w_F is as before.

The viscosity being used is the dynamic viscosity so $\nu = \frac{\eta}{\rho}$ and eq. (6.16) becomes

$$-\tilde{p}_{,i} + \tilde{t}_{ij,j} = 0 \quad (6.19)$$

where

$$\tilde{t}_{ij} = \eta(v_{i,ii} + v_{i,jj}). \quad (6.20)$$

So the governing Stokes equations for this problem are

$$-\tilde{p}_x + \eta(u_{xx} + u_{zz}) = 0, \quad (6.21)$$

$$-\tilde{p}_z + \eta(v_{xx} + v_{zz}) = 0, \quad (6.22)$$

$$\text{and} \quad u_x + v_z = 0, \quad (6.23)$$

where the third equation (6.23) is the incompressibility condition.

These equations can be non-dimensionalised by setting

$$x = L\hat{x} \quad z = M\hat{z} \quad \tilde{p} = P\hat{p} \quad (6.24)$$

$$u = U\hat{u} \quad v = V\hat{v}.$$

The lubrication approximation [40] is assumed which means that the length scale in the x direction is much greater than it is in the z direction, so

$$\left| \frac{M}{L} \right| \ll 1 \quad (6.25)$$

and eq. (6.23) becomes

$$\frac{U}{L} \frac{\partial \hat{u}}{\partial \hat{x}} + \frac{V}{M} \frac{\partial \hat{v}}{\partial \hat{z}} = 0. \quad (6.26)$$

This means that

$$V = \frac{M}{L} U \quad (6.27)$$

is a scale relation to give the normalised relation

$$\frac{\partial \hat{u}}{\partial \hat{x}} + \frac{\partial \hat{v}}{\partial \hat{z}} = 0. \quad (6.28)$$

If the scalings from (6.24) are substituted into eq. (6.21), they give

$$-\frac{P}{L} \frac{\partial \hat{p}}{\partial \hat{x}} + \eta \left[\frac{U}{L^2} \frac{\partial^2 \hat{u}}{\partial \hat{x}^2} + \frac{U}{M^2} \frac{\partial^2 \hat{u}}{\partial \hat{z}^2} \right] = 0 \quad (6.29)$$

$$\Rightarrow -\frac{P}{L} \frac{\partial \hat{p}}{\partial \hat{x}} + \eta \frac{U}{M^2} \left[\frac{M^2}{L^2} \frac{\partial^2 \hat{u}}{\partial \hat{x}^2} + \frac{\partial^2 \hat{u}}{\partial \hat{z}^2} \right] = 0 \quad (6.30)$$

$$\Rightarrow -\frac{P}{L} \frac{\partial \hat{p}}{\partial \hat{x}} + \eta \frac{U}{M^2} \left[\frac{\partial^2 \hat{u}}{\partial \hat{z}^2} + \mathcal{O} \left(\left(\frac{M}{L} \right)^2 \right) \right] = 0 \quad (6.31)$$

$$\Rightarrow -\frac{P}{L} \frac{\partial \hat{p}}{\partial \hat{x}} + \eta \frac{U}{M^2} \frac{\partial^2 \hat{u}}{\partial \hat{z}^2} = 0 \quad (6.32)$$

from the assumption (6.25) above. This suggests that the scale P should be

$$P = \eta \frac{UL}{M^2}. \quad (6.33)$$

If (6.33) is now inserted into eq. (6.22) along with (6.24) eq. (6.22) becomes

$$-\frac{UL}{M^3} \frac{\partial \hat{p}}{\partial \hat{z}} + \eta \left[\frac{V}{L^2} \frac{\partial^2 \hat{v}}{\partial \hat{x}^2} + \frac{V}{M^2} \frac{\partial^2 \hat{v}}{\partial \hat{z}^2} \right] = 0. \quad (6.34)$$

The scaling for V is known from (6.27) so this becomes

$$\frac{UL}{M^3} \frac{\partial \hat{p}}{\partial \hat{z}} + \eta \left[\frac{MU}{L^3} \frac{\partial^2 \hat{v}}{\partial \hat{x}^2} + \frac{U}{ML} \frac{\partial^2 \hat{v}}{\partial \hat{z}^2} \right] = 0 + \mathcal{O} \left(\left(\frac{M}{L} \right)^2 \right), \quad (6.35)$$

which becomes

$$-\frac{\partial \hat{p}}{\partial \hat{z}} + \mathcal{O} \left(\left(\frac{M}{L} \right)^2 \right) = 0 \quad (6.36)$$

$$\Rightarrow -\frac{\partial \hat{p}}{\partial \hat{z}} \approx 0 \quad (6.37)$$

by (6.25) above. This means that $\tilde{p} = p + w_F$ in the lubrication approximation is not a function of z so

$$p = p(x, t) \quad (6.38)$$

in the original variables, and w_F is already known not to be a function of z .

6.2.2 Laplace's formula

To find the pressure for this problem, Laplace's formula has to be considered. From Landau and Lifshitz [41], Laplace's formula says that the surface pressure between two different fluids is given by

$$p_1 - p_2 = \alpha \left(\frac{1}{R_1} + \frac{1}{R_2} \right) \quad (6.39)$$

where R_1 and R_2 are the radii of curvature of the surface and α is the surface tension between the two media. For $h(x, y)$ sufficiently small,

$$\frac{1}{R_1} + \frac{1}{R_2} = - \left(\frac{\partial^2 h}{\partial x^2} + \frac{\partial^2 h}{\partial y^2} \right) \quad (6.40)$$

so the change in pressure is given by

$$p_1 - p_2 = \alpha \left(\frac{\partial^2 h}{\partial x^2} + \frac{\partial^2 h}{\partial y^2} \right). \quad (6.41)$$

For this problem, α is replaced by γ_{lv} , the surface tension between the solid and liquid, and $h(x, y) = h(x)$, so with $h(x)$ given by (6.1) the pressure is given by

$$p(x, t) = p_0 - \gamma_{lv} \left(\frac{\partial^2 h}{\partial x^2} \right) \quad (6.42)$$

$$= p_0 + \gamma_{lv} \xi_0(t) q^2 \sin(qx). \quad (6.43)$$

6.2.3 Surface conditions

There are two surface conditions which all fluids must satisfy. These are the Kelvin condition and the continuity of the velocity across a boundary.

The Kelvin condition states that the surface of the fluid that is described by

$$F(x, y, z, t) = 0 \quad (6.44)$$

must always satisfy

$$\frac{DF}{Dt} = 0, \quad (6.45)$$

from [42] and [43, p. 7]. In this case, the surface is described by

$$F(x, z, t) = z - h(x, t). \quad (6.46)$$

The normal and tangential components of the velocity must be continuous also from Batchelor [42]. The difference in the stress on surface elements parallel to the boundary and on either side of it is a normal force due wholly to surface tension so the full stress tensor is needed to look at the condition. Also, from Landau and Lifshitz [41] (p233/4 and 7) for the dynamic equation

$$n_k \sigma_{2,ik} - n_k \sigma_{1,ik} = \alpha \left(\frac{1}{R_1} + \frac{1}{R_2} \right) n_i \quad (6.47)$$

which, also along the tangent τ , gives

$$n_k \sigma_{2,ik} \tau_i = n_k \sigma_{1,ik} \tau_i \quad (6.48)$$

and

$$n_k \sigma_{2,ik} \tau_i - n_k \sigma_{1,ik} \tau_i = \alpha \left(\frac{1}{R_1} + \frac{1}{R_2} \right) \quad (6.49)$$

where $\sigma_{ij} = -p\delta_{ij} + \sigma'_{ij}$ is the stress tensor and σ'_{ij} is the viscous stress tensor.

For the current problem, the Kelvin condition (6.45) gives the surface condition

$$u_z|_{z=h_0} = 0 \quad (6.50)$$

where the subscript z denotes derivative with respect to z , and the continuity of the velocity across a boundary gives

$$u|_{z=0} = 0 \quad (6.51)$$

from above, which is the standard no slip condition.

6.2.4 Solving the equations

The two equations to be solved are

$$(p + w_F)_{,i} = \tilde{t}_{ij,j} \quad (6.52)$$

and

$$u_x + v_z = 0. \quad (6.53)$$

These are the Stokes equation and the incompressibility condition. If the solution for $u(x, z)$ is found via eq. (6.52) then $v(x, z)$ can be found via (6.53). This means that eq. (6.52) only needs to be considered with $i = 1$. From eq. (6.32), the Navier–Stokes equation to be solved is

$$(p + w_F)_x = \eta u_{zz}. \quad (6.54)$$

From Laplace’s formula, the pressure is given by eq. (6.43) and we know from the formulation of the problem that

$$(p + w_F)_x = \gamma_{lv} \xi_0(t) q^3 \cos(qx) + \frac{K\theta^2}{h(x, t)^3} \frac{dh}{dx} - \frac{A}{2\pi h(x, t)^4} \frac{dh}{dx} \quad (6.55)$$

$$\begin{aligned} &= \gamma_{lv} \xi_0(t) q^3 \cos(qx) + K\theta^2 \frac{\xi_0(t) q \cos(qx)}{(h_0 + \xi_0(t) \sin(qx))^3} \\ &\quad - \frac{A}{2\pi} \frac{\xi_0(t) q \cos(qx)}{(h_0 + \xi_0(t) \sin(qx))^4} \end{aligned} \quad (6.56)$$

but since $\xi_0(t) \ll h_0$ this is approximated by

$$\begin{aligned} (p + w_F)_x &= \gamma_{lv} \xi_0(t) q^3 \cos(qx) + \frac{K\theta^2}{h_0^3} \xi_0(t) q \cos(qx) \\ &\quad - \frac{A}{2\pi h_0^4} \xi_0(t) q \cos(qx) \end{aligned} \quad (6.57)$$

$$= \xi_0(t) q \cos(qx) \left(\gamma_{lv} q^2 + \frac{K\theta^2}{h_0^3} - \frac{A}{2\pi h_0^4} \right) \quad (6.58)$$

$$= f(x, t). \quad (6.59)$$

This means that (6.54) becomes

$$\eta u_{zz} = f(x, t). \quad (6.60)$$

This can be integrated once with respect to z to get

$$\eta u_z = f(x, t)z + c_1, \quad (6.61)$$

where c_1 can be found by applying the boundary condition given by (6.50) which gives c_1 such that

$$\eta u_z = f(x, t)(z - h_0). \quad (6.62)$$

Eq. (6.62) can be integrating again to find the velocity in the x direction, $u(x, z)$, as

$$u(x, z, t) = \frac{f(x)}{\eta} \left(\frac{z^2}{2} - h_0 z \right) \quad (6.63)$$

$$= \frac{\xi_0(t)h_0}{2\eta} \alpha(q) \left(\frac{z}{h_0} - 2 \right) qz \cos(qx) \quad (6.64)$$

after applying the second boundary condition (6.51), where

$$\alpha(q) = \left(\gamma_w q^2 + \frac{K\theta^2}{h_0^3} - \frac{A}{2\pi h_0^4} \right). \quad (6.65)$$

Since $u(x, z, t)$ is now know, $v(x, z, t)$ can easily be found via eq. (6.53). The velocity in the z direction is found to be

$$v(x, z, t) = \frac{\xi_0(t)h_0}{6\eta} \alpha(q) \left(\frac{z}{h_0} - 3 \right) (qz)^2 \sin(qx) + c_3. \quad (6.66)$$

There is no slip on the lower boundary of the liquid crystal film so

$$v(x, 0, t) = 0 \quad (6.67)$$

which means $c_3 = 0$ so the final expression for the velocity in the z direction is

$$v(x, z, t) = \frac{\xi_0 h_0}{6\eta} \alpha(q) \left(\frac{z}{h_0} - 3 \right) (qz)^2 \sin(qx), \quad (6.68)$$

with $\alpha(q)$ given by (6.65).

6.2.5 Fluctuations

The boundary condition at the free interface is

$$\frac{\partial h}{\partial t} = v|_{z=h_0} \quad (6.69)$$

since there is no z component of velocity on the surface. This gives us

$$\frac{d\xi_0}{dt} \sin(qx) = \frac{-2\xi_0 h_0^3}{6\eta} \alpha(q) q^2 \sin(qx) \quad (6.70)$$

$$\Rightarrow \frac{d\xi_0}{dt} + s(q)\xi_0 = 0 \quad (6.71)$$

where

$$s(q) = \frac{h_0^3}{3\eta} q^2 \alpha(q). \quad (6.72)$$

The fluctuations will grow exponentially if $s(q) < 0$ and will decay exponentially if $s(q) > 0$. The spinodal dewetting of a nematic film may be initiated for long wavelength fluctuations (i.e., $q \rightarrow 0$) and if the Hamaker constant is positive. If this is the case the term in $\alpha(q)$

$$\frac{K\theta^2}{h_0^3} - \frac{A}{2\pi h_0^4} \quad (6.73)$$

is negative, i.e., $h_0 < h^*$ where h^* is found by setting $h_0 = h^*$ in (6.73) and setting (6.73) equal to zero. This gives

$$h^* = \frac{A}{2\pi K\theta^2}. \quad (6.74)$$

If we define an effective Hamaker constant, A_{eff} , as

$$A_{eff} = A \left(1 - \frac{h_0}{h^*} \right) \quad (6.75)$$

then instability will develop if $A_{eff} < 0$.

The critical wave vector, q_c , below which fluctuations grow and lead to the rupture of the film can now be expressed as a function of A_{eff} . If we look at $\alpha(q_c) = 0$ and rearrange we get

$$q_c = \sqrt{\frac{A_{eff}}{2\pi\gamma_{lv}h_0^4}} \quad (6.76)$$

where the positive square root is used since $q > 0$ physically.

To find the fastest growing mode we have to look at the minimum of $s(q)$. The function $s(q)$ can be restated as

$$s(q) = \frac{h_0^3}{3\eta} \gamma_{lv} [q^4 - q_c^2 q^2] \quad (6.77)$$

so

$$s'(q) = \frac{h_0^3}{3\eta} \gamma_{lv} [4q^3 - 2q q_c^2] . \quad (6.78)$$

There are three solutions to $s'(q)=0$. Of these three solutions, the minimum occurs when $s'(q_m) = 0$ and $s''(q_m) = 0$. This q_m is the wave vector corresponding to the fastest growing mode and is found to be

$$q_m = \frac{1}{\sqrt{2}} q_c . \quad (6.79)$$

The fastest growing mode is then given by

$$\lambda_m = \frac{2\pi}{q_m} \quad (6.80)$$

$$= \sqrt{\frac{16\pi^3 \gamma_{lv} h_0^4}{A_{eff}}} . \quad (6.81)$$

A solution to the differential equation (6.71) would be of the form

$$\xi_0(t) = A e^{-s(q)t} \quad (6.82)$$

so we can find an associated time constant by considering $-s(q)$. The associated time constant for the fastest growing mode would be given by

$$\frac{1}{\tau} = -s(q_m) \quad (6.83)$$

which gives us

$$\tau = \frac{48\pi^2 h_0^5 \eta \gamma_{lv}}{A_{eff}^2} . \quad (6.84)$$

6.2.6 Typical values

If the thin nematic film is a 30nm thick film of 5CB and $\eta = 0.01\text{Pa s}$ with $A_{eff} = 10^{-20}\text{ J}$ and the surface tension between air and the liquid crystal being $\gamma_{lv} = 30\text{ mN m}^{-1}$ then the fastest growing mode corresponds to

$$\lambda_m \approx 34.7 \mu\text{m}, \quad (6.85)$$

and

$$\tau \approx 34.5 \text{ s}. \quad (6.86)$$

At 25°C , a 20nm thick film of 5CB does not dewet but a 17nm thick film does. This means that 20nm can be taken as an approximate value for h^* and the angle θ at the surface can be calculated. If $K = 10^{-11}\text{ N}$ and $A = 10^{-20}\text{ J}$ then θ comes out to be approximately 0.089 radians.

6.3 Thin film with Leslie viscosities

The isotropic dynamic viscosity, η , can be replaced with the full viscosity for liquid crystals by using

$$\begin{aligned} \tilde{t}_{ij} = & \alpha_1 n_k A_{kp} n_p n_i n_j + \alpha_2 N_i n_j + \alpha_3 n_i N_j + \\ & \alpha_4 A_{ij} + \alpha_5 n_j A_{ik} n_k + \alpha_6 n_i A_{jk} n_k \end{aligned} \quad (6.87)$$

where

$$A_{ij} = \frac{1}{2} (v_{i,j} + v_{j,i}) \quad (6.88)$$

and

$$N_i = \dot{n}_i - W_{ij} n_j \quad \text{where} \quad W_{ij} = \frac{1}{2} (v_{i,j} - v_{j,i}). \quad (6.89)$$

For this problem, the director would be

$$\mathbf{n} = (1, 0, f(x, z, t)) \quad (6.90)$$

where $f(x, z, t)$ is given by (6.2).

6.3.1 Ericksen-Leslie equations

The equation for linear momentum from the Ericksen–Leslie equations is given by

$$\rho \dot{v}_i = \rho F_i - (p + w_F)_{,i} + \tilde{g}_j n_{j,i} + G_j n_{j,i} + \tilde{t}_{ij,j} \quad (6.91)$$

from section 2.2.4, where w_F here represents $e_P(h)$. For this problem, there is no external body force, no generalised body force, the material time derivative of the velocity is ignored and $\tilde{\mathbf{g}} = \mathbf{0}$ so the linear momentum equation becomes

$$(p + w_F)_{,i} = \tilde{t}_{ij,j}. \quad (6.92)$$

From the lubrication approximation, the linear momentum equation for $i = 1$ is

$$(p + w_F)_{,1} = \tilde{t}_{13,3} \quad (6.93)$$

and the equation for $i = 3$ gives

$$(p + w_F)_{,3} = \tilde{t}_{33,3} \quad (6.94)$$

$$0 = \tilde{t}_{33,3}. \quad (6.95)$$

Since we have the condition

$$u_z + v_x = 0, \quad (6.96)$$

only the $i = 1$ case has to be considered as this will give $u(x, z)$, and $v(x, z)$ can be found by 6.96.

For this problem, the non-zero components of the matrix A , given by (2.21), which is used in \tilde{t}_{ij} are

$$A_{11} = \frac{\partial u}{\partial x} \quad A_{33} = \frac{\partial v}{\partial z} \quad (6.97)$$

$$A_{13} = A_{31} = \frac{1}{2} \left(\frac{\partial u}{\partial z} + \frac{\partial v}{\partial x} \right) \quad (6.98)$$

but since the lubrication approximation is being assumed, the terms involving v are discarded along with any x derivatives leaving

$$A_{13} = A_{31} = \frac{1}{2} \frac{\partial u}{\partial z}. \quad (6.99)$$

For the same reasons, the only non-zero components of the matrix W , (2.23) are

$$W_{13} = -W_{31} = \frac{1}{2} \frac{\partial u}{\partial z}. \quad (6.100)$$

The terms in N_i are

$$N_1 = -\frac{1}{2} \frac{\partial u}{\partial z} f(x, z, t), \quad (6.101)$$

$$N_2 = 0, \quad (6.102)$$

$$N_3 = \frac{1}{2} \frac{\partial u}{\partial z}. \quad (6.103)$$

This means that \tilde{t}_{13} is given by

$$\begin{aligned} \tilde{t}_{13} &= \alpha_1 [A_{13}n_3 + n_3A_{31}]n_3 + \alpha_2 N_1 n_3 \\ &\quad + \alpha_3 N_3 + \alpha_4 A_{13} + \alpha_5 n_3 A_{13} n_3 + \alpha_6 A_{21} \end{aligned} \quad (6.104)$$

$$\begin{aligned} &= \alpha_1 \left[\frac{\partial u}{\partial z} f(x, z, t) \right] f(x, z, t) - \alpha_2 \frac{1}{2} \frac{\partial u}{\partial z} f^2(x, z, t) + \alpha_3 \frac{1}{2} \frac{\partial u}{\partial z} \\ &\quad + \alpha_4 \frac{1}{2} \frac{\partial u}{\partial z} + \alpha_5 \frac{1}{2} \frac{\partial u}{\partial z} f^2(x, z, t) + \alpha_6 \frac{1}{2} \frac{\partial u}{\partial z}, \end{aligned} \quad (6.105)$$

but since

$$f(x, z, t) = \frac{\theta}{h} z \quad (6.106)$$

and θ is assumed small, this becomes

$$\tilde{t}_{13} = \frac{1}{2} \frac{\partial u}{\partial z} (\alpha_3 + \alpha_4 + \alpha_6) \quad (6.107)$$

$$= \eta_1 \frac{\partial u}{\partial z}, \quad (6.108)$$

where η_1 is a Miesowicz viscosity. Differentiating this with respect to z then gives

$$\tilde{t}_{13,3} = \eta_1 \frac{\partial^2 u}{\partial z^2}. \quad (6.109)$$

The $p + w_F$ term is given by

$$p + w_F = p_0 + \gamma_{lv}\xi_0(t)q^2 \sin(qx) - \frac{1}{2} \frac{K\theta^2}{h^2} + \frac{A}{6\pi h^3}, \quad (6.110)$$

from (6.43) and (??). This gives

$$(p + w_F)_{,1} = \gamma_{lv}\xi_0(t)q^3 \cos(qx) + \frac{K\theta^2}{h^3} \frac{\partial h}{\partial x} - \frac{A}{2\pi h^4} \frac{\partial h}{\partial x} \quad (6.111)$$

$$\begin{aligned} &= \gamma_{lv}\xi_0(t)q^3 \cos(qx) + \frac{K\theta^2}{h_0^3} \xi_0(t)q \cos(qx) \\ &\quad - \frac{A}{2\pi h_0^4} \xi_0(t)q \cos(qx), \end{aligned} \quad (6.112)$$

since $\xi_0 \ll h_0$ and $h(x, t)$ is given by (6.1). This can be tidied up to give

$$(p + w_F)_{,1} = \xi_0(t)q \cos(qx) \left[\gamma_{lv}q^2 + \frac{K\theta^2}{h_0^3} - \frac{A}{2\pi h_0^4} \right] \quad (6.113)$$

$$= \xi_0(t)q \cos(qx) \alpha(q) \quad (6.114)$$

where

$$\alpha(q) = \gamma_{lv}q^2 + \frac{K\theta^2}{h_0^3} - \frac{A}{2\pi h_0^4} \quad (6.115)$$

for convenience.

This means that the Ericksen–Leslie linear momentum equation for $i = 1$ becomes

$$(p + w_F)_{,1} = \tilde{t}_{13,3} \quad (6.116)$$

$$\frac{\partial^2 u}{\partial z^2} = \frac{1}{\eta_1} \xi_0(t)q \cos(qx) \alpha(q). \quad (6.117)$$

This can easily be integrated twice with respect to z , using the boundary conditions

$$\eta_1 \left(\frac{\partial u}{\partial z} \right)_{z=h_0} = 0 \quad \text{and} \quad u(x, 0) = 0 \quad (6.118)$$

to give

$$u(x, z, t) = \frac{\xi_0(t)h_0}{2\eta_1} \alpha(q) \left(\frac{z}{h_0} - 2 \right) qz \cos(qx), \quad (6.119)$$

which is the same as the velocity in the x direction for the isotropic viscosity assumption except $\eta = \eta_3$ has been replaced with η_1 .

Similarly, the velocity in the z direction is given by

$$v(x, z, t) = \frac{\xi_0(t)h_0}{6\eta_1}\alpha(q)\left(\frac{z}{h_0} - 3\right)(qz)^2\sin(qx). \quad (6.120)$$

6.3.2 Fluctuations

When the same analysis is applied as was done for the isotropic viscosity in Section 6.2.5, it is found that all the analysis of the equations and the fluctuation carry through as before but η is replaced by η_1 . The value of θ which was used is still the value of θ here because the equation used to find θ did not use the viscosity.

To find the fastest growing mode and the time constant for 5CB at 25°C as before, the value of η_1 is needed. It has to be calculated, and this requires the values of the Leslie viscosities. These are given in the table below for 5CB at 25°C from [6].

α_i	Viscosity (Pa s)
α_1	-0.0060
α_2	-0.0812
α_3	-0.0036
α_4	0.0652
α_5	0.0640
α_6	-0.0208

For these values, $\eta_1 = 0.0408$ Pa s. With this η_1 and with the h_0 , γ_{lv} and A_{eff} values the same as before, the fastest growing mode and the time constant come out to be

$$\lambda_m \approx 34.7\mu\text{m}, \quad (6.121)$$

since the η value does not come into the equation for λ_m , and

$$\tau \approx 140.9, \quad (6.122)$$

respectively. This value of τ is almost 4 times higher than the previous value.

6.4 Leslie viscosities with more director freedom

The next logical progression in the problem was to remove the approximation on $f(x, z, t)$ that it was small so that the director is now represented by

$$\mathbf{n} = (\cos(f(x, z, t)), 0, \sin(f(x, z, t))) . \quad (6.123)$$

6.4.1 Ericksen-Leslie equations

As before, the only non-zero components of the matrix A , given by (2.21), after applying the lubrication approximation are

$$A_{13} = A_{31} = \frac{1}{2} \frac{\partial u}{\partial z} , \quad (6.124)$$

and the only non-zero components of the matrix W , (2.23) are

$$W_{13} = -W_{31} = \frac{1}{2} \frac{\partial u}{\partial z} . \quad (6.125)$$

For this different director, the N_i terms change. They are now

$$N_1 = -\frac{1}{2} \frac{\partial u}{\partial z} \sin f(x, z, t) , \quad (6.126)$$

$$N_2 = 0 , \quad (6.127)$$

$$N_3 = \frac{1}{2} \frac{\partial u}{\partial z} \cos f(x, z, t) . \quad (6.128)$$

The \tilde{t}_{13} term is now

$$\begin{aligned} \tilde{t}_{13} = & \alpha_1 [\cos(f)A_{13} \sin(f) + \sin(f)A_{31} \cos(f)] \sin(f) \cos(f) \\ & + \alpha_2 N_1 \sin(f) + \alpha_3 \cos(f)N_3 + \alpha_4 A_{13} + \\ & + \alpha_5 \sin(f)A_{13} \sin(f) + \alpha_6 \cos(f)A_{31} \cos(f) . \end{aligned} \quad (6.129)$$

After inserting the values of A_{13} , A_{31} and N_i simplifying, this becomes

$$\tilde{t}_{13} = \frac{\partial u}{\partial z} \left[\frac{1}{4} \alpha_1 \sin^2(2f) - \gamma_2 \sin^2(f) + \eta_1 \right] \quad (6.130)$$

$$= \frac{\partial u}{\partial z} \Upsilon(x, z, t) . \quad (6.131)$$

The $(p + w_F)_{,1}$ term is the same as before, so it is only a function of x and t .

The Ericksen–Leslie linear momentum equation for this problem is

$$\left(\frac{\partial u}{\partial z} \Upsilon(x, z, t) \right)_z = (p + w_F)_x, \quad (6.132)$$

where the subscripts denote differentiation with respect to that variable. Since the right hand side of this equation is only a function of x and t , the whole equation can be integrated with respect to z to give

$$\frac{\partial u}{\partial z} \Upsilon(x, z, t) = z(p + w_F)_x + C, \quad (6.133)$$

where C is an arbitrary function of x and t . From the Kelvin condition, (6.50), the boundary condition

$$\left. \frac{\partial u}{\partial z} \right|_{z=h_0} = 0 \quad (6.134)$$

allows C to be calculated and the resultant equation comes out to be

$$\frac{\partial u}{\partial z} \Upsilon(x, z, t) = (p + w_F)_x (z - h_0). \quad (6.135)$$

This means that

$$\frac{\partial u}{\partial z} = \frac{1}{\Upsilon(x, z, t)} (p + w_F)_x (z - h_0). \quad (6.136)$$

This equation can only be integrated numerically.

This gives the velocity in x direction to be

$$u(x, z, t) = \xi_0(t) q \cos(qx) \alpha(q) Y(x, z, t) \quad (6.137)$$

where

$$\alpha(q) = \gamma_l v q^2 + \frac{K \theta^2}{h_0^3} - \frac{A}{2\pi h_0^4} \quad (6.138)$$

as before.

From the incompressibility condition and (6.136), the velocity in the z direction can be calculated via

$$\frac{\partial v}{\partial x} = \frac{-1}{\Upsilon(x, z, t)} ((p + w_F)_x (z - h_0)), \quad (6.139)$$

$$= \frac{-1}{\Upsilon(x, z, t)} \xi_0(t) q \cos(qx) \alpha(q) (z - h_0). \quad (6.140)$$

This integration of this equation also has to be done numerically.

6.5 A perturbation to the known solution

If it is assumed that the Ericksen–Leslie equations are satisfied by some velocities, u_1 and v_1 , then perturbations to these solutions can be considered. The solutions are perturbed in x , z and t such that

$$u = u_1 + \bar{u} \exp(\tau t + i(\mathbf{q} \cdot \mathbf{x})) \quad \text{and} \quad (6.141)$$

$$v = v_1 + \bar{v} \exp(\tau t + i(\mathbf{q} \cdot \mathbf{x})), \quad (6.142)$$

where $\bar{u}, \bar{v} \ll 1$ and where

$$\mathbf{q} = \begin{bmatrix} q_x \\ 0 \\ q_z \end{bmatrix}. \quad (6.143)$$

If the director is considered to be of the form

$$\mathbf{n} = (1, 0, \theta_1) \quad (6.144)$$

where

$$\theta_1 := \frac{\theta_0 z}{h}, \quad (6.145)$$

with θ_0 the same as the θ used in the previous sections, then we can also perturb the director such that

$$\theta = \theta_1 + \bar{\theta} \exp(\tau t + i(\mathbf{q} \cdot \mathbf{x})) \quad (6.146)$$

where $\bar{\theta} \ll 1$.

We are assuming that the height and the pressure are not perturbed.

By perturbing the u , v and θ quantities we also perturb terms in the Ericksen–Leslie equations. The Ericksen–Leslie equations for our problem reduce to

$$-(p + w_F)_{,i} + \tilde{g}_j n_{j,i} + \tilde{t}_{ij,j} = 0 \quad (6.147)$$

$$\text{and} \quad \left(\frac{\partial w_F}{\partial n_{i,j}} \right)_{,j} - \frac{\partial w_F}{\partial n_i} + \tilde{g}_i = \lambda n_i, \quad (6.148)$$

so if these are perturbed via the above expressions then the perturbed terms are $\tilde{t}_{ij,j}$, \tilde{g}_j , w_F and n_j . These are perturbed such that

$$\tilde{t}_{ij,j} = t_{ij,j} + \bar{t}_{ij,j}, \quad (6.149)$$

$$\tilde{g}_j = g_j + \bar{g}_j, \quad (6.150)$$

$$w_F = w_{1F} + \bar{w}_F, \quad (6.151)$$

$$n_j = n_{1j} + \bar{n}, \quad (6.152)$$

where the first term in each is the original term and the expressions with a bar over them indicate the associated perturbation. This means that our linear momentum equation now becomes

$$0 = -(p + w_{1F} + \bar{w}_F)_{,i} + (g_j + \bar{g}_j)_{,j}(n_{1j} + \bar{n}_{j,i}) + t_{ij,j} + \tilde{t}_{ij,j}. \quad (6.153)$$

Since the unperturbed solutions automatically satisfy the equations, we have

$$0 = -\bar{w}_{F,i} + g_j \bar{n}_{j,i} + \bar{g}_j n_{j,i} + \bar{t}_{ij,j}. \quad (6.154)$$

From before, we know that

$$\begin{aligned} \tilde{t}_{ij} = & \alpha_1 n_k A_{kp} n_p n_i n_j + \alpha_2 N_i n_j + \alpha_3 n_i N_j + \\ & \alpha_4 A_{ij} + \alpha_5 n_j A_{ik} n_k + \alpha_6 n_i A_{jk} n_k \end{aligned} \quad (6.155)$$

but now the A_{ij} , N_i are also perturbed. The matrix A_{ij} is given by

$$\begin{aligned} A &= \begin{bmatrix} u_x & 0 & \frac{1}{2}(u_z + v_x) \\ 0 & 0 & 0 \\ \frac{1}{2}(v_x + u_z) & 0 & v_z \end{bmatrix} \quad (6.156) \\ &= \begin{bmatrix} u_x + iq_x \bar{u} \exp(P) & 0 & \frac{1}{2}(u_z + v_x + (q_z \bar{u} + q_x \bar{v})i \exp(P)) \\ 0 & 0 & 0 \\ \frac{1}{2}(v_x + u_z + (q_x \bar{v} + q_z \bar{u})i \exp(P)) & 0 & v_z + iq_z \bar{v} \exp(P) \end{bmatrix} \quad (6.157) \end{aligned}$$

where

$$P := \tau t + i(\mathbf{q} \cdot \mathbf{x}) \quad (6.158)$$

for convenience.

Also,

$$N_i = \dot{n}_i - W_{ij}n_j \quad (6.159)$$

where

$$W_{ij} = \frac{1}{2}(v_{i,j} - v_{j,i}) \quad (6.160)$$

as before, is perturbed. These result in the terms

$$N_i = N_{1i} + \bar{N}_i. \quad (6.161)$$

Similarly, the \tilde{t}_{ij} terms are of the form

$$\tilde{t}_{ij} = t_{ij} + \bar{t}_{ij}. \quad (6.162)$$

If we assume that the original solutions are linearised (which they are) then any products involving the solutions or perturbations can be neglected.

This means that our linear momentum equations are now

$$\bar{t}_{11,1} + \bar{t}_{13,3} = 0 \quad (6.163)$$

$$\bar{t}_{31,1} + \bar{t}_{33,3} = 0. \quad (6.164)$$

From (2.17),

$$\begin{aligned} \tilde{t}_{ij} = & \alpha_1 n_k A_{kp} n_p n_i n_j + \alpha_2 N_i n_j + \alpha_3 n_i N_j + \\ & \alpha_4 A_{ij} + \alpha_5 n_j A_{ik} n_k + \alpha_6 n_i A_{jk} n_k. \end{aligned} \quad (6.165)$$

The N_i values here are

$$\bar{N}_1 = 0 \quad \text{and} \quad \bar{N}_3 = \bar{\theta}\tau \exp(P) \quad (6.166)$$

and the \bar{t}_{ij} , the perturbed term in the \tilde{t}_{ij} , are

$$\bar{t}_{11} = iq_x \bar{u} [\alpha_1 + \alpha_4 + \alpha_5 + \alpha_6] \exp(P) \quad (6.167)$$

$$\bar{t}_{13} = \left[\alpha_3 \bar{\theta}\tau + \frac{1}{2} (\alpha_4 + \alpha_6) (iq_x \bar{v} + iq_z \bar{u}) \right] \exp(P) \quad (6.168)$$

$$\bar{t}_{31} = \left[\alpha_2 \bar{\theta}\tau + \frac{1}{2} (\alpha_4 + \alpha_5) (iq_x \bar{v} + iq_z \bar{u}) \right] \exp(P) \quad (6.169)$$

$$\bar{t}_{33} = \alpha_4 iq_z \bar{v} \exp(P) \quad (6.170)$$

meaning that the $\bar{t}_{ij,j}$ terms are

$$\bar{t}_{11,1} = -q_x^2 \bar{u} [\alpha_1 + \alpha_4 + \alpha_5 + \alpha_6] \exp(P) \quad (6.171)$$

$$\bar{t}_{13,3} = \left[iq_z \alpha_3 \bar{\theta} \tau + \frac{1}{2} (\alpha_4 + \alpha_6) (-q_x q_z \bar{v} q_z^2 \bar{u}) \right] \exp(P) \quad (6.172)$$

$$\bar{t}_{31,1} = \left[iq_x \alpha_2 \bar{\theta} \tau + \frac{1}{2} (\alpha_4 + \alpha_5) (-q_x^2 \bar{v} - q_x q_z \bar{u}) \right] \exp(P) \quad (6.173)$$

$$\bar{t}_{33,3} = -\alpha_4 q_z^2 \bar{v} \exp(P). \quad (6.174)$$

Putting these together gives us the linear momentum equations. The $\exp(P)$ term can be cancelled out since it is in all terms so the linear momentum equation for $i = 1$ is

$$-q_x^2 \bar{u} [\alpha_1 + \alpha_4 + \alpha_5 + \alpha_6] + iq_z \alpha_3 \bar{\theta} \tau + \frac{1}{2} (\alpha_4 + \alpha_6) (-q_x q_z \bar{v} q_z^2 \bar{u}) = 0 \quad (6.175)$$

and for $i = 3$ we have

$$-\alpha_4 q_z^2 \bar{v} + iq_x \alpha_2 \bar{\theta} \tau + \frac{1}{2} (\alpha_4 + \alpha_5) (-q_x^2 \bar{v} - q_x q_z \bar{u}) = 0. \quad (6.176)$$

The angular momentum equation, from (2.24), is given by

$$\left(\frac{\partial w_F}{\partial n_{i,j}} \right)_{,j} - \frac{\partial w_F}{\partial n_i} + \tilde{g}_i + G_i = \lambda n_i. \quad (6.177)$$

If we consider only the perturbed linearised equations then the equation for $i = 1$ is simply

$$\bar{g}_1 = \lambda. \quad (6.178)$$

The $i = 3$ angular momentum equation is

$$\bar{g}_3 = \lambda n_3, \quad (6.179)$$

so substituting the λ value from (6.178) and linearising leaves us simply with

$$\bar{g}_3 = 0 \quad (6.180)$$

which is

$$-\gamma_1 \bar{\theta} \tau - \frac{\gamma_2}{2} (iq_x \bar{v} + iq_z \bar{u}) = 0. \quad (6.181)$$

If we take the two linear momentum equations and the angular momentum equation and write them in matrix form we have

$$\begin{bmatrix} u_1 & v_1 & \theta_1 \\ u_2 & v_2 & \theta_2 \\ u_3 & v_3 & \theta_3 \end{bmatrix} \begin{bmatrix} \bar{u} \\ \bar{v} \\ \bar{\theta} \end{bmatrix} = \begin{bmatrix} 0 \\ 0 \\ 0 \end{bmatrix} \quad (6.182)$$

where

$$u_1 = -q_x^2(\alpha_1 + \alpha_4 + \alpha_5 + \alpha_6) - \frac{q_z^2}{2}(\alpha_4 + \alpha_6) - \rho\tau, \quad (6.183)$$

$$v_1 = -\frac{q_x q_z}{2}(\alpha_4 + \alpha_6), \quad (6.184)$$

$$\theta_1 = i q_z \alpha_3 \tau, \quad (6.185)$$

$$u_2 = -\frac{q_z^2}{2}(\alpha_4 + \alpha_6), \quad (6.186)$$

$$v_2 = -q_z^2 \alpha_4 - \frac{q_x q_z}{2}(\alpha_4 + \alpha_6) - \rho\tau, \quad (6.187)$$

$$\theta_2 = i q_x \alpha_4 \tau, \quad (6.188)$$

$$u_3 = -\frac{\gamma_2}{2} i q_z, \quad (6.189)$$

$$v_3 = -\frac{\gamma_2}{2} i q_x, \quad (6.190)$$

$$\theta_3 = -\gamma_1 \tau. \quad (6.191)$$

We are interested in the stability of the solutions subject to the perturbations as introduced above, so now we must consider the determinant of the 3x3 matrix in (6.182). The determinant of this matrix gives a cubic equation in τ

$$\begin{vmatrix} u_1 & v_1 & \theta_1 \\ u_2 & v_2 & \theta_2 \\ u_3 & v_3 & \theta_3 \end{vmatrix} = A\tau^3 + B\tau^2 + C\tau \quad (6.192)$$

where

$$A = -\gamma_1 \rho^2 \quad (6.193)$$

$$B = \frac{q_z^2 \rho}{2} (\gamma_2 \alpha_1 - 3\gamma_1 \alpha_4 - \gamma_1 \alpha_6) + \frac{q_x^2 \rho}{2} (\gamma_2 \alpha_4 - 2\gamma_1 (\alpha_1 + \alpha_4 + \alpha_5 + \alpha_6)) - \frac{q_x q_z \rho}{2} \gamma_1 (\alpha_4 + \alpha_6) \quad (6.194)$$

$$C = \frac{q_x^4}{2} \gamma_2 \alpha_4 (\alpha_1 + \alpha_4 + \alpha_5 + \alpha_6) - \frac{q_x^3 q_z}{2} \gamma_1 (\alpha_4 + \alpha_6) (\alpha_1 + \alpha_4 + \alpha_5 + \alpha_6) - q_x^2 q_z^2 \gamma_1 \alpha_4 (\alpha_1 + \alpha_4 + \alpha_5 + \alpha_6) + \frac{q_z^4}{2} \alpha_4 (\gamma_2 \alpha_1 - \gamma_1 (\alpha_6 + \alpha_4)). \quad (6.195)$$

A τ can be taken out as a common factor so that only the sign of the quadratic

$$f(\tau) := A\tau^2 + B\tau + C \quad (6.196)$$

needs to be considered for stability. If the function $f(\tau)$ is always negative then the solutions subject to the perturbations of the Ericksen–Leslie equations are always stable.

The solution $\tau = 0$ is also a solution to the determinant of the matrix. However, this would correspond to no perturbation in time, so we can neglect this solution.

The value of the constant A is always negative but B and C depend on the values of q_x and q_z as well as combinations of the Leslie viscosities. The values of the viscosities will change for each different nematic liquid crystal.

6.5.1 Different nematic liquid crystals

As mentioned previously, A is always negative for all nematic liquid crystal materials but the signs of B and C need to be considered more carefully. In this section we will look at different nematic materials and determine whether or not the solution subject to the perturbation is stable.

6.5.1.1 5CB

The first liquid crystal we consider in this section is 5CB. The Leslie viscosities for 5CB are:

α_i	Viscosity (Pa s)
α_1	−0.0060
α_2	−0.0812
α_3	−0.0036
α_4	0.0652
α_5	0.0640
α_6	−0.0208
γ_1	0.0777
γ_2	−0.0848

Substituting these values into A , B and C and using the value $\rho = 1 \text{ kg m}^{-3}$ for simplicity produces

$$A = -0.0777 \quad (6.197)$$

$$B = -0.00654q_z^2 - 0.0107q_x^2 - 0.00173q_xq_z \quad (6.198)$$

$$C = -0.000283q_x^4 - 0.000096q_z^4 \\ - 0.000519q_x^2q_z^2 - 0.000177q_x^3q_z. \quad (6.199)$$

If the roots of the quadratic $f(\tau)$ are now plotted in terms of q_x and q_z then if both roots are always negative for all values of q_x and q_z then the solution subject to the perturbation is stable since the τ will always be negative meaning the the perturbation will decay in time. The roots of the quadratic were found using the quadratic formula with τ_1 denoting the root with the square root added and τ_2 denoting the root with the square root subtracted.

The graph of τ_1 is shown in Fig. 26 and τ_2 is shown in Fig. 27. It is clear from both these graphs that τ_1 and τ_2 reach their maximum values at $q_x, q_z = 0$. At this point

$$f(\tau) = -0.0777\tau^2 \quad (6.200)$$

so the roots of the equation would be $\tau_1 = \tau_2 = 0$. This means that there would be no perturbation at all since τ , q_x and q_z would all be 0.

6.5.1.2 MBBA

The nematic liquid crystal MBBA is relatively stable at room temperature. The viscosities for this material are given below in the table.

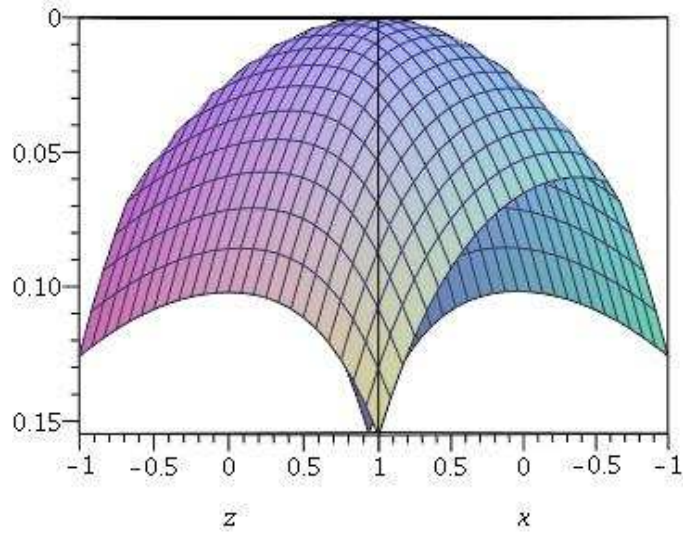


Figure 26: The graph of τ_1 as a function of $z = q_z$ and $x = q_x$ for 5CB close to the origin

α_i	Viscosity (Pa s)
α_1	-0.0181
α_2	-0.1104
α_3	-0.001104
α_4	0.0826
α_5	0.0779
α_6	-0.0336
γ_1	0.1093
γ_2	-0.1121

When these viscosities are substituted into the values for A , B and C then the graphs of τ_1 and τ_2 are given by Fig. 28 and Fig. 29 respectively.

As was the case with 5CB the maximum values of τ_1 and τ_2 are attained. This means that the solution subject to the perturbation above is stable for this particular sample of nematic liquid crystal.

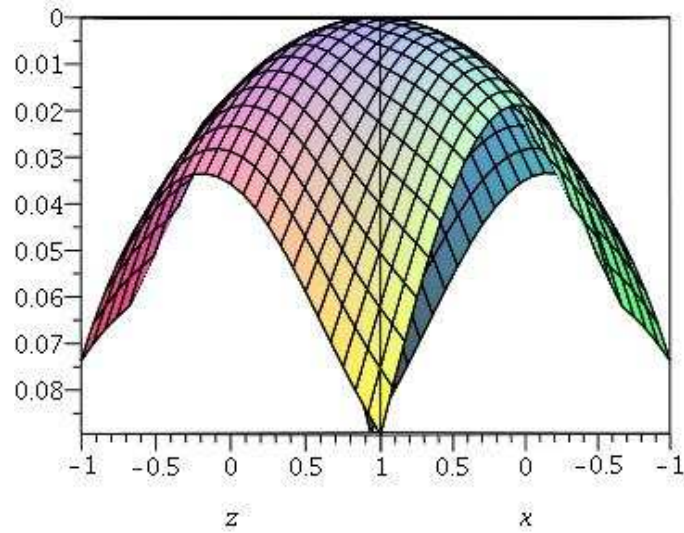


Figure 27: The graph of τ_2 as a function of $z = q_z$ and $x = q_x$ for 5CB close to the origin

6.5.1.3 DDA9

The nematic liquid crystal poly(4,4'-dioxy-2,2'-dimethylazoxybenzene-dodecanediyl), also known as DDA9 is a main-chain thermotropic nematic polymer. This sample has much higher viscosity values than the previously considered samples, as shown below in the table.

α_i	Viscosity (Pa s)
α_1	-1.620×10^2
α_2	-1.700×10^2
α_3	-2.000
α_4	1.601×10^1
α_5	1.620×10^2
α_6	-1.001×10^1
γ_1	1.680×10^2
γ_2	-1.720×10^2

Substituting these values into A , B and C and using the value $\rho = 1\text{kg m}^{-3}$

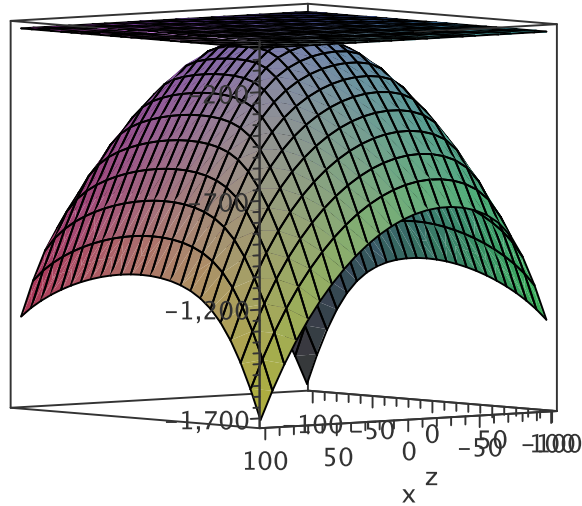


Figure 28: The graph of τ_1 as a function of $z = q_z$ and $x = q_x$ for MBBA

as before gives

$$A = -168.0 \quad (6.201)$$

$$B = 10740q_z^2 - 2380q_x^2 - 504q_xq_z \quad (6.202)$$

$$C = -8260q_x^4 + 0.00005q_xq_z^3 + 215000q_z^4 \\ - 16100q_x^2q_z^2 - 3020q_x^3q_z. \quad (6.203)$$

For this nematic liquid crystal, the graphs of τ_1 and τ_2 , given in Fig. 30 and Fig. 31 respectively. The graph for τ_1 is negative in the range but it is not as smooth as the graphs for the 5CB and MBBA even though the range of q_x and q_z is reduced. Where the graph appears to become jagged is where τ_1 and τ_2 become imaginary. If τ_2 turned out to be the same then more analysis would be needed to determine whether or not the solution subject to the perturbation is stable.

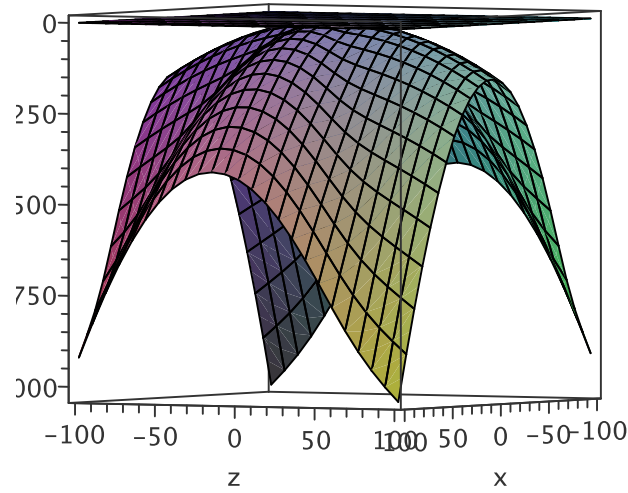


Figure 29: The graph of τ_2 as a function of $z = q_z$ and $x = q_x$ for MBBA

The graph for τ_2 clearly shows that this root is always positive when it is real. This is enough to know that perturbing the sample of DDA9 would cause dewetting.

The next step is to compare the viscosities of a nematic which is stable after being perturbed, 5CB for example, and this unstable sample. To compare the viscosities of 5CB and DDA9, the Miesowicz viscosities are used since these are the observable viscosities which can be measured by experiments.

Viscosity (Pa S)	5CB	DDA9
η_1	0.0204	2
η_2	0.1052	174
η_3	0.0326	8
η_{12}	-0.0060	-162

It is easily seen that the viscosities for DDA9 are much larger than those for 5CB. This is due to the molecular structure of the liquid crystals.

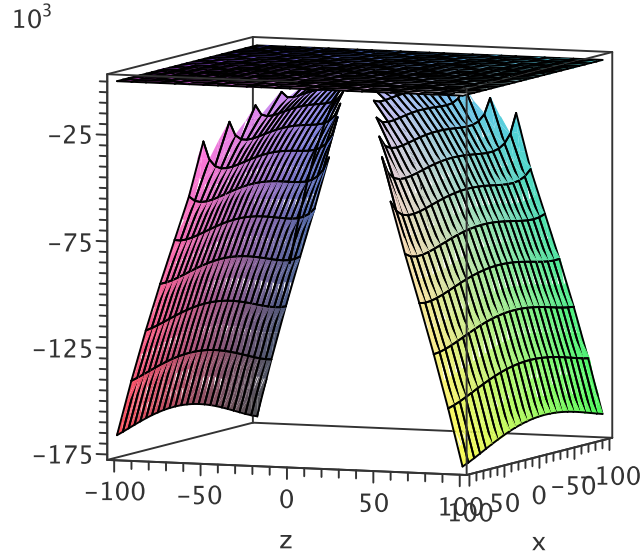


Figure 30: The graph of τ_1 as a function of $z = q_z$ and $x = q_x$ for DDA9

To try to determine which of the viscosities is driving the instability, we wanted to use a simple approximation of one viscosity value, α , but this still had to satisfy the Parodi relation. The approximation was made that

$$-\alpha_1 = -\alpha_2 = \alpha_5 = \alpha (> 0) \quad (6.204)$$

and

$$\alpha_3 = \alpha_4 = \alpha_6 = 0. \quad (6.205)$$

This time the determinant of the equation gives a quadratic in the form

$$\begin{vmatrix} u_1 & v_1 & \theta_1 \\ u_2 & v_2 & \theta_2 \\ u_3 & v_3 & \theta_3 \end{vmatrix} = A\tau^3 + B\tau^2 \quad (6.206)$$

$$= \tau^2(A\tau + B), \quad (6.207)$$

where

$$A = -\alpha\rho^2 < 0 \quad (6.208)$$

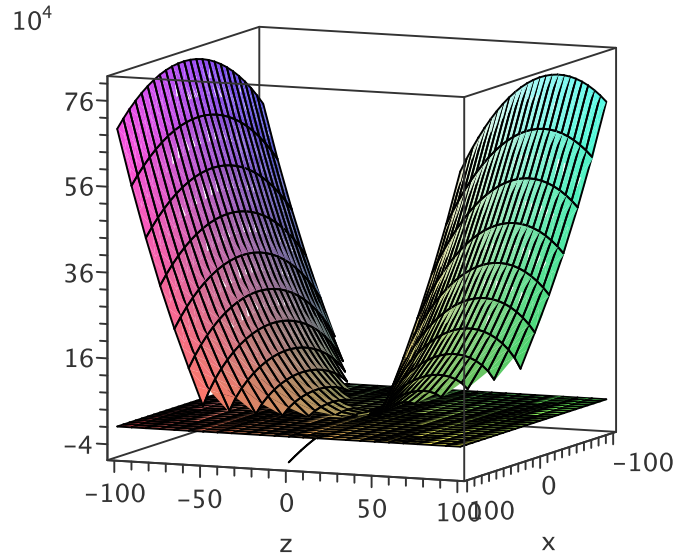


Figure 31: The graph of τ_2 as a function of $z = q_z$ and $x = q_x$ for DDA9

and

$$B = \frac{1}{2}\alpha^2 q_z^2 \rho > 0. \quad (6.209)$$

This means that the non zero root of this equation is given by

$$\tau = \frac{-B}{A} > 0 \quad (6.210)$$

so the perturbed solution is still unstable if you make that approximation.

6.6 Conclusions

Within this chapter, the work of Valignat, Vandenbrouck and Cazabat, [38], has been verified in a mathematical way. This work has then been extended by removing the assumption by Valignat et al. that the director angle θ is fixed at the surface and allowing it to vary and then considering the Ericksen–Leslie equations rather than the Navier–Stokes equations for the problem. The

Ericksen–Leslie equations were then considered with a perturbation to the known solutions for different nematic liquid crystals (5CB, MBBA and DDA9). While doing this, it was discovered that for DDA9 a perturbed solution was not stable and therefore some of the Leslie viscosities were ignored in an attempt to discover what was causing the instability.

7 A Blade Approaching a Free Surface

When an object approaches the free surface of a fluid, the fluid will spontaneously jump up to meet the approaching object. This is investigated by researchers by using the Wilhelmy plate technique to measure properties of the fluid-air interface. The Wilhelmy plate experiment involves the approaching edge-on emersion of a metal plate into the fluid. The surface initially rises up and eventually jumps to capture the blade. This is caused by van der Waals surface forces. From [44], these are weak non-chemical short range bonds that hold neutral molecules together because of their induced dipoles. As the distance between the blade and the original level of the fluid decreases, the fluid rises more and more until, at some height above the undisturbed level of the fluid, the fluid can no longer remain in its distorted shape and so the fluid is captured by the blade. Essentially, the fluid jumps up to meet the blade.

Within this chapter we will consider the work done by Miklavcic [45] where he considers a parabolic blade, and we extend this work by considering a different shape of blade. This allows us to draw comparisons between blade shapes, curvatures and heights.

7.1 Blade models

In the paper [45], Miklavcic looks at this problem with water as the fluid. The model for this problem is shown below in Fig. 32. This problem is in 2D only. The blade is assumed to be infinite in the y direction, as is the water. It is also assumed that the water sample is infinite in x and depth. In Fig. 32, $z_p(x)$ is the equation for the cross section of the blade, $z(x)$ is the profile of the fluid, and $D(x)$ is the shortest distance from the fluid at x to the blade.

The deformation to the free surface has an associated change in free energy. It is this that Miklavcic uses to look at the equilibrium stability of the problem.

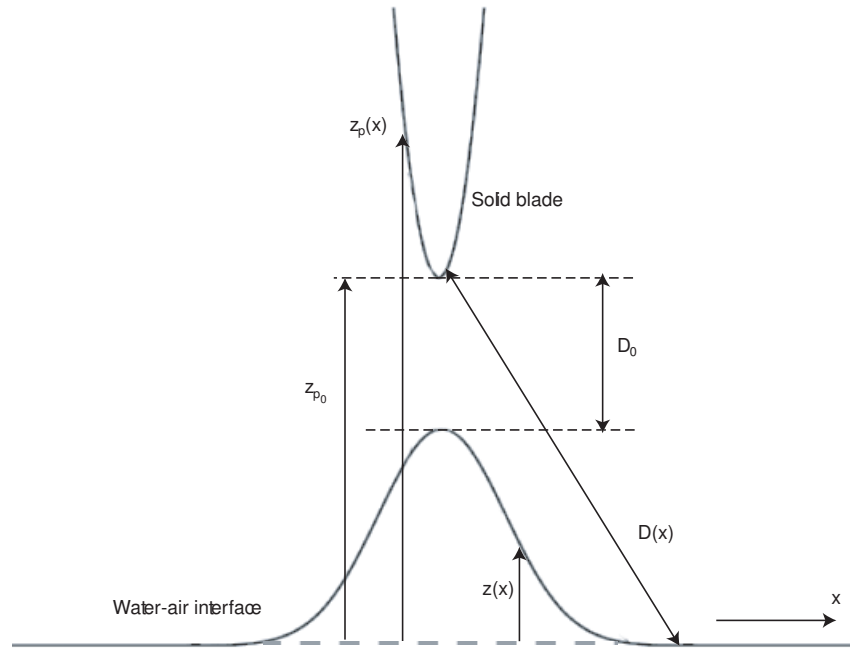


Figure 32: As the parabolic blade approaches the free surface, the surface rises up to meet the blade.

This change is caused by some of the fluid rising above the rest changing the gravitational potential, and by the increased surface area of the fluid, changing the surface tension. From [45], the change in free energy in F is given by

$$F = \gamma A_\Lambda + G \int \int \int_{\Delta V_\Lambda} z dV + \int \int_\Lambda \sigma dS. \quad (7.1)$$

In (7.1), γ is the interfacial tension given to be 72.8 mN m^{-1} , $G = g\Delta\rho$ where g is the acceleration due to gravity (taken to be 9.81 ms^{-2}), $\Delta\rho$ is the density difference between the air and the fluid taken to be 1 kg m^{-3} , and σ is the surface energy density. It was supposed by Miklavcic that σ has continuous partial derivatives up to order k , where $k \geq 2$. The deformed interface is denoted by Λ so the A_Λ means the area of the deformed fluid. This means that the three terms in (7.1) are the surface energy associated with the change in surface area, the gravitational potential energy and the interaction term, respectively. The change in free energy, (7.1), defines a functional over the space Ω_x , the set of all

possible profiles $z(x)$ of the interface.

Since we are only dealing with a two dimensional problem, the free energy change, (7.1), reduces to the one dimensional integral

$$\mathcal{F} = \gamma \int_{-\infty}^{\infty} W(\bar{z}_x) dx + \frac{1}{2}G \int_{-\infty}^{\infty} \bar{z}^2 dx + \int_{-\infty}^{\infty} W(\bar{z}_x) \sigma(x, \bar{z}) dx, \quad (7.2)$$

$$= \int_{-\infty}^{\infty} \left\{ W\bar{z}_x h(x, \bar{z}) + \frac{1}{2}G\bar{z}^2 \right\} dx, \quad (7.3)$$

$$= \int_{-\infty}^{\infty} f(x, \bar{z}(x), \bar{z}_x(x)) dx, \quad (7.4)$$

where $W(\bar{z}_x) = (1 + \bar{z}_x^2)^{\frac{1}{2}}$, and $h(x, \bar{z}) := \gamma + \sigma$.

From [45], the profile $z(x)$ that we are looking for should be even due to symmetry and it should be integrable, and it should also have continuous second-order derivatives, which should be square integrable. So $z(x)$ should be in Ω_x where

$$\Omega_x = \{ \eta : \eta^{(k)} \in C(\mathbb{R}) \cap L_2(\mathbb{R}), k = 0, 1, 2; \eta(x) = \eta(-x) \}. \quad (7.5)$$

From this, all functions in this set need to satisfy

$$\eta_x(0) = 0. \quad (7.6)$$

The unique function, $z(x)$, which is a member of Ω_x and is an extremal of (7.4), will be assumed to exist and shall be called the equilibrium profile.

In [45], the Euler–Lagrange equation of $f(x, \bar{z}(x), \bar{z}_x(x))$ in (7.4) is found to be

$$\left(\frac{h(x, z)z_x}{W(z_x)} \right)_x = Gz + h_z(x, z)W(z_x), \quad (7.7)$$

which is satisfied by $z(x)$, the equilibrium solution.

The van der Waals interaction is simplified in [45] by using the surface stress, π , to obtain the van der Waals surface energy density, σ since calculating the actual van der Waals interaction is very complicated. The surface stress is given by

$$\pi(D) = -\frac{C_H}{D^3}, \quad (7.8)$$

which arises from considering the van der Waals pressure acting between two infinite parallel planar surfaces separated by a distance D . The Hamaker constant for the problem is denoted C_H and here, $C_H = 10^{21}$ J. This Hamaker constant is constant used for describing the van der Waals force. The magnitude of the Hamaker constant reflects the strength of the forces between the blade, air and the surface. It is a parameter which depends upon the three different materials in the problem: the blade, the air and the water. Integrating (7.8) gives $\sigma(D)$,

$$\sigma(D) = - \int_{-\infty}^D \pi(\tau) d\tau, \quad (7.9)$$

$$= - \frac{C_H}{2D^2}. \quad (7.10)$$

This theory can be used for blades of different shapes, but the function for the shortest distance between the blade and the surface must be continuously differentiable so the blade cannot have corners.

7.1.1 Parabolic blade

The blade shape considered in [45] is parabolic. The blade profile is described by the curve

$$z_p(x_p) = z_{p0} + \lambda x_p^2, \quad (7.11)$$

where a point on the blade has co-ordinates (x_p, z_p) . The z_{p0} value is the height above the free surface that the blade is at for the solution, and $\lambda > 0$ is the curvature of the blade.

For this blade, the shortest distance between a point on the fluid $(x, z(x))$ and the blade (x_p, z_p) , is given by

$$D(x, z(x)) = \sqrt{(x - x_p)^2 + (z(x) - z_p)^2}. \quad (7.12)$$

The points $(x, z(x))$ and (x_p, z_p) are related by

$$\left(\frac{\partial}{\partial x_p}, \frac{\partial}{\partial z_p} \right) (z_{p0} + \lambda x_p^2 - z_p) = \alpha(x - x_p, z(x) - z_p), \quad (7.13)$$

which is a vector equation from [45]. Eliminating α and solving the resulting cubic equation, gives us only one real solution, namely

$$x_p(x) = R - \frac{1 + 2\lambda(z_{p_0} - z(x))}{6\lambda^2 R}, \quad (7.14)$$

where

$$R = \left[\frac{x}{4\lambda^2} + \sqrt{\frac{x^2}{16\lambda^4} + \frac{(1 + 2\lambda(z_{p_0} - z(x)))^3}{216\lambda^6}} \right]. \quad (7.15)$$

This means that the distance $D(x, z(x))$ depends upon x and the profile of the solution $z(x)$.

As was done in [45], a numerical routine was used to find the profiles $z(x)$ for specified z_{p_0} values. The boundary conditions were found by considering the physical problem. Far away from the blade, the van der Waals interaction will have a negligible effect. If we use this along with $|z_x| \ll 1$, the Euler–Lagrange equation (7.7) becomes

$$\gamma z_{xx} = Gz, \quad (7.16)$$

which has the solution

$$z(x) = Ce^{-\frac{|x|}{l_G}} \quad \text{with} \quad |x| \gg 1, \quad (7.17)$$

where $l_G = \sqrt{\gamma/G}$. The value of C is chosen to match the solution far away from the blade. A positive C value is chosen for an attractive interaction between the blade and the free surface. The boundary conditions used to find the solution were

$$z_x(0) = 0 \quad \text{and} \quad z(x_\infty) = Ce^{-\frac{x_\infty}{l_G}}. \quad (7.18)$$

The solutions were found numerically with $x_\infty = 0.1\text{m}$, and graphs of the profiles for $\lambda = 0.1\text{m}^{-1}$ are shown below in Fig. 33. These solutions are in agreement with those found by Miklavcic in [45].

The value of the highest point in the profiles, $z(0)$, is useful for comparisons between different blades and z_{p_0} values. For the three profiles shown above in Fig. 33, the $z(0)$ values were

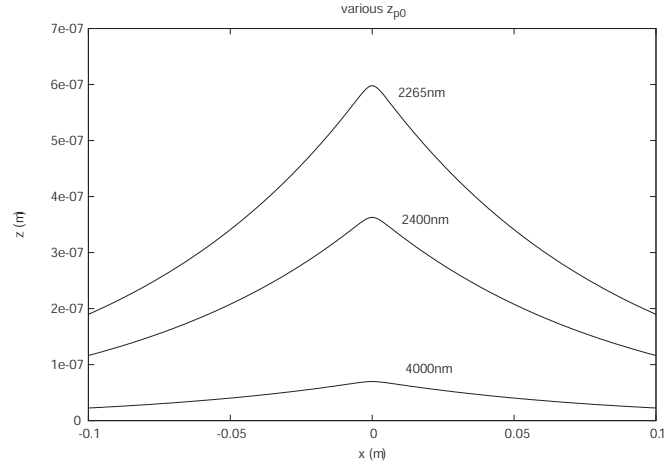


Figure 33: Profiles of the solutions for the parabolic blade for z_{p0} values of 4000nm, 2400nm and 2265nm with $\lambda = 0.1 \text{ m}^{-1}$.

z_{p0} (nm)	$z(0)$ (nm)
4000	69.8
2400	363
2265	598

for $\lambda = 0.1$.

The value of λ can be changed to represent blades of different curvature. If we increase λ , the blade becomes narrower, and if we decrease λ , the blade becomes wider. If λ is varied, the $z(0)$ values change. For $z_{p0}=4000$ nm, the $z(0)$ values obtained for different λ values are shown below.

λ (m^{-1})	$z(0)$ (nm)
0.005	335.1
0.01	229
0.05	99.3
0.1	69.9
0.5	30.7
1	21.6
5	9.5
10	6.59

It is clear from these that as the curvature of the blade increases, the surface below is affected less. This is as expected because the blade is more pointed and so less of the blade is close to the surface so the surface reacts less.

7.1.2 Circular ended blade

Solutions in (7.5) can exist only if the blade is smooth in the sense that the equation for the shortest distance between the surface and blade of the blade has to have continuous first derivatives. The next step was to change the parabolic blade to a blade with a circular end. This is a simpler profile than the parabolic blade and is more realistic. The profile of this circular blade is given by

$$z_{p0} = \left(\sqrt{R^2 - x^2} + (z_{p0} + R) \right) (1 - H(x - r)) \tag{7.19}$$

where R is the radius of the circular end, z_{p0} is the lowest point of the blade and $H(x - r)$ is the Heaviside function. The centre of the circle on the end of the blade is the point $(0, z_{p0} + R)$. Fig. 34 shows the geometry of the problem. The

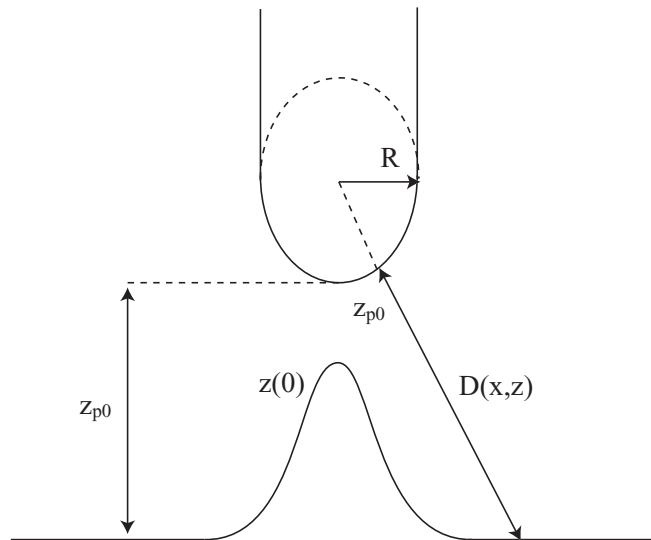


Figure 34: This is the basic geometry for the circular blade approaching the free surface of fluid.

distance function for this model can be written explicitly as a function of $z(x)$ and x , since the closest distance from any x on the free surface is a straight line to the centre of the circle with the size of the radius subtracted, i.e.,

$$D(x, z(x)) = \sqrt{x^2 + (z(x) - (z_{p0} + R))^2} - R. \tag{7.20}$$

This makes the problem less complicated than it was for the parabolic blade as the distance function is only a function of x and $z(x)$.

The profile solutions for the free surface were found in the same way as they were for the parabolic blade, but this time the peaks of the profiles were slightly lower. With the radius, R , set to be 5, the values for $z(0)$ were

z_{p_0} (nm)	$z(0)$ (nm)
4000	58.1
2400	273
2265	358

and the plots of these solutions are shown below in Fig. 35.

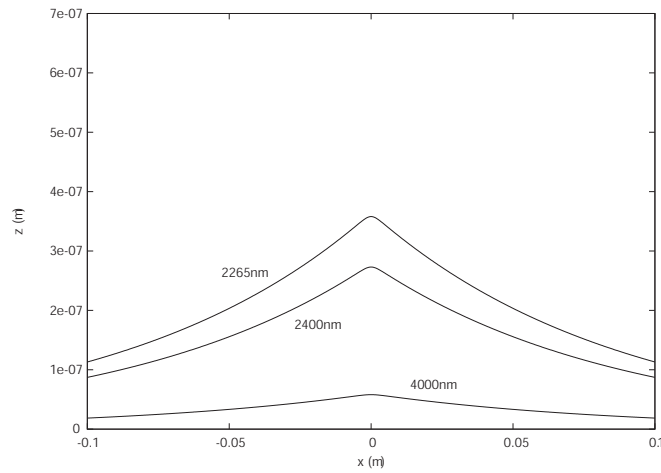


Figure 35: Profiles of the solutions for the circular ended blade for z_{p_0} values of 4000nm, 2400nm and 2265nm.

The value of R can be changed to represent blades of different curvature, as was done previously for λ . If we increase R , the blade becomes wider, and if we decrease R , the blade becomes narrower. If R is varied, the $z(0)$ values for $z_{p_0} = 4000\text{nm}$ change.

R (m)	$z(0)$ (nm)
0.001	0.791
0.01	2.541
0.1	8.11
0.5	18.21
1	25.51
5	57.81
10	82.31
20	117.51
30	144.91
50	189.41
100	274.81

The larger R becomes, the higher the free surface raises. This is to be expected since there would be more surface area of the blade interacting with the free surface. The size of the radius could be increased to 636 m which gives a $z(0)$ height of 1131.1 nm but if this is increased to 637 m then no solution for the free surface can be obtained. When the value of R is plotted against the $z(0)$ value, the graph in Fig. 36 is obtained. As the value of the radius R reaches its

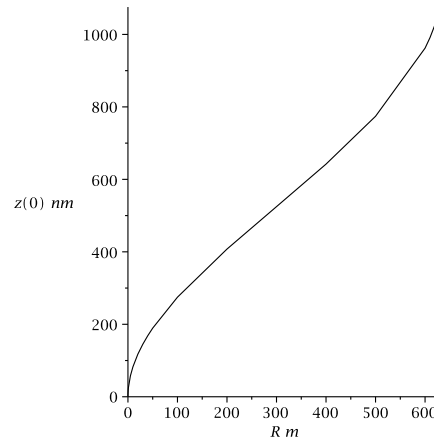


Figure 36: The graph of the radius of the blade against the height the free surface rises shows that as the blade increases in radius, the surface rises more.

critical value the height that the free surface rises to begins to increase quicker than before. This is not what we expected. As the radius of the blade increases, we expected the $z(0)$ value to asymptote to a value because as R increases we

are approximating bringing a plate to the surface. The reason our results does not give this is unknown, it may be down to numerical error within our system.

7.1.3 Comparison of blade shapes

To compare the two different blade shapes fairly for the same z_{p0} , blades with the same curvature at $x = 0$ were considered. The curvature of the circle ended blade is given by

$$k_c = \frac{1}{R} \quad (7.21)$$

For the parabolic blade, the curvature is calculated from the equation for the parabola. The curvature of a twice differentiable function y is given by [46, p. 890]

$$k = \frac{|y''|}{(1 + (y')^2)^{3/2}}. \quad (7.22)$$

For the parabolic blade

$$y = \lambda x_p^2 + z_{p0}, \quad (7.23)$$

so the curvature is given by

$$k_p = \frac{2\lambda}{(1 + (2\lambda x_p)^2)^{3/2}}. \quad (7.24)$$

When $x = 0$, $x_p = 0$ so the comparable curvature for the parabolic blade is

$$k_p = 2\lambda, \quad (7.25)$$

so for comparison

$$\lambda = \frac{1}{2R}. \quad (7.26)$$

This means that when $\lambda = 0.1 \text{ m}^{-1}$, the circular ended blade which it should be compared with had radius $R = 5 \text{ m}$.

The following table shows the comparable values for the different blades at a z_{p0} value of 4000nm.

λ (m ⁻¹)	R (m)	$z_\lambda(0)$ (nm)	$z_R(0)$ (nm)	$z_\lambda(0) - z_R(0)$ (nm)
1000	0.0005	0.380	0.551	-0.171
100	0.005	1.867	1.791	0.076
10	0.05	6.59	5.721	0.869
1	0.5	21.6	18.21	3.39
0.1	5	69.875	57.81	12.065
0.01	50	229.0	189.41	39.59

As the curvature decreases, it can be seen that the parabolic blade causes the free surface to rise more than the circle ended blade.

Two blades with the same curvature were considered for varying z_{p_0} values. The curvature for both blades was set to be 0.1 m⁻¹.

z_{p_0} (nm)	Parabolic $z(0)$ (nm)	Circular $z(0)$ (nm)
4000	69.8	58.1
2400	363	273
2265	598	358

It is clear from this table that the parabolic blade causes the free surface to rise more at the peak than the circle ended blade.

7.2 Stability of the profiles

Miklavcic [45] gives two sufficient conditions with regards to the stability of the solutions for the deformed surface.

Condition 1: Stability

Let $z \in \Omega_x$ be the solution of the Euler–Lagrange equation (7.7) for the equilibrium profile of the fluid interface subject to a local van der Waals stress. Furthermore, let $z(x)$ satisfy the constraint that $\Phi = \Phi(x, z(x))$ remains bounded for all $x \in R$ such that

$$\begin{cases} L < \Phi < U & \forall x \in R \\ \Phi \rightarrow U & \text{as } |x| \rightarrow \infty \end{cases} \quad (7.27)$$

Then, there exists a positive constant E^* such that if

$$\Phi(x) \geq \frac{1 - E \exp\left(-\left(\frac{x}{l_G}\right)^2\right)}{l_G^2} \quad \forall x \in R \quad (7.28)$$

for some $E \leq E^*$ then the equilibrium profile will be stable to arbitrary infinitesimal perturbations $\nu \in \Omega_x$.

Miklavcic calculated the value of E^* to be 5.

Condition 2: Instability

Let $z \in \Omega_x$ be the solution of the Euler–Lagrange equation (7.7) for the equilibrium profile of the fluid interface subject to a local van der Waals stress. Furthermore, let $z(x)$ satisfy the constraint that $\Phi = \Phi(x, z(x))$ remain bounded for all $x \in R$ as described above in Condition 1. Then there exists a positive constant E_* such that if

$$\Phi(x) \leq \frac{1 - E \exp\left(-\left(\frac{x}{l_G}\right)^2\right)}{l_G^2} \quad \forall x \in R \quad (7.29)$$

for some $E > E_* > 5 \left(\frac{3}{2}\right)^{3/2}$, then the equilibrium profile will not be stable to arbitrary perturbations $\nu \in \Omega_x$.

These conditions are proved in the appendix of [45] where Miklavcic considers the second variation of the problem then applies the Rayleigh–Ritz method. These conditions are based upon a lot of inequalities so they are not the optimal stability conditions.

These conditions do not take into account the shape of the blade and it would be expected that the shape of the blade would play some part in the stability. Here the stability of both blade shapes is considered using the second variation and Rayleigh–Ritz method applied to numerical solutions obtained. Since these solutions are known, they are also known to be stable but the comparison of the eigenvalues of the two different blades allows comparisons to be drawn.

7.2.1 Second Variation

The second variation for this problem (regardless of blade shape) is given by

$$\delta^2 F = \int_{-\infty}^{\infty} [v_x^2 + \Phi(x)v^2] dx \quad (7.30)$$

where

$$\Phi(x) = \frac{1}{2} \left(\frac{(f_{pp})_x}{f_{pp}} \right)_x + \frac{[(f_{pp})_x]^2}{4f_{pp}^2} + \frac{(f_{zz} - (f_{zzx})_x)}{f_{pp}} \quad (7.31)$$

and $p = z_x$. Each term in $\Phi(x)$ can be expressed as

$$\frac{1}{2} \left(\frac{(f_{pp})_x}{f_{pp}} \right)_x = \frac{1}{2} \left[\frac{6z_x^2 z_{xx}^2}{W(z_x)^4} - \frac{3(z_{xx}^2 + z_x z_{xxx})}{W(z_x)^2} - \frac{(h_z z_x + h_z)^2}{h^2} + \frac{(h_{xx} + 2z_x z_x + h_{zz} z_x^2 + h_z z_{xx})}{h} \right], \quad (7.32)$$

$$\frac{[(f_{pp})_x]^2}{4f_{pp}^2} = \frac{1}{4} \left[\frac{1}{h} (h_z z_x + h_z) - \frac{3z_x z_{xx}}{W(z_x)^2} \right]^2, \quad (7.33)$$

$$\frac{(f_{zz} - (f_{zzx})_x)}{f_{pp}} = \frac{1}{h} [GW(z_x)^3 - h_z z_{xx} - (h_{zx} z_x + h_{zz}) W(z_x)^2]. \quad (7.34)$$

As before, if the integrand is positive definite then the integral is positive definite meaning that the solution for the deformation of the $z(x)$ is stable. Unfortunately, $\Phi(x)$ changes sign so it cannot be guaranteed that the integral is positive definite.

The second variation here is an integral from $-\infty$ to ∞ but, since the problem is assumed to be symmetric around the z axis, we can consider double the integral from 0 to ∞

$$\delta^2 F = 2 \int_0^\infty [v_x^2 + \Phi(x)v^2] dx. \quad (7.35)$$

Since it is the sign of the integral and not the value of the integral which is of interest, the factor two can be ignored. Since the surface far from the centre of the sample would be undisturbed by the presence of the blade, this integral can be considered over a finite domain only and then stitched together with a function which is zero from the finite end point to infinity. If the finite end point is set to be $x = 1$ then the integral becomes

$$\int_0^1 [v_x^2 + \Phi(x)v^2] dx. \quad (7.36)$$

The Poincaré inequality [27] says

$$\int_0^1 [v_x^2] dx \geq \pi \int_0^1 [v^2] dx \quad (7.37)$$

so

$$\int_0^1 [v_x^2 + \Phi(x)v^2] dx \geq \int_0^1 [(\pi + \Phi(x)) v^2] dx. \quad (7.38)$$

From this, if

$$\pi + \Phi(x) > 0 \quad (7.39)$$

then the second variation is positive and therefore the solution is stable, i.e. for stability

$$\Phi(x) > -\pi. \quad (7.40)$$

This result does not improve upon the results in the Miklavcic paper [45].

As in the Atkin–Stewart Equations chapter, the positivity criterion from Section 3.4 was applied to the second variation of the problem for the solutions which are known. The positivity criterion confirmed that the solutions which we already have are stable but it could not be applied to solutions we had not obtained so this did not progress the stability argument.

7.2.2 Rayleigh–Ritz method

The Rayleigh Ritz method was applied to the solutions for both blade shapes. The eigenvalues given by the method were noted for different heights of z_{p_0} .

For the circular ended blade the following eigenvalues, μ , were found for $R = 5$ m.

z_{p_0} (nm)	μ
4000	112.1632437
2400	112.1335002
2265	112.1216989
2200	112.1165040
2151	112.0881887

As the z_{p_0} value is decreased, the eigenvalue also decreases. However, when z_{p_0} was lowered beyond 2151 nm, the first eigenvalue for the solution could no longer be found. This could be because the solutions become unstable and so

the imposed initial condition of $z'(0) = 0$ may fail or it could be the limitations of the program. We would have expected the value of μ to change sign near the instability.

The parabolic blade used had $\lambda = 0.1 \text{ m}^{-1}$.

z_{p0} (nm)	μ
4000	112.1631827
2400	112.1292251
2265	112.1021386
2264	112.1001536
2263	112.0996178

These eigenvalues also reduce but they are slightly lower than the eigenvalues for the circular ended blade. A first eigenvalue cannot be found for 2262 nm which is a higher limit than the circular ended blade. These different eigenvalues mean that the shape of the blade must have an impact upon the stability of the raised surface. This means that the work by Miklavcic can be improved.

7.3 Conclusions

Having compared the two different blade shapes, it has been seen that they affect the free surface differently. The circular ended blade is closer to the surface over a wider x range and so the surface does not rise by as much in the middle than the parabolic blade. It also appears that the circular ended blade can be taken closer to the surface before any instabilities may occur than the parabolic one (2151 nm compared with 2262 nm).

It was also noticed that the shape of the blade had some effect on the stability of the profile (as would be expected). The degree to which the shape of the blade affects the stability of the solution is something which could be looked at in a lot more depth.

8 Conclusions and Outlook

This thesis looks at the stability of different fluids using a range of perturbation methods from the calculus of variations.

In chapter 1 the history of liquid crystals are introduced along with a basic description of the liquid crystal phases: nematic, smectic and cholesteric. Although cholesteric liquid crystals are not used within the thesis, the information is given here for completeness.

Chapter 2 then gives a brief description of three important mathematical theories for the dynamics of liquid crystals. The Ericksen–Leslie dynamic theory for nematic liquid crystals is described first and then the theory of smectic liquid crystals is introduced. The smectic theory is based upon the Leslie, Stewart and Nakagawa (LSN) theory. This is used in Chapters 4 and 5 while the nematic theory is used in Chapter 6.

Some methods in the calculus of variations are introduced in chapter 3. These methods are applied in later chapters using the new inequality from section 3.4. These methods are used within the chapters which followed. The inequality that was introduced from [24] was used to prove the stability for two different solutions without the need for further investigation (one solution from Chapter 4 and one from Chapter 5). Without this useful inequality, a lot more work would have been needed to solve the Jacobi equation for the solution. With a little further work, this inequality proved stability for another 3 cases in the cylindrical geometry.

Five solutions to a differential equation which arises from considering a magnetic field to a sample of smectic liquid crystals are looked at in terms of stability in chapter 4. These five Atkin–Stewart equations were found by Atkin and Stewart a stability condition was known for one of them. The full stability is now known for 4 of the 5 solutions and the final solution was shown to be unstable un-

der certain conditions. The work within Chapter 4 is extended to the case when a planar layer of smectic liquid crystals have an electric field applied in chapter 5. The resulting equation produced a qualitatively different phase portrait to those found in the previous chapter. All of the solutions within this different phase plane were found for specific values of the variables b and k . the stability of these solutions were considered briefly but only one solution has a complete stability story. The work in these chapters is motivated by the little experimental data on the elastic constants A_{ij} . It is hoped that the solutions may lead to experiments which can determine these values or give us more information.

Within Chapter 6, the work of Valignat, Vandenbrouck and Cazabat looking at the wetting and dewetting of thin nematic films of liquid crystals is considered and then extended. Valignat et al. considered the stability of a perturbation using the Navier–Stokes equation. Here, the Ericksen–Leslie equations were considered as an extension of the Navier–Stokes equation by introducing some freedom to the director angle at the free surface and by considering the leslie viscosities rather than an isotropic viscosity. The stability of the Ericksen–Leslie equations is considered by introducing a small perturbation to the terms. This chapter concludes with different smectic materials being considered to compare stabilities. The work in this chapter is important for coating processes. Depending on whether you want wetting or dewetting, the nematic liquid crystal would have to be chosen carefully.

A blade approaching a free surface of fluid is considered within Chapter 7. The work of Miklavcic is followed for his original parabolic blade and then with the blade model changed to a circular ended blade. The results for both sets of blades were compared and the stability was looked at using the second variation methods.

The stability work in this thesis could be extended to consider different types of stability. Here the stability work focused on the stability of small perturbation

to the solutions. Instead of this, energy stability methods could have been used. Also, here it was only the linear stability that was considered. This could be extended to consider non-linear effects. There are also potential applications of the work within the thesis including applying the work to other phases of liquid crystals as well as non-Newtonian fluids such as Oldroyd-B [47]. The work within chapter 6 has already been extended by Miklavcic and Cortat in [48] and [49]. Within this work they have found results for the original parabolic shaped blade for blade heights, z_{p0} , much less than we were able to compute.

A Solutions to the Planar Layer Integral

In Section 5.1, the solution to the integral equation

$$\int \frac{d\psi}{\sqrt{2b \cos^2 \psi + 4bk \cos \psi + c - b}} = \int ds \quad (\text{A.1})$$

was considered. This problem was rearranged using substitutions into the form of (5.29) where denominator has three roots. From [37] here are eight solutions to this problem. In Section 5.1, case 1 is given where the roots of (5.29) are such that $r_1 > r_2 > r_3 \geq u$. For completeness, the remaining seven solutions u to the integral equation given by (5.29) are given below.

Case 2: $r_1 > r_2 > r_3 > u$

If u is strictly less than the three distinct roots then

$$\int_u^{r_3} \frac{dx}{\sqrt{(r_1 - x)(r_2 - x)(r_3 - x)}} = \frac{2}{\sqrt{r_1 - r_3}} F(\beta, p) \quad (\text{A.2})$$

where F is the elliptic integral of the first kind (from [37]) which is

$$\begin{aligned} F(\varphi, k) &= \int_0^\varphi \frac{d\alpha}{\sqrt{1 - k^2 \sin^2 \alpha}} \\ &= \int_0^{\sin \varphi} \frac{dx}{\sqrt{(1 - x^2)(1 - k^2 x^2)}}, \end{aligned} \quad (\text{A.3})$$

and

$$\beta = \arcsin \left(\sqrt{\frac{r_3 - u}{r_2 - u}} \right) \quad (\text{A.4})$$

and p is given by

$$p = \sqrt{\frac{r_1 - r_2}{r_1 - r_3}}. \quad (\text{A.5})$$

In this case, after substituting back in for the original variables, the solution for the differential equation (A.1) turns out to be

$$\psi = 2 \arctan \left(\sqrt{-r_3 \sec^2(z(s)) - r_2 \tan^2(z(s))} \right) \quad (\text{A.6})$$

where

$$z(s) := \text{am} \left(\frac{\sqrt{r_1 - r_3}}{2} \sqrt{a_1} s, \sqrt{\frac{r_1 - r_2}{r_1 - r_3}} \right) \quad (\text{A.7})$$

for ease. Here $\text{am}(u)$ is the amplitude function.

Case 3: $r_1 > r_2 \geq u > r_3$

If the solution lies in the range where is is greater than the least root of the polynomial, r_3 but is less than or equal to r_2 then

$$\int_{r_3}^u \frac{dx}{\sqrt{(r_1-x)(r_2-x)(x-r_3)}} = \frac{2}{\sqrt{r_1-r_3}} F(\gamma, q) \quad (\text{A.8})$$

with F being the elliptic function of the first kind (A.3),

$$\gamma = \arcsin \left(\sqrt{\frac{u-r_3}{r_2-r_3}} \right) \quad (\text{A.9})$$

and

$$q = \sqrt{\frac{r_2-r_3}{r_1-r_3}}. \quad (\text{A.10})$$

In this case the solution is given by

$$\psi = 2 \arctan \left(\sqrt{r_3 + (r_2 - r_3) \sin^2 \left(\text{am} \left(\frac{\sqrt{r_1 - r_3}}{2} \sqrt{a_1} s, \sqrt{\frac{r_2 - r_3}{r_1 - r_3}} \right) \right)} \right) \quad (\text{A.11})$$

Case 4: $r_1 > r_2 > u \geq r_3$

If u is strictly less than r_2 but greater than r_3 then

$$\int_u^{r_2} \frac{dx}{\sqrt{(r_1-x)(r_2-x)(x-r_3)}} = \frac{2}{\sqrt{r_1-r_3}} F(\delta, q) \quad (\text{A.12})$$

where F is the elliptic function of the first kind as before,

$$\delta = \arcsin \left(\sqrt{\frac{(r_1-r_3)(r_2-u)}{(r_2-r_3)(r_1-u)}} \right) \quad (\text{A.13})$$

and q is given by (A.10).

For this case, the solution ψ is given by

$$\psi = 2 \arctan \left(\sqrt{\frac{\left(r_1 \frac{(r_2-r_3)}{(r_1-r_3)} \sin^2(z(s)) - r_2 \right)}{\left(\frac{(r_2-r_3)}{(r_1-r_3)} \sin^2(z(s)) - 1 \right)}} \right) \quad (\text{A.14})$$

with

$$z(s) := \text{am} \left(\frac{\sqrt{r_1-r_3}}{2} \sqrt{a_1} s, \sqrt{\frac{r_2-r_3}{r_1-r_3}} \right). \quad (\text{A.15})$$

Case 5: $r_1 \geq u > r_2 > r_3$

If the solution u lies in the range such that it is less than or equal to the greatest of the roots r_1 but greater than the lower two roots then

$$\int_{r_2}^u \frac{dx}{\sqrt{(r_1-x)(x-r_2)(x-r_3)}} = \frac{2}{\sqrt{r_1-r_3}} F(\chi, p) \quad (\text{A.16})$$

where F is the standard elliptic function of the first kind given by (A.3),

$$\chi = \arcsin \left(\sqrt{\frac{(r_1-r_3)(u-r_2)}{(r_1-r_2)(u-r_3)}} \right) \quad (\text{A.17})$$

and p is give by (A.5).

In this case, ψ is given by

$$\psi = 2 \arctan \left(\sqrt{\frac{\left(-r_3 \frac{(r_1-r_2)}{(r_1-r_3)} \sin^2(z(s)) + b \right)}{\left(1 - \frac{(r_1-r_2)}{(r_1-r_3)} \sin^2(z(s)) \right)}} \right) \quad (\text{A.18})$$

with

$$z(s) := \text{am} \left(\frac{\sqrt{r_1-r_3}}{2} \sqrt{a_1} s, \sqrt{\frac{r_1-r_2}{r_1-r_3}} \right). \quad (\text{A.19})$$

Case 6: $r_1 > u \geq r_2 > r_3$

If u is strictly less than r_1 but greater than r_2 and r_3 then

$$\int_u^{r_1} \frac{dx}{\sqrt{(r_1-x)(x-r_2)(x-r_3)}} = \frac{2}{\sqrt{r_1-r_3}} F(\lambda, p) \quad (\text{A.20})$$

with F as in (A.3),

$$\lambda = \arcsin \left(\sqrt{\frac{r_1-u}{r_1-r_2}} \right) \quad (\text{A.21})$$

and p is give by (A.5).

For this range, the solution ψ is given by

$$\psi = 2 \arctan \left(\sqrt{r_1 - (r_1 - r_2) \sin^2 \left(\text{am} \left(\frac{\sqrt{r_1-r_3}}{2} \sqrt{a_1} s, \sqrt{\frac{r_1-r_2}{r_1-r_3}} \right) \right)} \right) \quad (\text{A.22})$$

Case 7: $u > r_1 > r_2 > r_3$

If u is strictly greater than all of the roots then

$$\int_{r_1}^u \frac{dx}{\sqrt{(x-r_1)(x-r_2)(x-r_3)}} = \frac{2}{\sqrt{r_1-r_3}} F(\mu, q) \quad (\text{A.23})$$

with F representing the elliptic function of the first kind (A.3),

$$\mu = \arcsin \left(\sqrt{\frac{u-r_1}{u-r_2}} \right) \quad (\text{A.24})$$

and q given by (A.10).

In this case, the solution is given by

$$\psi = 2 \arctan \left(\sqrt{-r_2 \tan^2(z(s)) + r_1 \sec^2(z(s))} \right) \quad (\text{A.25})$$

where

$$z(s) := \text{am} \left(\frac{\sqrt{r_1-r_3}}{2} \sqrt{a_1} s, \sqrt{\frac{r_2-r_3}{r_1-r_3}} \right) \quad (\text{A.26})$$

Case 8: $u \geq r_1 > r_2 > r_3$

If u is greater than or equal to the largest of the roots then

$$\int_u^\infty \frac{dx}{\sqrt{(x-r_1)(x-r_2)(x-r_3)}} = \frac{2}{\sqrt{r_1-r_3}} F(\nu, q) \quad (\text{A.27})$$

where F is the elliptic function of the first kind (A.3),

$$\nu = \arcsin \left(\sqrt{\frac{r_1-r_3}{u-r_3}} \right) \quad (\text{A.28})$$

and q given by (A.10).

In this case, the solution is given by

$$\psi = 2 \arctan \left(\sqrt{(a-c) \csc^2 \left(\text{am} \left(\frac{\sqrt{r_1-r_3}}{2} \sqrt{a_1} s, \sqrt{\frac{r_2-r_3}{r_1-r_3}} \right) \right) + r_3} \right) \quad (\text{A.29})$$

References

- [1] P. J. Collings. *Liquid Crystals: Nature's Delicate Phase of Matter*. Adam Hilger, Bristol, 1990.
- [2] F. Reinitzer. Beiträge zur kenntnis des cholesterins. *Monatsh. Chem.*, 9:421–441, 1888.
- [3] H. Kelker. History of liquid crystals. *Molecular Crystals and Liquid Crystals*, 21:1–48, 1973.
- [4] G. Friedel. Les états mésomorphes de la matière. *Ann. Phys. (Paris)*, 18:273–474, 1922.
- [5] F. Schneider H. Knepe and N. K. Sharma. Rotational viscosity γ_1 of nematic liquid crystals. *Journal of Chemical Physics*, 77:3203–3208, 1982.
- [6] I. W. Stewart. *The Static and Dynamic Continuum Theory of Liquid Crystals: A Mathematical Introduction*. Taylor and Francis, London, 2004.
- [7] M. R. Fisch and S. Kumar. *Liquid Crystals: Experimental Study of Physical Properties and Phase Transitions*. Cambridge University Press, Cambridge, 2001.
- [8] H. Zöcher. Über die Einwirkung magnetischer, elektrischer und mechanischer Kräfte auf Mesophasen. *Physik. Zeitschr.*, (28):790–796, 1927.
- [9] H. Zöcher. The effect of a magnetic field on the nematic state. *Trans. Faraday Soc.*, (29):745–957, 1933.
- [10] C. W. Oseen. Flüssige Kristalle, Tatsachen, Theorien. *Fortschr. d. Chemie, Eucken. A. Ed.*, 1929.
- [11] F. C. Frank. On the theory of liquid crystals. *Discuss. Faraday Soc.*, 1958.

- [12] J. L. Ericksen. Conservation laws for liquid crystals. *Trans. Soc. Rheol.*, (5):23–36, 1961.
- [13] F. M. Leslie. Some constitutive equations for anisotropic fluids. *Q. Jl. Mech. Appl. Math.*, 19:357–370, 1966.
- [14] F. M. Leslie. Some constitutive equations for liquid crystals. *Arch. Rat. Mech. Anal.*, 28:265–283, 1968.
- [15] P. G. de Gennes and J. Prost. *The Physics of Liquid Crystals*. Clarendon Press, Oxford, 1993.
- [16] O. Parodi. Stress tensor for a nematic liquid crystal. *J. de Physique*, 31:581–584, 1970.
- [17] J. K. Moscicki. Measurements of viscosities in nematics. *Physical Properties of Liquid Crystals: Nematics*, pages 387–404, 2001.
- [18] A. Rapini and M. Papoular. Distortion d’une lamelle nématique sous champ magnétique. Conditions d’ancrage aux parois. *Journal de Physique*, 30 C4:54–56, 1969.
- [19] I.W. Stewart F. M. Leslie and M. Nakagawa. A continuum theory for smectic c liquid crystals. *Molecular Crystals and Liquid Crystals*, 198:443–454, 1991.
- [20] C. W. Oseen. The theory of liquid crystals. *Trans. Faraday Soc.*, 29:883–899, 1933.
- [21] I. W. Stewart T. Carlsson and F. M. Leslie. Theoretical studies of smectic C liquid crystals confined in a wedge: Stability considerations and Frederiks transitions. *Liquid Crystals*, 9:661–678, 1991.

- [22] T. Carlsson F. M. Leslie, I.W. Stewart and M. Nakagawa. Equivalent smectic c liquid crystal energies. *Continuum Mechanics and Thermodynamics*, 3:237–250, 1991.
- [23] Orsay Group. Simplified elastic theory for smectics c. *Solid State Commun.*, 9:653–655, 1971.
- [24] E. C. Gartland and I. W. Stewart. Private communication.
- [25] H. Sagan. *Introduction to the Calculus of Variations*. Dover, 1992.
- [26] I. M. Gelfand and S. V. Fomin. *Calculus of Variations*. Prentice-Hall, 1963.
- [27] J. D. Logan. *An introduction to nonlinear partial differential equations*. Wiley, Chichester, 1994.
- [28] J. L. Troutman and M. Bautista. *Boundary Value Problems of Applied Mathematics*. PWS Publishing Company, Boston, 1994.
- [29] J. C. Clegg. *Calculus of Variations*. Oliver and Boyd, Edinburgh, 1968.
- [30] R. J. Atkin and I. W. Stewart. Static solutions for smectic C liquid crystals. *CIMNE, Barcelona*, 1996.
- [31] R. J. Atkin and I. W. Stewart. Static domain wall solutions for smectic C liquid crystals and nematic liquid crystals in cylindrical geometry. *Journal of Non-Newtonian Fluid Mechanics*, 119:105–113, 2004.
- [32] R. J. Atkin and I. W. Stewart. Non-linear solutions for smectic C liquid crystals in wedge and cylinder geometries. *Liquid Crystals*, 22(5):585–594, 1997.
- [33] E. G. Virga. *Variational Theories for Liquid Crystals*. Chapman and Hall, London, 1994.

- [34] R. J. Atkin and I. W. Stewart. Stability of domain walls in cylindrical layers of smectic c liquid crystals. *Q. Jl. Mech. Appl. Math.*, 55(2):163–177, 2002.
- [35] I. W. Stewart and E. J. Wigham. Dynamics of cylindrical domain walls in smectic C liquid crystals. *J. Phys A: Math. Theor*, 42(235501), 2009.
- [36] R. J. Atkin and I. W. Stewart. Static domain wall solutions for smectic C liquid crystals. *Mol. Cryst. Liq. Cryst.*, 413:261/[2397]–270/[2406], 2004.
- [37] I. S. Gradstein and I. M. Ryshik. *Tables of Series, Products and Integrals*. Verlag Harri Deutsch, Thun, 1981.
- [38] M. P. Valignat F. Vandenbrouck and A. M. Cazabat. Thin nematic films: Metastability and spinodal dewetting. *Physical Review Letters*, 82(13):2693–2696, 1999.
- [39] P. Neogi and X. Zhang. Wettability of nematic liquid crystals. *Journal of Colloid and Interface Science*, 237:145–146, 2001.
- [40] D. J. Acheson. *Elementary Fluid Dynamics*. Clarendon Press, Oxford, 2003.
- [41] L. D. Landau and E. M. Lifshitz. *Fluid Mechanics*. Pergamon Press, London, 1959.
- [42] G. K. Batchelor. *An Introduction to Fluid Dynamics*. Cambridge University Press, Cambridge, 1987.
- [43] H. Lamb. *Hydrodynamics*. Cambridge University Press, Cambridge, 6th edition, 1945.
- [44] H. Benson. *University Physics, Revised Edition*. John Wiley and Sons, New York, 1996.

- [45] S. J. Miklavcic. On the stability of planar fluid interfaces under van der Waals surface forces. *Journal of Physics A: Mathematical and General*, 36:8829–8850, 2003.
- [46] S. L. Salas and E. Hille. *Calculus: One and Several Variables*. John Wiley and Sons, New York, 7th edition, 1995.
- [47] D. O. Olagunju and L. P. Cook. Secondary flows in cone and plate flow of an Oldroyd-B fluid. *J. Non-Newtonian Fluid Mech.*, 46:29–47, 1993.
- [48] F. P. A. Cortat and S. J. Miklavcic. How closely can a solid approach an air-water surface without becoming wet? *Phys. Rev. E*, 68(052601), 2003.
- [49] F. P. A. Cortat and S. J. Miklavcic. Using stable and unstable profiles to deduce deformation limits of the air-water interface. *Langmuir*, 20, 2004.